QATAR UNIVERSITY

COLLEGE OF HEALTH SCIENCES

THE IMPACT OF HSA-MIR-146A-5P ON HUMAN RETINAL ENDOTHELIAL CELLS IN DIABETIC CONDITIONS

BY

AISHA MOEEN KHAN

A Thesis Submitted to

the College of Health Sciences

in Partial Fulfillment of the Requirements for the Degree of

Masters of Science in Biomedical Sciences

June 2021

COMMITTEE PAGE

The members of the Committee approve the Thesis of

Aisha Moeen Khan defended on 15/04/2021.

Nasser Moustafa Rizk
Thesis/Dissertation Supervisor

Mohamed Aghar N M Elrayess
Committee Member

Abdelali Agouni
Committee Member

Approved:

Hanan Abdul Rahim, Dean, College of Health Science

ABSTRACT

KHAN, AISHA, M., Masters of Science : June : [2021:], Biomedical Sciences

Title: The Impact of hsa-mir-146a-5p on Human Retinal Endothelial Cells in Diabetic Conditions

Supervisor of Thesis: Nasser M. Rizk.

Background: Diabetic retinopathy (DR) is a microvascular complication of diabetes that leads to visual impairment in the adult population with effective available therapy. Micro-Ribonucleic acids (miRNAs) are small (~22 nucleotides) expressed RNA molecules that do not code for protein. They affect the expression of the target gene at the post-transcriptional level, hence, affecting several cellular processes. Clinical and experimental studies demonstrated that miRNAs are implicated in the pathogenesis of diabetic retinopathy. We identified hsa-miR-146a-5p is differentially expressed in human retinal microvascular endothelial cells (HRECs) under hyperglycemic conditions treated with adiponectin using RNA-seq for miRNA and qRT-PCR.

Aim and objectives: To explore the impact of hsa-miR-146a-5p in hyperglycemia condition in vitro using HRECs and evaluate whether miR-146a-5p could mimic adiponectin's actions and effects in ameliorating the hyperglycemic effect in HRECS *in vitro*.

Methods: HRECs were treated with 25 mM glucose, then transfected with a low dose of 10 nM or high dose of 50 nM of miR-146a-5p mimic to overexpress the miR-146a-5p. Moreover, we transfected HRECs using 10 nM of miR-146a-5p inhibitory to silence the expression. Apoptosis and oxidative stress were evaluated. Total RNA was extracted from different HRECs-treated groups, and the gene expression of miR-146a-5p, TRAF6, TNF-α, ICAM-1, PPAR-α and antioxidant

enzymes were evaluated using qRT-PCR. Further, we utilized RT-PCR profile array technology to explore the gene panel for inflammatory, cytokine receptor molecules and angiogenesis in HRECs under hyperglycemic conditions transfected with 50nM miR-146a-5p mimic. Bioinformatic analysis tools were used to explore the impact of 50 nM miR-146a-5p mimic transfection on inflammatory, oxidation, and angiogenesis pathways.

Results and discussion: Transfection with miR-146a-5p inhibitory and 10 nM of miR-146a-5p mimic upregulated the expression of TNF-α, ICAM-1, and ROS production in HRECs, indicating a pro-inflammatory effect. Transfection of HRECs with 50nM miR-146a-5p mimic revealed anti-inflammatory impact and significantly reduced the expression of TRAF-6, TNF-α, and ICAM-1, whereas PPAR- α expression was not affected. Pathway analysis demonstrated a pleiotropic effect of miR-146a-5p miRNA on gene expression via different pathways such as Il-17 signaling pathway, IL-8 Signaling, Toll-like Receptor Signaling, PPAR Signaling, and IL-6 Signaling, and also via inhibiting several transcription factors such as HMGB1, Jun, STAT4, NFKB1, and RELA.

Conclusion: These results propose that miR-146a-5p could be involved in the amelioration of hyperglycemia-induced endothelial inflammation. High expression of miR-146a-5p and its anti-inflammatory, anti-oxidant, and anti-angiogenesis impact could be a potentially promising therapeutic and preventive option for DR patients.

DEDICATION

To my Mom and My brother Yar Mohammad

To my sisters Zainab, Fatima, Maryam, nieces and nephews

To our dearest angel Mariyam Sohail Alabadla (May Allah bless her soul and grant her the highest state in the Jannah)

ACKNOWLEDGMENTS

First, I would like to praise Allah the almighty for the countless blessing, so that I have been able to accomplish this thesis.

Apart from the countless efforts of me, I would like to express gratitude to so many people for their support and encouragement that facilitated the completion of this thesis. I would like to show my greatest appreciation to the supervisor of this thesis Dr. Nasser Rizk for his trust and support throughout the project. Many thanks to Dr. Mohamed Elrayees, Dr. Layla Al Mansouri, Dr. Sudheer (From Sedeer Medical), who shared with me their treasured knowledge about cell culture and research skills and kept on providing me constructive comments throughout the project to improve this thesis. I would also like to thank the assistants at Dr. Nasser Rizk and Dr. Abdelali Agouni labs, Maram Hassan and Omnia Mohamed, for their help and support. Special thanks, gratitude, and love are extended to Ms. Samira Abdullah Saleh, supervisor of Immunology and Histocompatibility & Immunogenetics laboratories at Hamad Medical Corporation, for encouraging me and the other technologists to develop and gain knowledge through earning higher degrees. Without her trust, love, flexibility, support and understanding, I would not have been able to start and accomplish this chapter of my life. I would also like to extend my gratitude to my colleagues Dalal Alhababi, Zahra Ali, Alaa Hassiba, Rejisha Shukkoor, Hazar, and my friends Muna Yousef, Abeer Qush, Enas, Marie Joy, Sherlene, Buthaina Shaheen, Fatima Alkuwari, Fatima Alzahraa for their support, encouragement, and kindness during my master's degree journey.

Finally, my forever non ending thanks and love to my superheroes, my mother and my brother Yar Mohammed for raising me up to be the human being that I'm today.

TABLE OF CONTENTS

LIST OF TABLES

LIST OF FIGURES

LIST OF ABBREVIATIONS

3’UTR	3 prime untranslated region
ADAR1	Adenosine deaminase 1
AGE	Advanced glycation end product
AGO	Argonaute protein
AGTR1	Angiotensin II Receptor Type 1
AMD	Age-Related Macular Degeneration
AMP	Adenosine monophosphate
AMPK	AMP-activated protein kinase
APN	Adiponectin
apo-A1	Apolipoprotein A1
BRB	Blood retinal barrier
cDNA	Complementary deoxyribonucleic acid
circRNA	Circular Ribonucleic acid
CXCR4	C-X-C Motif Chemokine Receptor 4
CXCL8	C-X-C Motif Chemokine Ligand 8
DGCR8	DiGeorge syndrome critical region 8
DME	Diabetic macular edema
DNA	Deoxyribonucleic acid
DR	Diabetic retinopathy
FADD	Fas Associated Death Domain
FLK1	Fetal Liver Kinase 1
FLT1	Fms Related Receptor Tyrosine Kinase 1
FOXO4	Forkhead Box O4 FOXO4
GATA2	GATA Binding Protein 2

GSK3B	Glycogen Synthase Kinase 3 Beta
HIF-1	Hypoxia-inducible factor 1
HRECs	Human retinal endothelial cells
HUVEC	Human umbilical vein endothelial cells
ICAM-1	Intercellular Adhesion Molecule 1
IFN-γ	Interferon-gamma
IL-10	Interleukin 10
IL-6	Interleukin 6
IL-8	Interleukin 8
IRAK1	Interleukin 1 Receptor Associated Kinase 1
IRS-1	Insulin receptor substrate 1
JAK/STAT3	Janus kinase/signal transducers and activators of transcription 3
lncRNA	Long non-coding Ribonucleic acid
LPS	Lipopolysaccharide
MCP-1	Monocyte chemoattractant protein 1
MCP2	Monocyte chemoattractant protein 2
MENA	Middle East and North Africa
MGC	Müller glial cell
miRNA	micro Ribonucleic acid
mRNA	Messenger Ribonucleic acid
mtDNA	Mitochondrial Deoxyribonucleic acid
ncRNA	Non-coding Ribonucleic acid
NF-κB	Nuclear Factor kappa-light-chain-enhancer of activated B cells
NPDR	Non-proliferative diabetic retinopathy
PAK4	p21-activated kinase 4

PDCD4	Programmed Cell Death 4
PDR	Proliferative diabetic retinopathy
PI3K	Phosphoinositide-3-kinase
PKB/Akt	Protein kinase B
PKC	Protein kinase C
PNPT1	Polyribonucleotide Nucleotidyl transferase 1
Poly II	Polymerase II
PPAR-α	Peroxisome proliferator-activated receptor-- α
Pre-miRNA	Precursor micro ribonucleic acid
Pri-miRNA	Primary micro ribonucleic acid
PTEN	Phosphatase and tensin homolog
RAX	Retina and Anterior Neural Fold Homeobox
RISC	RNA Induced Silencing Complex
RNA	Ribonucleic acid
ROP	Retinopathy of Prematurity
ROS	Reactive oxygen species
RPE	Retinal Pigment Epithelium
RT-PCR	Reverse transcription-polymerase chain reaction
SCF	Stem cell factor
Sema6A	Semaphorin 6A
SPRED1	Suppressing sprouty related protein 1
STZ	Streptozotocin
TAB2	Transforming growth factor Activated Kinase 1 Binding Protein 2
TCR	T Cell Receptor
TFMA	Mitochondrial transcription factor A

TGF-β	Transforming growth factor-beta
TLR	Toll-like receptor
TNF-α	Tumor necrosis factor-- α
TRAF6	TNF Receptor Associated Factor 6
TRBP	Transactivation response element ribonucleic acid-binding protein
VCAM-1	Vascular cell adhesion molecule 1
VEGF	Vascular endothelial growth factor

CHAPTER 1: INTRODUCTION

Diabetes is a chronic disease characterized by hyperglycemia, and as of the year 2019, about 463 million people worldwide have either type 1 or type 2 diabetes, and the numbers are expected to reach 700 million by the year 2045 (IDF, 2019). The constant status of hyperglycemia in diabetes leads to many complications categorized as macrovascular such as coronary artery disease or microvascular complications like nephropathy and retinopathy.

Diabetic retinopathy (DR) is a serious microvascular complication of diabetes, and it is the main cause of visual disability and blindness among the working-age population (20–65 years) (Qiaoyun Gong, Xie, Liu, Li, & Su, 2017). It is estimated that the probability of a person with type 1 diabetes developing DR is 75%, while a type 2 diabetes person has a chance of 50% to suffer from DR (Cohen & Gardner, 2016). A study reported that DR is responsible for 4.8% of the total blindness cases worldwide (Al-Kharashi, 2018). In addition, DR is called the silent cause of blindness (Srivastava et al., 2019) because no symptoms are observed in the early stages, and visual impairment begins when DR has already progressed (Al-Kharashi, 2018), which is characterized by vascular abnormalities in the retina (W. Wang & Lo, 2018). In the later stage of DR, the severe retinal ischemia condition due to blockage of blood vessels leads to the secretion of vascular endothelial growth factor (VEGF), stimulating the formation of new blood vessels in a process known as neovascularization (angiogenesis) (Tarr, Kaul, Chopra, Kohner, & Chibber, 2013). The pathogenesis of DR is complicated, and the exact process is incompletely understood and remains controversial due to the involvement of multiple factors (Q. Gong & Su, 2017).

The primary factor of DR is the consistent state of hyperglycemia, followed by numerous secondary mechanisms and pathways that contribute to disease development

and progression (W. Wang & Lo, 2018). Oxidative stress and inflammation have been widely reported to be of the main factors involved in developing DR. Emerging studies reported numerous protein-coding and non-coding genes related to hyperglycemia to have a role in DR development and progression. Among the non-coding RNAs (ncRNAs), miRNAs (miRNAs) function and involvement in DR pathology have been widely studied. MiRNAs are biomarkers and molecules with regulatory roles in several biological processes (Condorelli, Latronico, & Cavarretta, 2014). Interestingly, miRNAs are reported to regulate pro-inflammatory pathways (E.-A. Ye & Steinle, 2017b), expression of VEGF, and endothelial cells' response to VEGF (Suárez & Sessa, 2009) and therefore can regulate DR.

One of the largely studied anti-inflammatory miRNAs is miR-146a-5p, which is reported to downregulate activation of NF-κB by targeting its signaling molecules IRAK1, TRAF6, and MyD88 (Ma, Becker Buscaglia, Barker, & Li, 2011; L. Zhang, Dong, Tang, Li, & Zhang, 2020) and reduce expression of adhesion molecule ICAM-1 on epithelial cells (P. Zhuang, Muraleedharan, & Xu, 2017). Many studies demonstrated downregulation in miR-146a-5p expression in hyperglycemic conditions; therefore, the downregulation of miR-146a-5p plays a potential role in the pathogenesis of DR by enhancing inflammation in the vascular system of the retina. Adiponectin is another factor that is reported to be decreased in hyperglycemia and to have a potential role in DR. In a study by Al-Sadeq, 2018, results showed that exposing of HRECs to adiponectin in hyperglycemic condition increases miR-146a-5p expression (Al-Sadeq, 2018). Hence, we predicted that miR-146a-5p might prevent inflammation in HRECs by mimicking adiponectin action and increase the PPAR-α expression, which is involved in the genesis of DR.

Currently, there are several therapeutic options for DR, such as eye surgery, laser photocoagulation, anti-VEGF injections, steroids, and PPAR-α agonist (Duh, Sun, & Stitt, 2017; Mohamed, Gillies, & Wong, 2007). However, the failure of a successful response to these available treatments is common among DR patients (Stewart, 2016). Therefore, researchers focus on studying miRNAs association with DR through gene regulation to develop novel and effective molecular therapeutic strategies for the disease development, progress, and maintenance.

In this study, we aimed to extend the previous work to explore the impact of hsa-miR-146a-5p on diabetic milieu and to highlight the impact of using miR-146a-5p to mimic adiponectin actions, especially in diabetic subjects who are characterized by low adiponectin levels. We exposed HRECs to 25mM glucose for 96 hours and then transfected the cells with miR-146a-5p mimic and inhibitory using low dose (10 nM) and high dose (50nM) to examine the effect on 1) inflammatory cytokine and adhesion factors including PPAR-α, TNF-α, ICAM-1 and TRAF-6 2) ROS production and 3) cell viability and apoptosis rate. Our data revealed the anti-inflammatory role of miR-146a-5p in DR and hypothetically in other vascular complications of diabetes by decreasing TNF-α, ICAM-1, and TRAF6 expression. In addition, our data showed no significant effect of miR-146a-5p mimic on the expression of PPAR-α. Therefore, our hypothesis that miR-146a-5p may regulate inflammation mainly through the PPAR-α pathway needs further investigation. Finally, our study's findings show that determining the effective dose of miR-146a-5p is essential since it was demonstrated that using a low dose could result in adverse effects. Hence, bioinformatic analysis using inflammation and angiogenesis profiles was performed, in addition to the assessment of oxidative stress genes to explore the possible pathways and the mechanistic regulation of hsa-miR-146a-5p in HRECs exposed to the hyperglycemic condition.

CHAPTER 2: LITERATURE REVIEW

Diabetic retinopathy (DR)

DR has resulted from abnormal retinal blood vessels (Duh et al., 2017), and it is classified into an early non-proliferative diabetic retinopathy (NPDR) and an advanced proliferative diabetic retinopathy (PDR) (Solomon et al., 2017). NPDR is further classified into three stages mild, moderate, and severe (Martinez & Peplow, 2019). During NPDR, the tiny blood vessels of the retina swell, leading to the appearance of microaneurysms. Consequently, the blood capillaries rupture, and the vascular permeability increase due to the break of the tight junctions between the capillaries leading to hemorrhage and accumulation of fluid in the retinal vasculature (Zaki et al., 2016). This is followed by swelling and blockage of the vessels that nourish the retina (Martinez & Peplow, 2019). As the disease progress, in PDR, the severe retinal ischemia due to blockage of blood vessels leads to the secretion of growth factor VEGF stimulating the formation of new blood vessels, in PDR, the severe retinal ischemia due to blockage of blood vessels leads to the secretion of growth factor VEGF, stimulating new blood vessels formation in a process known as neovascularization (angiogenesis) (W. Wang & Lo, 2018). The newly formed abnormal fragile blood vessels can bleed into the vitreous, causing vitreous hemorrhage-, and tissue contract can cause tractional retinal detachment or distortion, both together lead to severe vision impairment (Kollias & Ulbig, 2010; Weinreb, Aung, & Medeiros, 2014). The reason that can complicate the condition and lead to complete vision loss in DR patients is diabetic macular edema (DME), which can occur at any stage of the disease (Cohen & Gardner, 2016; W. Wang & Lo, 2018). DME is the swelling of the macula due to the accumulation of fluid as a result of increased retinal vascular permeability (Musat et al., 2015).

Epidemiology and risk factors

The number of people suffering from DR worldwide was estimated to be 93 million, according to a pooled meta-analysis study performed in 2012 (Yau et al., 2012). Moreover, another meta-analysis published in 2016 reported that as of 2010, 3.7 million people globally had a visual impairment or were blind because of DR, a data that reflected 64% and 27% increase in each group respectively compared to 1990 (Leasher et al., 2016). Furthermore, by the year 2045, 10% of the world adult population are predicted to develop DR as a complication of diabetes which is estimated to affect 700 million people leading to disastrous social and economic consequences (IDF, 2019). A recent review article published in 2019 which studied the global prevalence of DR based on studies performed between 2015 and 2018 showed that on average, 27% of all diabetes patients had a form of DR, with NPDR being the most common, accounting for 25% (Thomas, Halim, Gurudas, Sivaprasad, & Owens, 2019).

The factors that increase the risk of developing DR are several, including but not limited to ethnic background, duration of diabetes, uncontrolled diabetes, and hypertension. A recent review article indicated that the highest DR prevalence was in the Western Pacific (36%), followed by Africa and the Middle East and North Africa (MENA) region each had (33.8%), then Europe with (20.6%) while South East Asia had the lowest rate of DR with (12.5%) only (Thomas et al., 2019). Similarly, A previous meta-analysis study showed that Caucasians had a much higher rate of DR (46.7%) in comparison to Asians, where the prevalence was (20.8%) (Yau et al., 2012). The variability in DR prevalence between the different ethnic populations can be due to possible genetic susceptibility and socioeconomic differences, including lifestyle, nutrition, and the available medical care. Additionally, the 2019 review showed that in Europe, the DR occurrence was higher in type 1 diabetic patients, particularly in those

over age 30 years, while in Africa, it was much higher in those with type 2 diabetes. Likewise, in two other studies, the prevalence of DR was higher in type 1 diabetes patients than in type 2 diabetes (Konstantinidis et al., 2017; Nentwich & Ulbig, 2015). In contrast, another study found that the DR rate was higher in patients with type 2 diabetes (Magliah, Bardisi, Al Attah, & Khorsheed, 2018). The conflict of the prevalence of DR suggests that the probability of getting DR is due to diabetes and glycemic control duration rather than its type. Several studies had shown a significant association between increased duration of diabetes and developing DR (Abougalambou & Abougalambou, 2015; Bansal, Gupta, & Kotecha, 2013; Magliah et al., 2018; Yau et al., 2012). Bansal et al., 2013 reported that having diabetes for more than 15 years increases the risk of DR, hence suggesting screening all the patients with diabetes of 10 years or more for DR regularly (Bansal et al., 2013). Moreover, many studies proved that poorer glycemic control and high HbA1c values increase the risk of developing DR, whereas proper diabetes control can decrease the DR possibilities (Magliah et al., 2018; Yau et al., 2012; Yun et al., 2016). Furthermore, like uncontrolled diabetes, high blood pressure is shown to increase the risk of developing DR (Magliah et al., 2018; Yau et al., 2012). Besides, no significant link was found between DR and sex, serum lipids, and smoking (Magliah et al., 2018).

Current DR treatment strategies

The current treatment options of DR include laser photocoagulation, surgical interventions (vitrectomy), anti-VEGF drugs, steroids, and peroxisome proliferator-activated receptor-α (PPAR-α) agonist. Both laser photocoagulation and vitrectomy are the earliest to be implemented to treat DR and are used mainly to treat only the disease's advanced stages (Sorrentino, Matteini, Bonifazzi, Sebastiani, & Parmeggiani, 2018). In laser photocoagulation, the laser is applied into the retina to destroy the newly formed

blood vessels and the ischemic tissue to prevent further angiogenesis (Evans, Michelessi, & Virgili, 2014). On the other hand, vitrectomy is used to remove vitreous hemorrhage, tractional retinal detachment parts, and DME (Heij et al., 2004; Mohamed et al., 2007). However, both procedures are only applied when the retina is already damaged and cannot be used as part of the DR preventative approach. In addition, laser photocoagulation and vitrectomy can have adverse consequences and may lead to color blindness, night blindness, tractional retinal detachment, and hemorrhage (Sorrentino et al., 2018).

Anti-VEGF agents and steroids are used to prevent the development of DR as they interfere with the pathogenies process of the disease. As mentioned earlier, the overexpression of VEGF stimulates the process of angiogenesis which is the hallmark of DR (W. Wang & Lo, 2018). Consequently, the newly formed blood vessels can leak and cause vitreous hemorrhage leading to vision impairment (Kollias & Ulbig, 2010; Weinreb, Aung, & Medeiros, 2014). However, the anti-VEGF treatment also has several challenges. The procedure of administrating the anti-VEGF drug in the eye is invasive and requires highly skilled personnel to apply it (Simó & Hernández, 2009). Moreover, anti-VEGF treatment is shown to be effective in 50% of patients only (Duh et al., 2017). In addition, the anti-VEGF levels should be maintained at the therapeutic level necessitating regular intravitreal injection, which can lead to adverse effects such as hemorrhage and tractional retinal detachment (Cornel et al., 2015). On the other hand, steroids are effective in treating DME. Corticosteroids downregulate ant-inflammatory mediators and VEGF levels; hence, they improve: 1) blood-retinal barrier (BRB), 2) tight junctions between the capillary epithelial cells, and 3) retinal oxygen level (Zur, Iglicki, & Loewenstein, 2019). However, the negative impact of using steroids is the increased intraocular pressure and cataracts (Barot, Gokulgandhi, Patel,

& Mitra, 2013).

PPAR-α activators are also a potential treatment used to prevent DR. PPAR-α agonists such as fenofibrate are reported to increase the expression of apolipoprotein A1 (apo-A1) (Simó & Hernández, 2009). It is suggested that Apo-A1 is the major transporter of lipids in the retina; therefore, it inhibits lipid accumulations and thus lipotoxicity (Simó & Hernández, 2009). Moreover, PPAR-α inhibits the process of angiogenesis by downregulating VEGF receptor 2 expression (Meissner et al., 2004). Furthermore, PPAR-α is reported to enhance antioxidant enzyme production and prevent adhesion molecules' expression on epithelial cells, inhibiting leukostasis and inflammation (Bordet et al., 2006; Israelian-Konaraki & Reaven, 2005).

Pathophysiology

Several mechanisms and biological processes are involved in DR pathogenesis, including oxidative stress, inflammation, and neuroglial alterations. (Roy, Kern, Song, & Stuebe, 2017)

- ***Oxidative stress and reactive oxygen species***

The role of oxidative stress in diabetic complications of the retinal cells has been extensively studied, and significantly increased levels of intracellular reactive oxygen species (ROS) have been detected in the retina in studies on diabetes patients and diabetic animal models (Whitehead, Wickremasinghe, Osborne, Van Wijngaarden, & Martin, 2018). Oxidative stress is induced by several biochemical and molecular pathways such as polyol, protein kinase C (PKC), hexosamine, and accumulation of advanced glycation end products (AGEs), which causes mitochondrial overproduction of ROS (Calderon, Juarez, Hernandez, Punzo, & De la Cruz, 2017). The overload of ROS downregulates endogenous antioxidative mechanisms causing oxidizing of biomolecules like DNA and proteins, leading to oxidative stress, which in consequence,

causes apoptosis of retina cells (Birben, Sahiner, Sackesen, Erzurum, & Kalayci, 2012). ROS can directly damage endothelial cells, leading to pro-inflammatory and pro-constrictive effects (Cristina, Adina, Simona Georgiana, Valerica, & Maria, 2013). In addition, as will be discussed in the following section, ROS also has a role in inflammation by activating the nuclear factor kappa B (NF-κB) pathway (Jixiang Zhang et al., 2016). In normoglycemic conditions, the mitochondrial transcription factor A (TFMA) increases the transcription of mitochondrial DNA (mtDNA); however, in diabetes, due to hyperglycemia, mitochondrial function is impaired, and TFMA is ubiquitylated (Calderon et al., 2017). Consequently, a protein encoded by mtDNA is decreased (Santos, Tewari, & Kowluru, 2012), and ROS production is increased, and the apoptosis mechanism is activated (Madsen-Bouterse, Mohammad, & Kowluru, 2010).

- ***Inflammation***

Inflammation is well studied to be the etiology of many vascular complications of diabetes (Negi, Kumar, Joshi, P K, & Sharma, 2011). Inflammation is the immune system response that includes various mediators against invading pathogens (L. Chen et al., 2017). These pathogens are recognized by several recognition receptors such as Toll-like receptors (TLRs) and AGEs receptors (Sun et al., 2014). When TLRs are activated due to stress conditions such as oxidative stress, they activate the production of NF-κB, which is a transcription factor. NF-κB increases the transcription of pro-inflammatory cytokines and chemokines, which recruit and activate leukocytes and therefore initiate inflammation (Anne Rübsam, Sonia Parikh, & Patrice E. Fort, 2018). Several studies on DR animal models and human patients identified inflammation characteristics such as leukostasis, increased cytokines production, increased blood flow, vascular hyperpermeability, and edema in the very early stages. One study

identified retinal Müller glial cells (MGCs) as the main source of inflammatory cytokines and chemokines, which were activated in diabetic patients without clinical signs of DR (Vujosevic et al., 2015). MGCs are thought to be responsible for the onset of inflammation in DR. The role of MGCs is supported by the increased levels of Intercellular Adhesion Molecule 1 (ICAM-1), an adhesion molecule located on endothelial cells, monocyte chemoattractant protein 2 (MCP2), vascular cell adhesion molecule 1 (VCAM-1), selectins (E-selectin), all involved in leukostasis which is observed in the early stage of DR (Khalfaoui, Lizard, & Ouertani-Meddeb, 2008; Noda, Nakao, Ishida, & Ishibashi, 2012; Vujosevic et al., 2016). Another study performed on rats injected with streptozotocin showed increased leukostasis, and interestingly, BRB breakdown started after only two weeks of hyperglycemia, indicating the vascular hyperpermeability (Rungger-Brändle, Dosso, & Leuenberger, 2000).

As the disease progress, the elevated systemic expression of pro-inflammatory cytokines enhances the angiogenesis process by targeting the endothelial cells (Aplin, Gelati, Fogel, Carnevale, & Nicosia, 2006). In a study where human retinal pigment epithelial cells and human Müller cells were exposed to hyperglycemic conditions, it was demonstrated that endothelial cell injury in diabetes is mostly because of the released pro-inflammatory cytokines rather than the elevated glucose (Busik, Mohr, & Grant, 2008). In addition, another study reported that the increased release of pro-inflammatory cytokines leads to the release of adhesion molecules such as ICAM-1, which, as mentioned above, causes leukostasis (W. Chen, Esselman, Jump, & Busik, 2005). As the inflammation progresses, the extravasation leads to the loss of capillary pericytes and, consequently, the tight junctions between the endothelial cell break and the fluid leaks (A. Rübsam, S. Parikh, & P. E. Fort, 2018). Furthermore, the ischemic condition in the retina stimulates the endothelial cells and MGCs to upregulate the

production of VEGF, ICAM-1, Monocyte chemoattractant protein-1 (MCP-1), and tumor necrosis factor-- α (TNF-α) through hypoxia-inducible factor 1 (HIF-1), which is a transcription factor (dell'Omo et al., 2013; Tang & Kern, 2011).

It is important to highlight the main features of VEGF due to its role in inflammation. There are four isoforms of VEGF, which are 121, 165, 189, and 206 (Park, Keller, & Ferrara, 1993), and only VEGF-165 has been reported to be involved in the development of DR (Adamis et al., 1993). VEGF binds to the endothelial cells, leading to the activation of membrane tyrosine kinase receptors VEGFR1 (FLT1) and VEGF-R2 (FLK1) (Shibuya, 2011). This binding, in turn, activates calcium influx channels and MAPK signaling pathways (Shibuya, 2011), leading to neovascularization, BRB breakdown, and increases vascular permeability and leukostasis, which are the hallmark of DR (Al-Kharashi, 2018). The increased VEGF production, MCP-1, and TNF-α increase vascular permeability, which is the case in NPDR and DME (Yoshida, Yoshida, & Ishibashi, 2004). In addition, these inflammatory cytokines and growth factors enhance neovascularization (angiogenesis), which is seen in PDR; thus, inhibiting inflammation, which can interrupt neovascularization (Yoshida et al., 2004). In a study on the murine model in which ICAM-1 and its cognate receptor CD18 were deleted, deceased neovascularization was observed (Sakurai et al., 2003).

- ***Adipokines***

Adipokines are hormones and cytokines that are secreted by white adipose tissues (Mancuso, 2016). Adipokines include several members performing pro-inflammatory or anti-inflammatory functions such as TNF-α, Interleukin 6 (IL-6), leptin, adiponectin (APN), and Visfatin (Zorena, Jachimowicz-Duda, Ślęzak, Robakowska, & Mrugacz, 2020). APN binds to the membrane protein AdipoR1 and

AdipoR2, an interaction that increases the activity of PPARα through AMP-activated protein kinase (AMPK) phosphorylation (Kim & Park, 2019). The upregulation of PPARα, a ligand-activated transcription factor, leads to an increase in fatty acid oxidation (Kim & Park, 2019). Moreover, decreased circulating adiponectin levels have been associated with insulin resistance in obese diabetes animal models and patients (Kwon & Pessin, 2013).

Adipokines are modulators for several vascular diseases and are suggested to be involved in DR pathogenesis (Yilmaz et al., 2004). For instance, TNF-α is a well-studied pro-inflammatory, and it is involved in inflammation and angiogenesis processes. TNFα stimulates the production and transcription of cytokines and vascular adhesion molecules, induces BRB breakdown, and is a chemotactic factor for neutrophils and monocytes (Zorena et al., 2020). A study on the Asian population consisted of 327 diabetic controls without DR, and 158 diabetic patients with DR showed that the levels of leptin and adiponectin levels were much higher in DR patients (Tan et al., 2014). In another study, significantly higher visfatin levels were detected in diabetes patients with PDR than without DR or with NPDR (Y. Wang, Yuan, & Jiang, 2014). Furthermore, another study results revealed elevated mRNA and protein expression of IL-6 in type 2 diabetes patients with PDR (Lu et al., 2017).

microRNAs

Overview of miRNA: Function and biogenesis

miRNAs were first identified in 1993, and its account, along with the other ncRNAs, long non-coding RNAs (lncRNAs), and circular RNAs (circRNAs), more than 98.5% of the total human genome (C.-H. Liu, Huang, Britton, & Chen, 2020). ncRNAs were considered as junk RNAs till recently; they were identified to have a role in plentiful various physiological and pathological processes in the human body,

making them attractive research interest to understand diseases (Palazzo & Lee, 2015). miRNAs are very conserved ncRNAs with a small size of around 22 nucleotide bases in length (He & Hannon, 2004). The main function of miRNAs is to regulate approximately 60% of the protein-coding gene expression at the post-transcriptional level, and therefore it is involved in the different several cellular processes such as proliferation, differentiation, and apoptosis (Friedman, Farh, Burge, & Bartel, 2009; Osada & Takahashi, 2007). This is done through the complementary binding of miRNAs to the 3′-untranslated region (3'UTR) sequence of the messenger RNAs (mRNAs) that translate genetic information into proteins and thus terminating its translation or degrading it (Krol, Loedige, & Filipowicz, 2010).

Over the last few years, studies revealed the clinical importance of understanding the involvement of thousands of miRNAs in several diseases. Interestingly, dysregulation of specific miRNAs in diseases such as cardiovascular diseases and various types of cancers has been identified. To name a few, miR-9 and miR-21 are downregulated in breast cancer (Singh & Mo, 2013), while miR-1, miR-145, and miR-499 are decreased in coronary heart disease (Cavarretta & Frati, 2016). Additionally, some inherited diseases have been linked to the genetic difference of the miRNAs. For example, mutations in miR-17~92 cluster are associated with the growth detects (de Pontual et al., 2011). Furthermore, due to their involvement in multiple biological processes, miRNAs are considered as clinical biomarkers and therapeutic targets for many diseases (Kreth, Hübner, & Hinske, 2018).

miRNAs biogenesis is initiated in the nucleus of the cells. First, RNA polymerase II (Poly II) transcribes miRNA to generate primary miRNA (pri-miRNA), forming one or more hairpin loop structures. After that, the Drosha enzyme (RNaseIII endonuclease) and its cofactor DiGeorge syndrome critical region 8 (DGCR8) digest

the pri-miRNA into shorter precursor miRNA (pre-miRNA), which exportin-5 exports to the cytoplasm. Next, the Dicer enzyme (RNaseIII endonuclease) and transactivation response element RNA-binding protein (TRBP) will subsequently cleave the pre-miRNA and remove its terminal loop, yielding a double-strand molecule called miR: miR*duplex. Then, the argonaute (AGO) protein interacts with the Dicer enzyme, unwinding the double-strand miRNA to a passenger strand, which is degraded, and a mature guide strand. Finally, AGO protein interacts with the mature strand and form RNA Induced Silencing Complex (RISC) which binds to the targets through binding to the complementary sequence of the 3'UTR region of mRNA as mentioned earlier and negatively regulate gene expression (Catalanotto, Cogoni, & Zardo, 2016).

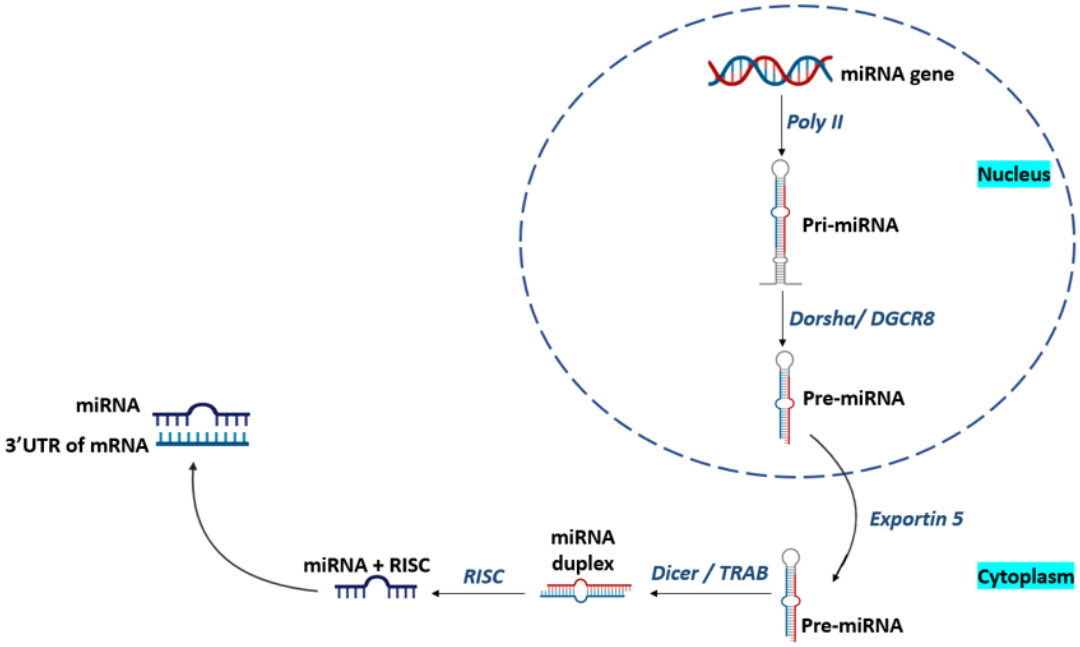

Figure 1: Biogenesis of miRNA

miRNA and DR

During the last decade, studies focused on studying changes in miRNAs expression in neovascular eye diseases as an approach to use these miRNAs as

biomarkers and therapeutic targets. For instance, a study on serum from a patient with Age-Related Macular Degeneration (AMD) showed upregulation in the expression of miR-146a-5P, miR-126, miR-34a, miR-27a, miR-23a, and miR-9 levels, while it revealed a decrease in the expression of miR-155 (Romano et al., 2017). Moreover, in a study on premature infants diagnosed with stage 3 Retinopathy of Prematurity (ROP), results revealed the upregulation of miR-23a and miR-200b-3p; in contrast, miR-27b-3p and miR-214-3p were downregulated (Metin et al., 2018). Concerning the role of miRNAs in DR, several studies investigated miRNAs' roles in DR in animals, human retinal endothelial cells (HRECs), and Retinal Pigment Epithelium (RPE) models and humans. These studies revealed changes in the expression of many miRNAs in DR, as some were upregulated while others were downregulated (Mastropasqua et al., 2014). To understand the function of miRNAs in DR disease development and progression, it is important to highlight the role of miRNAs in the inflammation and angiogenesis process in general.

- ***Role of miRNAs in angiogenesis***

Angiogenesis refers to a regulated process of forming new vessels from pre-existing vessels through several stimulators and inhibits (Otrock, Mahfouz, Makarem, & Shamseddine, 2007). The function of angiogenesis is crucial to maintaining physiological homeostasis through the vascular system, which nourishes the tissues and organs and eliminates waste (C.-H. Liu et al., 2020). Defects in angiogenesis cause interruption in delivering adequate amounts of oxygen and nutrients to the tissues leading to improper metabolism (Maier, 2006). Consequently, the affected tissues suffer from structural instability and loss of their functions (Maier, 2006). This is observed in several diseases with vascular components such as cardiovascular diseases, vascular eye diseases, and cancers (Khurana, Simons, Martin John, & Zachary Ian,

2005; Usui et al., 2015; Zuazo-Gaztelu & Casanovas, 2018). miRNAs role in angiogenesis can be either targeting angiogenesis genes or responding to angiogenic factors (Caporali & Emanueli, 2011), and this was observed initially in the mouse embryos model. Mouse embryos with mutation resulting in an insufficient amount of Dicer and Drosha enzymes showed defective miRNA biosynthesis, dysregulation of angiogenic genes, and defective angiogenesis (Kuehbacher, Urbich, Zeiher Andreas, & Dimmeler, 2007; Otsuka et al., 2008; W. Yang et al., 2005). Additionally, these mouse embryos' endothelial cells showed a reduction in their angiogenic functions such as sprouting, proliferation, migration, and tubulogenesis (Kuehbacher et al., 2007). Numerous studies have reported high expression of several miRNAs in human vascular endothelium cells and called them angiomiRs due to their association with angiogenesis genes (Shusheng Wang & Olson, 2009). A study performed on Streptozotocin (STZ) induced diabetic rats discovered that VEGF secretion is controlled by miR-200b (McArthur, Feng, Wu, Chen, & Chakrabarti, 2011). Another study on the mice model showed that miR-126 enhances the VEGF secretion by suppressing sprouty-related protein-1 (SPRED1), which downregulates the VEGF in Ras-MAP kinase pathway, hence promoting angiogenesis (Fish et al., 2008). In addition, miR-210 overexpression during hypoxic conditions has an important role in cell survival by enhancing angiogenesis. One study on human umbilical vein endothelial cells (HUVEC) revealed that miR-210 enhances endothelial cell migration and tubulogenesis by targeting tyrosine kinase receptor Ephrin A3 (Fasanaro et al., 2008). Moreover, miR-23 and miR-27 of miR-23-27-24 cluster are reported to function as angiogenesis enhancers by targeting antiangiogenic proteins Semaphorin 6A (Sema6A) and Sprouty2, which inhibits RAF (Zhou et al., 2011), while miR-24 is suggested to suppress cardiac angiogenesis, targeting GATA Binding Protein 2 (GATA2), the p21-activated kinase-

4 (PAK4) (Fiedler et al., 2011). Like miR-24, miR-221/222 has also been recognized as angiogenesis inhibit. It functions by blocking c-Kit, a tyrosine kinase receptor of the proangiogenic stem cell factor (SCF), thus inhibiting endothelial cell migration and tubulogenesis (Song et al., 2017). Likewise, miR-15a and miR-410 are found to downregulate VEGF expression in the retinal cells (N. Chen et al., 2014; Q. Wang et al., 2016). miR-140 inhibits AGTR1, enhancing the expression of VEGF (Guo, Gu, Zhang, Wang, & Gu, 2015). Furthermore, miR-155 is found to downregulate retinal neovascularization through regulating the phosphoinositide-3-kinase–protein kinase B/Akt (PI3K-PKB/Akt) pathway (Z. Zhuang et al., 2015). Conflict findings were reported regarding the role of miR-146 role in angiogenesis. Su et al. conducted a study in which they assessed the effect of miR-146 on endothelial progenitor cells in response to acute ischemic stroke using a mice model. Their finding revealed that miR-146a/b enhanced angiogenesis by targeting TRAF6 and IRAK1 genes (Su et al., 2017). The pro-angiogenic role was also supported by a study that evaluated the impact of miR-146a on angiogenesis in hepatocellular carcinoma. Zhu et al. found that miR-146a inhibits the expression of BRCA1, leading to an increase in platelet-derived growth factor receptor α (PDGFRA), which is associated with microvascular invasion (Zhu et al., 2013). On the other hand, Knoepp et al. found miR-146a to be anti-angiogenic in ischemic myocardium mice (Knoepp et al., 2020). They found that inhibition of miR-146a significantly enhanced the angiogenesis process. Likewise, in another study, miR-146a was also reported act as anti-angiogenic through downregulating extracellular matrix metalloproteinase inducer (EMMPRIN) which increases VEGF levels in many tumors (Amit-Cohen, Rahat, & Rahat, 2013). The effect of the different miRNAs on angiogenesis is summarized in Table 1 and Figure 2.

Table 1: Summary of effect of miRNAs on angiogenesis

Effect	miRNA	Target	Reference
Downregulated	miR-200b	VEGF	(McArthur et al., 2011)
Upregulated	miR-126	SPRED1	(Fish et al., 2008)
Upregulated	miR-210	Ephrin A3	(Fasanaro et al., 2008)
Upregulated	miR-23/ miR-27	Sema6A, Sprouty2,	(Zhou et al., 2011)
Downregulated	miR-24	GATA2, PAK4	(Fiedler et al., 2011)
Downregulated	miR-221/222	c-Kit	(Song et al., 2017)
Downregulated	miR-15a	VEGF	(N. Chen et al., 2014; Q. Wang et al., 2016)
Downregulated	miR-410	AGTR1	(N. Chen et al., 2014; Q. Wang et al., 2016), (Guo et al., 2015)
Downregulated	miR-155	PI3K-PKB/Akt	(Z. Zhuang et al., 2015)

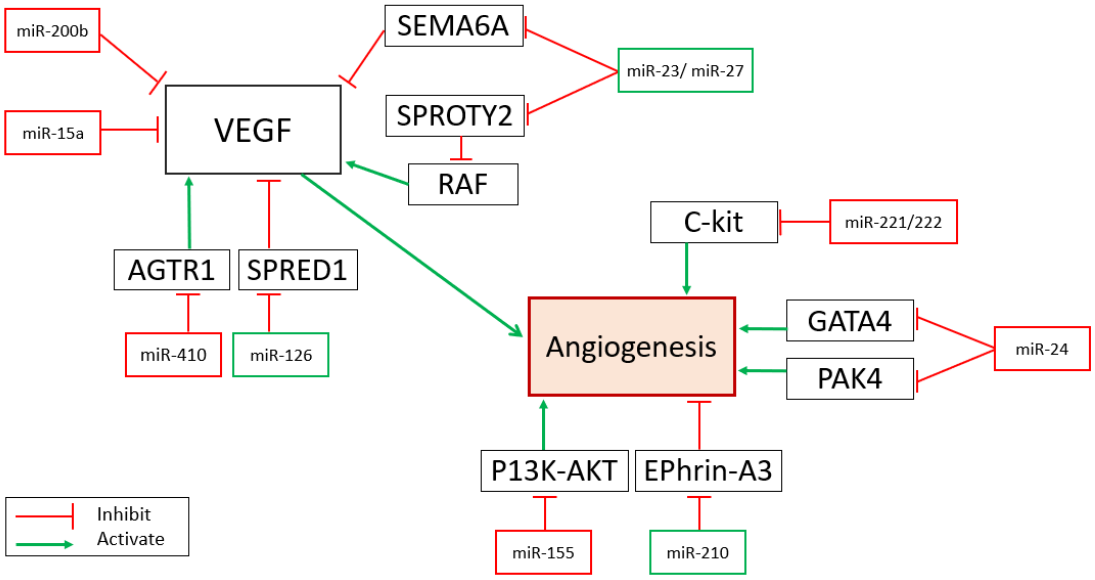

Figure 2: Effect of the different miRNAs on angiogenesis process

- ***Role of miRNAs in inflammation***

NF-κB is a transcription factor, and as described earlier, it is activated by TLRs and induces the production of pro-inflammatory cytokines and chemokines. Apart from this, NF-κB activations enhance the transcription of several miRNAs, which are released as a feedback response to inflammation (K. Taganov, Boldin, & Baltimore, 2007). Moreover, adenosine deaminase 1 (ADAR1) and Polyribonucleotide Nucleotidyl transferase 1 (PNPT1), which are enzymes involved in RNA metabolism, are also reported to influence the production of miRNA (O'Connell, Rao, Chaudhuri, & Baltimore, 2010). The feedback function of miRNAs in inflammatory conditions is a host protection response. miRNAs prevent the inflammation from becoming chronic, hence prevent host damage (Nejad, Stunden, & Gantier, 2018). Some examples of miRNAs that are extensively studied in inflammation are miR-146a-5P, miR-155, and miR-21.

miR-146 has two types, miR-146a-5p located on chromosome 5 and miR-146b located on chromosome 10. Upregulation of miR-146a-5P/b expression is NF-κB

dependent, and it is promoted by direct binding of NF-κB to its promoter following lipopolysaccharide (LPS) stimulation (Ma et al., 2011; K. D. Taganov, Boldin, Chang, & Baltimore, 2006). Interestingly, both miR-146a-5p/b, in turn, targets TNF Receptor Associated Factor 6 (TRAF6) and Interleukin 1 Receptor Associated Kinase 1 (IRAK1), which are two major signaling molecules required for activation of NF-κB in the TLR/NF-κB pathway (Ma et al., 2011). Moreover, a study using human lung fibroblasts cells, in which LPS induced pulmonary injury, reported that miR-146b targets MyD88, a signaling mediator, inhibiting NF-κB activation (L. Zhang et al., 2020). Hence, miR-146a-5p/b functions as a negative feedback regulator of NF-κB. Besides that, a study showed that miR-146a-5p has an anti-apoptotic role through targeting Fas Associated Death Domain (FADD) (Curtale et al., 2010). The study results also revealed lower expression of miR-146a-5p in T naïve cells than T memory cells, suggesting a regulatory role of miR-146a-5p in T cell activation by targeting T Cell Receptor (TCR) (Curtale et al., 2010).

miR-155, similarly to miR-146, is also secreted as a feedback response to inflammation. However, miR-155 is reported to have both a pro-and anti-inflammatory effect (Nejad et al., 2018). There are two mature forms of miR-155: miR-155-3p, which is upregulated earlier once stimulated by the TLR/NF-κB pathway, and miR-155- 5p that is enhanced later (Mahesh & Biswas, 2019). In addition, a study on human dermal lymphatic endothelial cells showed that miR-155 is induced by TNF-α and Interferon-γ (IFN-γ) (Yee, Shah, Coles, Sharp, & Lagos, 2017). In contrast, the expression of miR-155 is suppressed by Interleukin-10 (IL-10) to maintain hemostasis (Y. Li & Shi, 2013). Interestingly, miR-155 suppresses the activation of TLRs and the NF-κB pathway by targeting several signaling molecules such as TGF-β Activated Kinase 1 Binding Protein 2 (TAB2) and MyD88 (Nejad et al., 2018). Moreover, miR-155 downregulates

TNF-α and Interleukin-8 (IL-8) – also known as C-X-C Motif Chemokine Ligand 8 (CXCL8) (Y. Li & Shi, 2013). Furthermore, miR-155 is reported to inhibit the Suppressor of cytokine signaling 1 (SOCS1), which is a negative regulator in the JAK/STAT3 pathway and enhances the promoted inflammatory response of macrophages (J. Ye et al., 2016).

miR-21 is expressed widely in many tissues, and it is enhanced by pro-inflammatory signals produced by various immune cells (Sheedy, 2015). miR-21 has been reported to protect the host against inflammation by downregulation of TNF-α through silencing phosphatase and tensin homolog (PTEN), Glycogen Synthase Kinase 3 Beta (GSK3b), and Programmed Cell Death 4 (PDCD4) (Das, Ganesh, Khanna, Sen, & Roy, 2014). In contrast, like miR-155, the expression of miR-21 is suppressed by Interleukin-10 (IL-10) (Das et al., 2014). Moreover, the upregulated expression of miR-21 has been detected in cancer and cardiovascular diseases (Kumarswamy, Volkmann, & Thum, 2011). Furthermore, a study on lung cancer cell lines showed that miR-21 could be used as a circulating biomarker and agonist for TLR (Fabbri et al., 2012).

- ***Role of miRNAs in DR pathogenesis***

miR-200b, as mentioned earlier, is inhibiting angiogenesis and endothelial cell migration by downregulating VEGF levels (McArthur et al., 2011). In DR, the suggested role of miR-200 in the disease pathogenesis is that the hyperglycemic condition in diabetes induces dysregulation of miR-200 level. Consequently, VEGF expression is increased and thus leads to angiogenesis and disease progression. This proposed role of miR-200 in DR pathogenesis is supported by the findings of several studies which reported a significant decrease in miR-200 expression in hyperglycemic conditions. McArthur et al., 2011 found that diabetic rat retina and epithelial cells exposed to high glucose showed decreased expression of miR-200, whereas the level

of VEGF was increased (McArthur et al., 2011). Similarly, in another study, the hyperglycemic environment's effect on HRECs showed a significant decrease in miR-200b expression (Qun Jiang, Zhao, Liu, Li, & Liu, 2015). Likewise, significantly downregulated expression of miR200b was detected in a study on 255 DR patients compared to the healthy controls (E.-H. Li, Huang, Li, Xiang, & Zhang, 2017). Moreover, a study on the plasma of type 2 diabetes patients, 91 without DR, 46 with NPDR, and 49 with PDR, showed lower miR-200b in PDR patients than those without DR (Dantas da Costa E Silva et al., 2019).

miR-29b proposed a role in DR pathogenesis based on its function in regulating cell apoptosis and angiogenesis. miR-29b downregulates Forkhead Box O4 (FOXO4) expression, which inhibits cell proliferation and enhances cell death, hence protecting MGCs from apoptosis and enhancing eye nerves regeneration (Fu & Tindall, 2008; J. Zhang et al., 2018). Additionally, like miR-200b, miR-29b also downregulates VEGF expression, thus inhibiting angiogenesis (J. Zhang et al., 2018). Therefore, a reduction in miR-29b expression due to high glucose levels can favor DR development. Dantas da Costa E Silva et al., 2019 reported elevated VEGF and decreased miR-29b expression in PDR patients compared to those with healthy retina (Dantas da Costa E Silva et al., 2019). Moreover, J. Zhang et al., 2018 found that when miR-29b was downregulated, diabetic rats showed increased expression of FOXO4 and MGCs impairment (J. Zhang et al., 2018). In contrast, another study on retinas of STZ induced diabetic rats reported upregulated miR-29b and suggested that it may indirectly regulate Retina And Anterior Neural Fold Homeobox (RAX) expression and thus preventing MGCs apoptosis (Silva et al., 2011).

miR-146a-5p is reported to have an anti-inflammatory effect through downregulating activation of NF-κB by targeting several of its signaling molecules,

including IRAK1, TRAF6, and MyD88 (Ma et al., 2011; L. Zhang et al., 2020). In addition, miR-146a-5P reduces the expression of adhesion molecule ICAM-1 on epithelial cells, hence inhibiting leukostasis (P. Zhuang et al., 2017). Therefore, the downregulation of miR-146a-5p plays a potential role in the pathogenesis of DR by enhancing inflammation in the vascular system of the retina. Supporting this proposed mechanism, several studies conducted on HRECs exposed to hyperglycemic conditions showed a steady decrease in the expression of miR-146a-5p (Qiaoyun Gong et al., 2017; Q. Wang et al., 2014). Q. Wang et al., 2014 found that with inhibiting miR-146a-5p, the expression of IRAK1 and ICAM-1 increased (Qiaoyun Gong et al., 2017; Q. Wang et al., 2014). In another interesting study, STZ induced Sprague-Dawley diabetic rats were injected with lentivirus after one week of diabetes. The results revealed that miR-146a-5P expressed by the lentivirus inhibited the upregulation of NF-κB and ICAM1 expression, hence, prevented the diabetes-induced retina microvascular defects (P. Zhuang et al., 2017). Further, miR-146a is also reported to have an anti-angiogenic role through inhabiting IL-6 signaling and consequently suppressing STAT3-VEGF pathway (E.-A. Ye & Steinle, 2017a). Figure 3 summarizes the role of miR-146a in DR through regulating inflammation and angiogenesis.

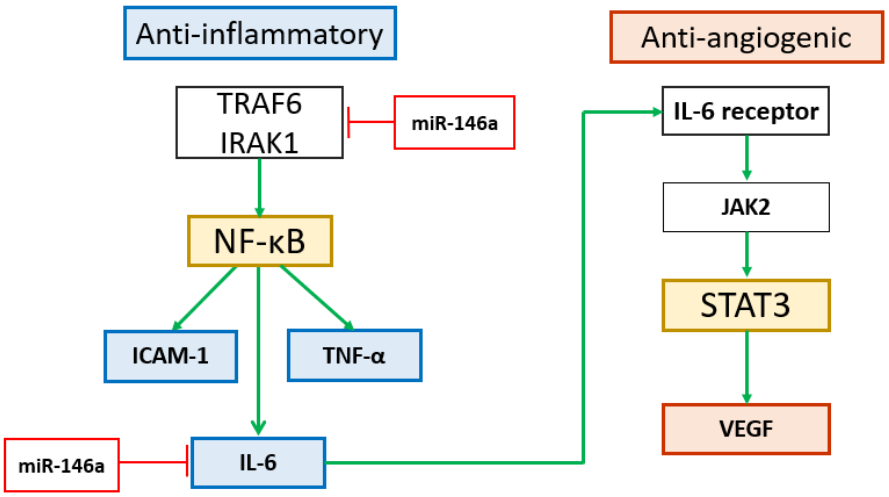

Figure 3 Role of miR-146a in DR.

miRNA-126 role is still under investigation, and different studies have reported contradictory roles in angiogenesis and cell invasion. Fang et al., 2017 showed that miR-126 inhibits angiogenesis by downregulating VEGF expression through targeting Insulin receptor substrate 1 (IRS-1) (Fang, Ma, Guo, & Lu, 2017). They found that mimic of miR-126 in epithelial cells downregulated IRS-1 level and consequently decreased the release of VEGF (Fang et al., 2017). In contrast, S. Wang et al. concluded from their study on miR-126 mutant mice that miR-126 induces angiogenesis by enhancing VEGF expression through inhibiting Spred-1, which is an angiogenic inhibit (S. Wang et al., 2008). Interestingly in DR, the miR-126 level of expression was found to be downregulated. A research study conducted on diabetes mellitus patients, 44 without DR, 42 with NPDR, and 39 PDR found that the expression level of miR-126 was downregulated significantly in patients with PDR compared to no DR and NPDR groups. (Qin, An, Liu, Xu, & Lu, 2017). Similarly, a study by Rezk et al., 2016 detected a significant reduction in miR-126 expression in type 2 diabetes DR (Rezk, Sabbah, & Saad, 2016). Overall, downregulation in miR-126 expression is suggested to impact DR

development; however, more studies are needed to understand its exact pathogenesis mechanism.

miR-150-5p inhibits angiogenesis, epithelial cell migration, and tubulogenesis through downregulating angiogenic genes such as C-X-C Motif Chemokine Receptor 4 (CXCR4) (C.-H. Liu et al., 2020; Mazzeo et al., 2018). Thus, the downregulated expression of miR-150-5p can enhance angiogenesis and lead to the development of DR. Mazzeo et al., 2018 study on samples from type 1 diabetes patients, 7 with DR and 7 without DR showed significantly reduced expression of miR-150-5p in patients with DR as compared to those without DR supporting its proposed role in DR pathogenesis (Mazzeo et al., 2018).

Besides the miRNAs mentioned above, the level of several other miRNAs was reported to be upregulated in DR. A study performed on type 2 diabetes patients, in which 20 without DR, 20 with NPDR, and 20 with PDR using RT-qPCR showed that the levels of miR-155 were greater in those with PDR followed by NPDR compared to those without DR. The obtained results suggested that miR-155 may be used as a biomarker to monitor the progression of the disease (T. T. Yang et al., 2015). Moreover, additional studies showed upregulation in the expression of miR-18b, miR19b, miR-211, and miR-320a in type 1 diabetes patients with DR, while expression of miR-21, miR-181c and miR-1179 was found to be higher in type 2 diabetes patients with DR (Qi Jiang, Lyu, Yuan, & Wang, 2017; Y. Liu et al., 2017; Qing et al., 2014; Zampetaki et al., 2016; Zou, Wang, Gang, Zhang, & Sun, 2017).

Among the above-mentioned miRNAs, miR-146a-5p is largely and well-identified to have an anti-inflammatory effect. Because miR-146a-5p was reported in a previous study by Al-Sadeq, 2018 to be upregulated by adiponectin treatment in HRECs

exposed to hyperglycemia (Al-Sadeq, 2018), the current project focused on studying miR-146a-5p.

CHAPTER 3: RESEARCH QUESTION AND HYPOTHESIS

DR is a complication of diabetes disease, and many different mechanisms cause it. In hyperglycemic conditions, both adiponectin and hsa-mir-146 5p are downregulated. A previous study showed that treating HERCS exposed to diabetic conditions with adiponectin increases miR-146a-5P expression (Al-Sadeq, 2018); this finding suggested that adiponectin actions are potentially mediated through miR-146a-5P. Both adiponectin and hsa-mir-146 5p target and regulate NF-κB, TNF-α, and ICAM-1 expression.

Therefore, in the current research study, we hypothesize that miR-146a-5p may ameliorate the inflammation in HRECs via the peroxisome proliferator-activated receptor-α signaling pathway (PPAR-α) and its target molecules, which is involved in the genesis of early changes in HRECs when exposed to hyperglycemic conditions mimicking the adiponectin effect.

Therefore, this study aims to extend the previous work to explore the impact of hsa-mir-146-5p on diabetic milieu and to highlight the impact of using miR-146a-5p to mimic adiponectin actions, especially in diabetic subjects who are characterized by low adiponectin levels.

To achieve the aim, the objectives of this study are to examine and assess the effect of hsa-miR-146a-5p in HRECs exposed to high glucose on:

- The total cellular ROS production and oxidative stress status
- Rate of apoptosis
- The expression of PPARα, inflammatory/apoptotic biomarker TNF-α, adhesion molecule biomarker ICAM1, and TRAF6 as target genes for hsa-miR-146a-5p

- Profiling of genes involved in inflammation and angiogenesis to determine the molecular pathways
- Gathering data of the current study will reveal the role of hsa-miR-146a-5p in DR in vitro and highlight its potential signaling pathway and mechanisms

CHAPTER 4: MATERIALS AND METHODS

Biosafety approval

The Qatar university institutional Bio-safety committee has approved the present study# QU-IBC-2020/077 (See Appendix).

Reagents and instruments:

Reagents and instruments used in the study for the different experiments and assays are listed in Table 2.

Table 2: List of reagents and instruments used in the study

Item	Company	Catalog number
Human Retinal Microvascular Endothelial Cells (HRMECs) passage	Cell System Corporation	**ACBRI 181**
Complete Classic Medium Kit with Serum	Cell System Corporation	**4Z0-500**
Culture Boost	Cell System Corporation	**4CB-500**
Complete Medium Formulated at Normal Blood Glucose Level with Serum and Culture Boost-R™	Cell System Corporation	**4N0-500-R**
Complete Serum-Free Medium Kit with RocketFuel	Cell System Corporation	**SF- 4Z0-500-R**
CSC Attachment Factor	Cell System Corporation	**4Z0-210**
CSC Cell Freezing Medium	Cell System Corporation	**4Z0- 705**
BAC-OFF® ANTIBIOTIC TONIC	Cell System Corporation	**4Z0-644**
Trypan Blue (powder)	Sigma-Aldrich	**T6146**

Item	Company	Catalog number
D-Glucose	Sigma-Aldrich	**G-7021**
D-Mannitol	Sigma-Aldrich	**M4125**
Phosphate Buffered Saline (PBS) Tablets	Gibco	**18912-014**
0.05% Trypsin-EDTA (1X)	Gibco	**25300-054**
Gibco™ Opti-MEM™ I Reduced Serum Medium	Gibco	**31985070**
mirVana hsa-miR-146a-5p ID:MC10722 miRNA mimic	Ambion	**4464066**
mirVana hsa-miRNA mimic Negative Control #1	Ambion	**4464058**
mirVana hsa-miR-146a-5p ID:MH10722 miRNA inhibit	Ambion	**4464084**
Anti-miR Negative Control #1	Ambion	**AM17010**
Lipofectamine RNAiMAX	Invitrogen	**LMRNA015**
HUMAN TNF-- A 50 UG BIOSOURCE	Invitrogen	**PHC3016**
QIAzol Lysis Reagent	Qiagen	**79306**
Chloroform	Sigma-Aldrich	**650498**
Ethanol	Sigma-Aldrich	**32221**
Qubit™ RNA IQ Assay Kit	Invitrogen	**Q33221**

Item	Company	Catalog number
Qubit™ Assay Tubes	Invitrogen	**Q32856**
High capacity RNA to cDNA kit	Applied Biosystems	**4387406**
TaqMan® Advanced miRNA Assays cDNA Synthesis Kit	Applied Biosystems	**A28007**
TaqMan® Fast Advanced Master Mix	Applied Biosystems	**A44360**
TaqMan® Gene Expression Assay (Hs00947536_ml) PPAR- α	Applied Biosystems	**4331182**
TaqMan® Gene Expression Assay (Hs00377558_ml) TRAF6	Applied Biosystems	**4331182**
TaqMan® Gene Expression Assay (Hs00174128_ml) TNF-α	Applied Biosystems	**4331182**
TaqMan® Gene Expression Assay (Hs00164932_ml) ICAM-1	Applied Biosystems	**4331182**
TaqMan® Gene Expression Assay (Hs99999903_ml) ACTB	Applied Biosystems	**4331182**
TaqMan® Advanced miRNA Assay (478399_mir) hsa-miR-146a-5P-5p	Applied Biosystems	**A25576**
TaqMan® Advanced miRNA Assay (478594_mir) hsa-miR-320a	Applied Biosystems	**A25576**
CellROX™ Orange Reagent	Invitrogen	**C10443**
Tali® Cellular Analysis Slides	Invitrogen	**T10794**
Muse™ Annexin V & Dead Cell Kit (MCH100105)	Millipore Corporation	**4700-1485**

Instrument	Company
Thermocycler (Gene Amp®, PCR System 9700)	**Applied Biosystem**
7500 Real-time PCR system	**Applied Biosystem**
Tali™ Image-Based Cytometer	**Invitrogen**
Qubit® 4.0 Fluorometer	**Invitrogen**
Nanodrop™ Lite Spectrophotometer	**Thermo Scientific**
EVOS XL Core Imaging System	**Invitrogen**
Muse™ Cell Analyzer	**Millipore Corporation**

Study design:

The different treatment and transfection groups and downstream experiments are illustrated in Figure 4.

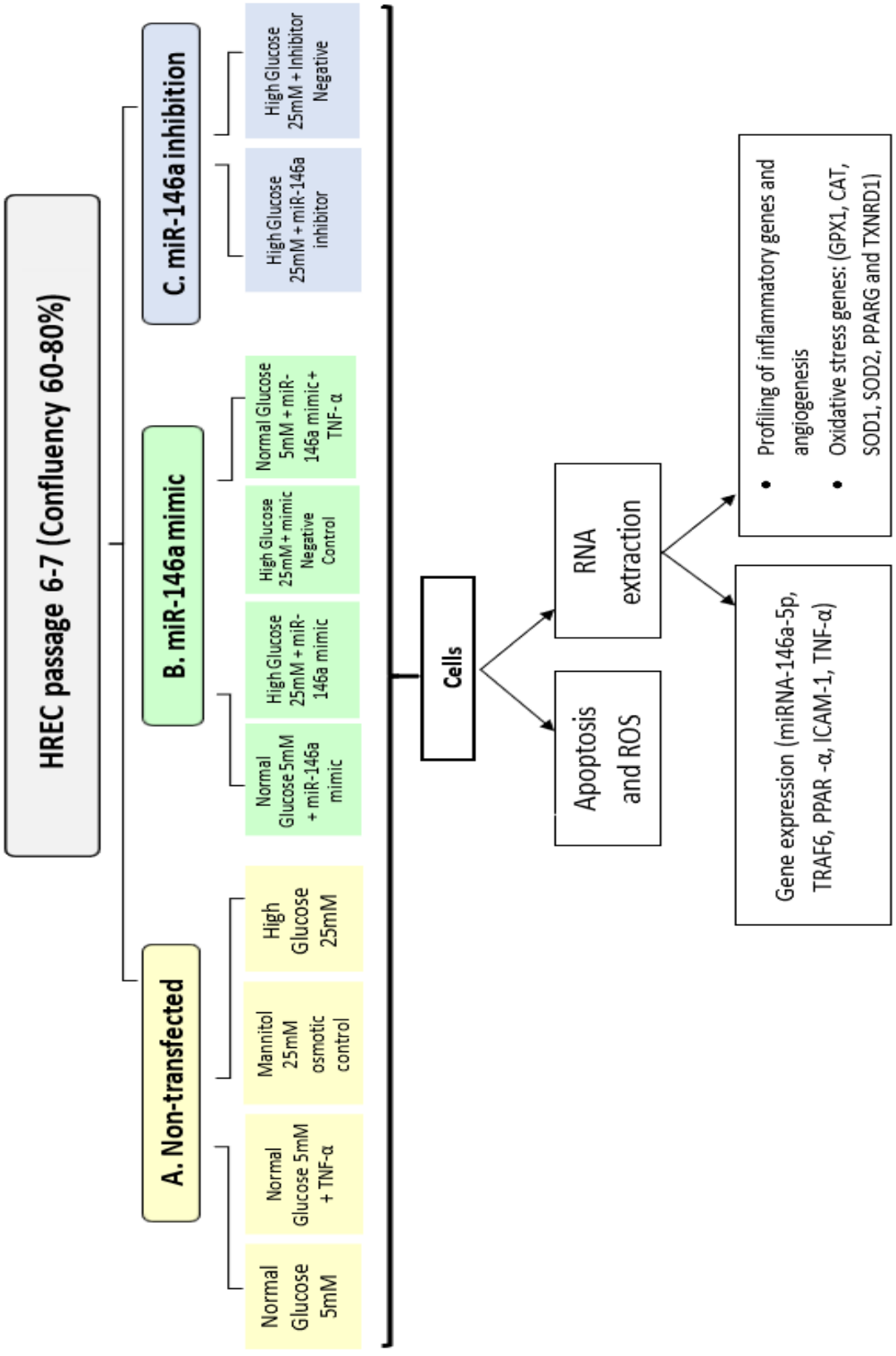

Figure 4: Study design and workflow

Methods:

Human Retinal Endothelial Cells (HRECs) culture and passage

First, a T75 flask was prepared using 5ml of attachment factor to cover the surface and then was removed and returned to the original bottle to reuse. In addition, 15ml of complete classic media (with culture boost and Bac-off) was warmed to 37°C. Then a vial with 1ml of cryopreserved passage 5 (P5) HRECs was warmed and thawed in hands, then immediately in ambient temperature, complete classic media was added. Thawed cells were added to the prepared flask, and then 15ml of warmed complete classic media was added. Flask was moved flask in (east-west, north-south) motion to ensure even spread of cells over flask surface and then the flask was incubated in 5% CO2 incubator at 37°C until 80% - 90% confluency. After 48 hours of growth, the complete classic media was changed. Upon confluency, cells were passaged to P6, which were then seeded and used in the study.

Before seeding, HRECs were counted using Trypan blue. In a well, 20µl of Trypan blue and 20µl of cell suspension were mixed, then 20µl of the mixture was loaded on a hemocytometer and was viewed under an inverted microscope. The cell number counted in two corner squares and the middle square were used in the following formula to retrieve the total cells number:

[Total number of cells counted / (No. of squares)] × 2(dilution factor) × 10,000

In this study, three P5 HRECs vials were used, which represented three different biological samples.

HRECs treatment

A total of 1 x 105 of P6 HRECs were seeded per well on 24 well plates according to the number of conditions and experiments for 96 hours for chronic treatment using three different treatment media: Normal Glucose (NG) using complete

media with 5 mM glucose (4N0-500-R), High Glucose (HG) where D-glucose powder was added to complete media with 5 mM glucose (4N0-500-R) to reach a final concentration of 25mM, and osmotic control Mannitol (M), where D-mannitol powder was added to complete media with 5 mM glucose (4N0-500-R) to reach a final concentration of 25mM. Then the plates were incubated in 5% CO2 incubator at 37°C.

HRECs transfection

In this study, we studied the effect of two concentrations of miR-146a-5p. For low dose study: miR-146a-5p transfection, miR-146a-5p mimic, miR-146a-5p inhibit, and the scramble sequences were used at a concentration of 10 nM, while for high dose study; miR-146a-5P-5p mimic and the scramble sequence were used at a concentration of 50 nM. The procedures in brief, after 48 hours of treatment with various glucose concentrations, and with ~80% confluency (cell count: 24 well plate = $0.5–2 \times 10^5$; 6 well plate= $0.25\text{-}1 \times 10^6$), the treatment media were replaced with serum-free media for 6 hours to serum starve the HRECs. Then, the serum-free media was removed, and cells were divided into three groups for transfection for 48 hours in 5% CO2 incubator at 37°C.

Group (A) non-transfected group: contained four control samples with treatment media as mentioned above:

1) NG,
2) NG+TNF-α
3) HG
4) M as osmotic control

Group (B) overexpression of miRNA-146a-5p: as a mimic group contained four samples/ treatment:

1) miR-146a-5p mimic in NG media

2) miR-146a-5p mimic in HG media

3) mimic negative control in HG media

4) miR-146a-5p mimic+ TNF-α

Group (C) knockout or silencing group of miRNA-146a-5p: as inhibitory group contained two samples/ treatment:

1) miR-146a-5p inhibitory in HG media, and

2) Scrambled inhibitory negative control both in HG media.

Upon completion of 48 hours incubation, TNF-α at 1ng/ml was added to the specific wells and incubated for additional 4 hours.

Table 3: Groups treatment and duration. L: Low dose (10 nM); H: High dose (50 nM)

Group	Treatment	Incubation duration
NG	Normal glucose (5 mM)	96 hours
NG + miR-146a-5p mimic (L)	Normal glucose (5 mM) + 10 nM miR-146a-5p mimic	96 hours treatment + 48 hours transfection
NG + TNF - α	Normal glucose (5 mM) + 1ng/ml TNF-α	96 hours treatment + 4 hours TNF - α treatment
NG + miR-146a-5p mimic + TNF-α (L)	Normal glucose (5 mM) + 10 nM miR-146a-5p mimic + 1ng/ml TNF-α	96 hours treatment + 48 hours transfection + 4 hours TNF - α treatment
HG	High glucose (25 mM)	96 hours
HG + miR-146a-5p mimic (L)	High glucose (25 mM) + 10 nM miR-146a-5p mimic	96 hours treatment + 48 hours transfection
HG + miR-146a-5p inhibit (L)	High glucose (25 mM) + 10 nM miR-146a-5p inhibit	96 hours treatment + 48 hours transfection
HG + scramble sequences (L)	High glucose (25 mM) + 10 nM scramble sequences	96 hours treatment + 48 hours transfection

Group	Treatment	Incubation duration
NG + miR-146a-5p mimic (H)	Normal glucose (5 mM) + 50 nM miR-146a-5p mimic	96 hours treatment + 48 hours transfection
HG + miR-146a-5p mimic (H)	High glucose (25 mM) + 50 nM miR-146a-5p mimic	96 hours treatment + 48 hours transfection
HG + scramble sequences (H)	High glucose (25 mM) + 50 nM scramble sequences	96 hours treatment + 48 hours transfection

- **miR-146a-5p inhibit:** A single oligonucleotides strand that binds to mature miR-146a-5p to knock it out.
- **miR-146a-5p mimic:** A double stand RNA that, when introduced to the cell, it increases the expression of miR-146a-5p and mimics its function.
- **Scramble sequence:** A stand with similar size of mimic and inhibit stands; however, it consists of a randomly arranged (ACGT) sequence.
- **Lipofectamine® RNAiMAX:** A lipid media formulation that is used to transfect siRNA and miRNA into the cell.

Cell growth parameters

- *Apoptosis and viability*

Trypsinized HRECs were washed using 1ml classic complete media, centrifuged at 500x g for 5 minutes, and the supernatant was discarded. The cell pellet was then resuspended in 100µl, to which 100µl of Annexin V & Dead Cell Kit (MCH100105) and then incubated for 20 minutes in the dark. Following that, tubes were analyzed on Muse™ Cell Analyzer using NG sample as the control.

- *ROS* production

Trypsinized HRECs were washed using 1ml classic complete media, centrifuged at 500x g for 5 minutes, the supernatant was discarded, and then cells were resuspended in 2ml of media. Two microcentrifuge tubes were retrieved for each sample, one labelled as stained and the other as unstained, and 1ml of cell suspension was added to each tube. Then, CellROX™ Orange Reagent was used to measure ROS production in live cells. In brief, 2 µL of the reagent was added to cells in a tube labelled as stained, mixed with a pipette, and both tubes were incubated at 37°C for 30 minutes in the dark. After that, tubes were centrifuged, and the supernatant was discarded. Next, cells were washed by adding 1ml PBS, mixing, and centrifugation, for a total of three times. Finally, cells were resuspended with 1 mL PBS and 25 µL were loaded on Tali slide. The samples were analyzed on Tali following the instrument instructions with using the unstained sample as the reference.

Genes expression

RNA extraction:

Briefly, culture media was removed from the wells, then 400µl of QIAzol lysis reagent was added to each well to homogenize the cells. Using a scraper, cells were detached and then were collected in microcentrifuge tubes. After that, 200µl of chloroform was added to each tube, shaken for 10 seconds vigorously, and incubated at room temperature for 3 minutes. Following incubation, tubes were centrifuged for 15 minutes at 12000xg and 4oC. Next, inside a clean hood, the clear upper aqueous layer ~ about 200µl (containing RNA) was carefully collected and transferred to new microcentrifuge tubes. Then, to precipitate the RNA, 500µl of isopropanol was added to each tube, mixed by inverting, and incubated at room temperature for 10 minutes. Following incubation, tubes were centrifuged for 10 minutes at 12000xg and 4oC. Afterward, the liquid layer was carefully removed and discarded without touting the

white RNA pellet in the bottom of the tube. After that, the pellet was washed with 500µl of 75% ethanol, centrifuged for 5 minutes at 7500xg and 4oC. The liquid layer was carefully removed and discarded, and the pellet was air-dried for 5-10 minutes. Finally, 20µl of nuclease-free water was added to the pellet, mixed by pipetting up and down gently, and immediately tubes were kept on ice for immediate use in downstream applications or stored at -80oC until used for further analysis.

Total RNA concentration, integrity, and quality

Total RNA concentration of samples was measured using the Nanodrop Lite instrument, and 260/280 ratio >1.8 was used to assess the purity. After that, to measure the total RNA's integrity and quality, RNA IQ Assay Kit was used following the manufacturer's instructions, and the samples were analyzed on Qubit® 4.0 Fluorometer. RNA integrity number (RIN) >8 was considered acceptable for miRNA and gene expression assays. Examples of RNA purity and integrity data are shown in a Table in the appendix

cDNA preparation

- *cDNA from RNA*

cDNA was synthesized from mRNA using the High Capacity RNA to cDNA reverse transcription kit following the manufacture instructions. In brief, for each sample, a reaction mixture was prepared (total volume = 20µl) by mixing the indicated volumes of following components in order: 10µl of 2X RT Buffer Mix, 1 µl of 20X RT Enzyme Mix, up to 9µl RNA sample (up to 2 µg in 20µL reaction) and nuclease-free water to complete quantity to 20µl. Then, tubes were briefly mixed, centrifuged, and placed in a Gene Amp thermocycler to perform reverse transcription by incubating at 37oC for 60 minutes, followed by reaction stopping at 95oC for 60 minutes and finally holding at 4oC.

- *cDNA from miRNA*

miRNA was converted to cDNA using the TaqMan® Advanced miRNA Assays reverse transcription kit following the manufacturer's instructions. The process of synthesizing cDNA is performed in 4 stages. In the first stage, the mature transcript is extended by adding poly(A) to the 3' end. Then the 5’ is elongated. After that, reverse transcription is performed, followed by a miR-Amp reaction to increasing the quantity of cDNA. The resulted product is then used as the template for RT-PCR assay. Detailed component volumes and thermocycler programs are indicated in manufacturer protocol.

Quantitative Real-time PCR

Quantitative RT-PCR was performed using TaqMan® Fast Advanced Master Mix and the specific primers set on 7500 Real-time PCR system. In brief, for each gene, 4µL of cDNA was pipetted in the bottom in 96 well PCR plate, then reaction master mix was prepared for each gene by mixing the volumes of specific Primer sequence, Fast Advanced Master Mix and RNase-free water as shown in Table 4. After that total of 16µL of reaction master mix was added to each well-containing DNA sample for a total volume of 20µL. Finally, the plate was mixed, centrifuged, and processed on 7500 Real-time PCR system.

Table 4: Components and primers sequences used for genes and miRNA expression

Genes expression	
Reagent	**Volume per reaction (ul)**
TaqMan® Gene Expression Assay	1
TaqMan® Fast Advanced Master Mix	10

Reagent	**Volume per reaction (ul)**
cDNA template	4
RNase-free water	5
Total volume	20
Primers	
PPAR-α	Hs00947536_m1
ICAM-1	Hs00164932_m1
TNF-α	Hs00174128_m1
TRAF	Hs00377558_ml
ACTB	Hs99999903_ml
GPX1	Hs00829989_gH
CAT	Hs00156308_m1
SOD2	Hs00167309_m1
SOD1	Hs00916176_m1
PPARG	Hs01115513_m1
TXNRD1	Hs00917067_m1
miRNA expression	
Reagent	Volume per reaction (ul)
TaqMan® Fast Advanced Master Mix	10

Reagent	Volume per reaction (ul)
TaqMan® Advanced miRNA Assay (20X)	1
Diluted cDNA	5
RNase-free water	4
Total volume	20
Primers	
hsa-miR-146a-5p	478399_mir
hsa-miR-320a	478594_mir

Optimization Protocol

- *Optimization of seeding density*

The current study includes treating HRECs with different media (NG, HG, and classic complete media) for 96 hours followed by 48 hours of transfection incubation, thus optimizing the initial cell count to be used for seeding to avoid over confluency during incubation days was important.

A T75 flask with confluent HRECs and 6 wells plates were obtained, and cells were seeded with three different cell counts 5 x 104, 1 x 105, and 2 x 105 and the three different media that will be used in the experiment as shown in the below Figure 5, and then plates were incubated for 96 hours in 5% CO2 incubator at 37°C

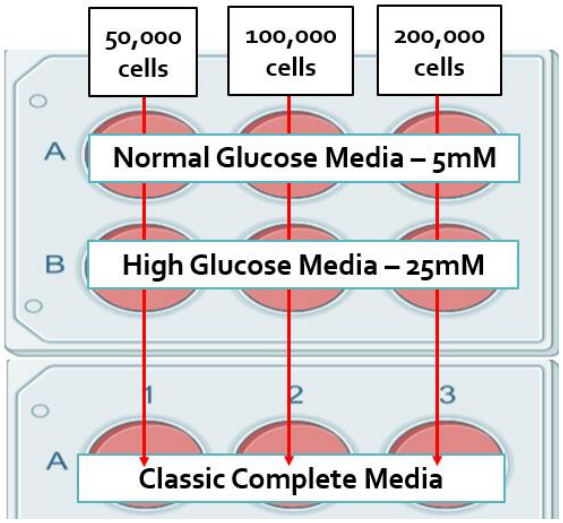

Figure 5: Seeding optimization experiment plate layout

After that, the wells were examined using EVOS XL Core Imaging System, and wells seeded with 5 x 104 were confluent and viable in all three media, while the wells with 1 x 105 and 2 x 105 counts had a large percentage of floating cells as shown in Figure 6, thus seeded with 5 x 104 was selected to start seeding with.

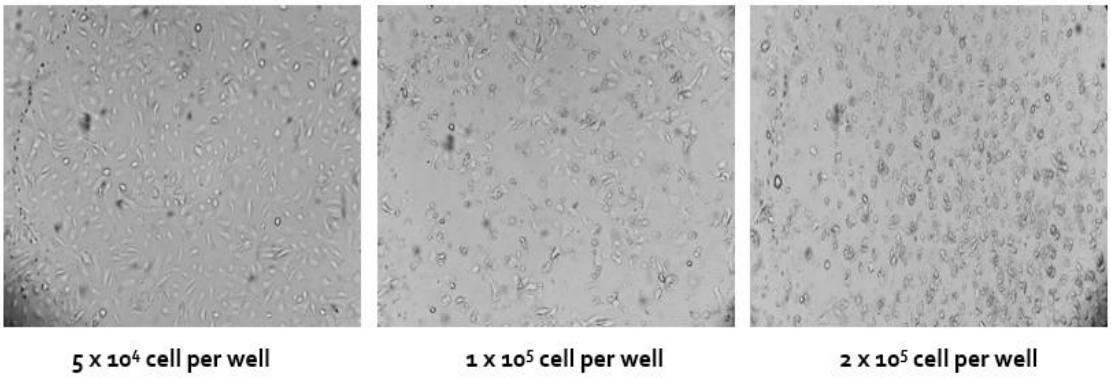

Figure 6: Seeding optimization experiment results. Microscopic images of the different seeding count of HRECs by the end of 96 hours incubation.

- *Assessing transfection efficacy*

Since transfection is the main point in the entire study and all the outcomes depend on it, assessing the efficacy of transfection is essential. In brief, HRECs P5 were

cultured in a T75 flask for 2 days in a complete culture media, then sub-cultured for 2 days in two T75 flasks. After that, cells were seeded in a 6 wells plate and was incubated in 5% CO2 incubator at 37°C until ~80% confluency. Then transfection with miR-146a-5p mimic (double-stranded RNA molecules), miR-146a-5p inhibit (single-stranded oligonucleotides), and negative control for mimic and inhibit miR-146a-5p (scramble sequence) were performed using Lipofectamine according to the manufacturer instructions, and the plate was incubated for 48 hours in 5% CO2 incubator at 37°C. Then total RNA was extracted, and the expression of miR-146a-5p was measured using RT-PCR.

RT^2 Profiler PCR Arrays (Inflammatory and Angiogenesis)

Two RT^2 Profiler PCR Arrays, Human Inflammatory cytokines, and receptors array (PAHS-011ZA-12) and Human Angiogenesis array (PAHS-024ZA-12), were used to assess the inflammatory cytokines and angiogenesis genes in HRECs exposed to hyperglycemia and transfected with 50nM miR-146a-5p. An array of each profile comes in a 96 well format that includes preloaded primers of specific 84 genes (cytokines, receptors, chemokines, adhesion molecules, inhibitors, etc.) depending on the type of array, in addition to primers for negative and endogenous controls. See Appendix C and Appendix D for a list of genes included in each array. In brief, a master mix was prepared by combining 1350 ul of 2x RT2 SYBR Green Master Mix, 102 ul of cDNA, and 1248 ul of RNase-free water. Then 25 ul were loaded per well, and the plate was mixed, centrifuged, and processed on 7500 Real-time PCR system. Differentially expressed genes (Group et al.) were generated using Gene Globe analysis software available on the Qiagen website. The threshold for significance in expression change was set at FC of $\leq$ -1.4 for downregulated and upregulated genes. Also, the Student's t-test of the replicate 2(-Delta CT) values for each gene in the control group

and treatment groups were determined using Gene Globe analysis from Qiagen. The options selected on Gene Globe were as the following: based on the type of the array, inflammatory or angiogenesis, the correct catalogue was selected. Then, CT value was set to 35, the fold regulation was set to 2, and P-value to 0.05. Normalization was done based on the geometric mean of five housekeeping genes: Actin-beta, B2M, GAPDH, HPRT1, RPLPO.

Bioinformatic Analysis

To determine the biological significance and functional classification of the genes, we performed bioinformatic analysis using the Metscape enrichment pathways analysis tool (metascape.org) and Ingenuity Pathway Analysis (IPA) software.

Statistical Analysis

Three biological replicates and 3-9 technical replicates were performed for each sample and experiment; hence, data are presented as mean with standard deviation. Statistical significance was determined by comparing the different treatment groups to the NG as the control followed by sub-comparisons between the different groups as specified using one-way ANOVA and Student T-test through GraphPad prism 9 or manually. A significant two-tailed P value was defined as 0.05 or less.

CHAPTER 5: RESULTS

A - Effect to a low dose (10 nM) of both miR-146a-5p mimic and inhibit

Apoptosis and viability

The apoptosis percentages (sum of early and late phases) obtained by Annexin V & Dead Cell Kit on Muse cell analyzer showed no significant difference in apoptosis percentage of HG-treated HRECs when compared with NG treated cells. In addition, transfection with miR-146a-5p mimic in normoglycemic did not significantly affect the apoptosis percentage compared to NG sample. Moreover, miR-146a-5p mimic and inhibit transfection in hyperglycemic did not significantly affect the apoptosis rate. In fact, all the HRECs samples showed similar apoptosis percentages to the NG sample, as shown in Figure 7a, b. Then we compared the percentage of live and dead cells percentages between the samples. Hyperglycemia did not affect the percentage of live and dead cells in comparison to the normoglycemia condition. Furthermore, we compared the impact of transfecting 10nM miR-146a-5p mimic and inhibitor in samples exposed to hyperglycemia in terms of live and dead percentages. Percentage of live and dead cells was not affected by neither miR-146a-5p mimic nor miR-146a-5p inhibit Figure 7a, c.

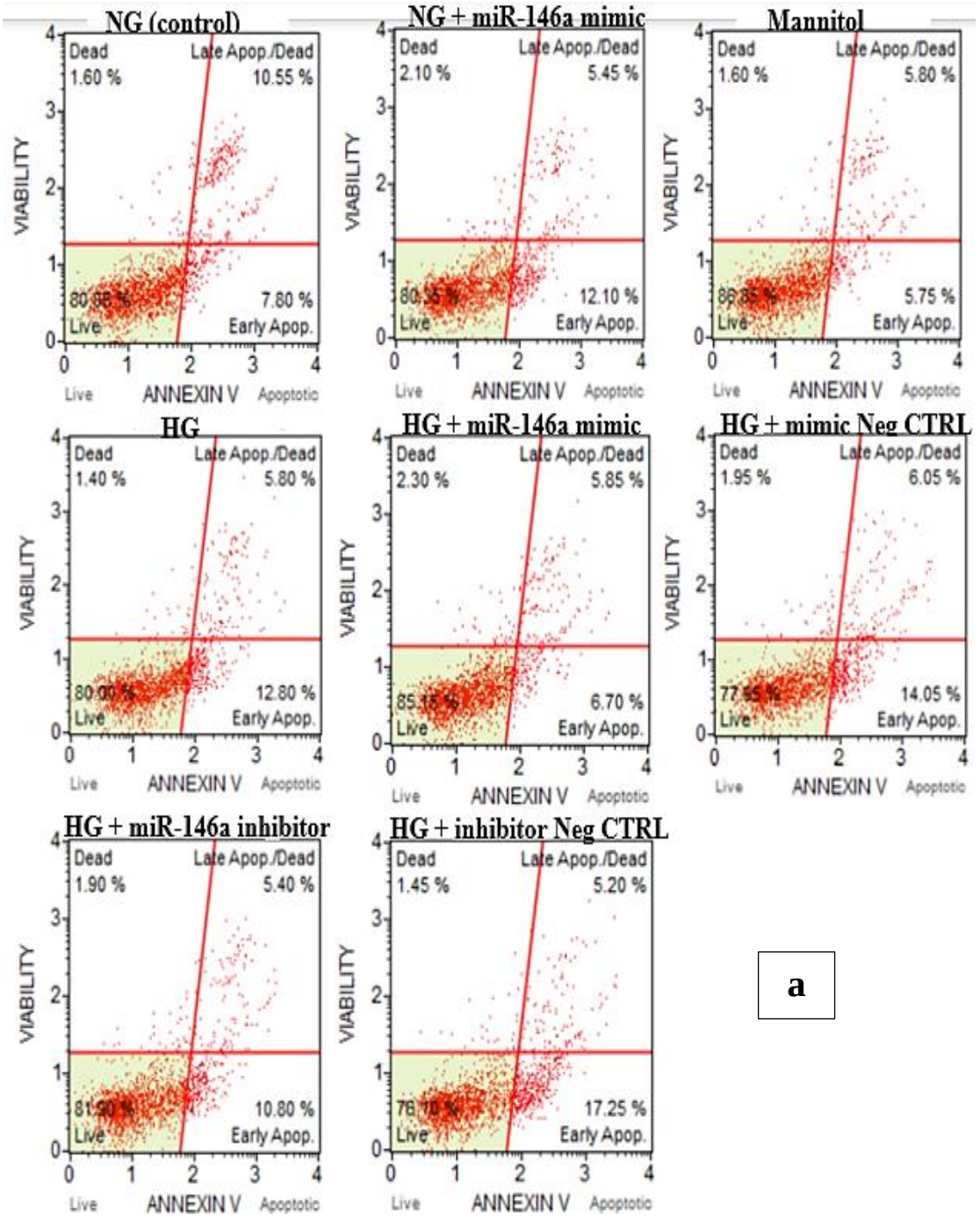
NG (control)
Dead
1.60 %
Late Apop./Dead
10.55 %
7.80 %
Early Apop.
Live
VIABILITY
ANNEXIN V
Apoptotic
NG + miR-146a mimic
Dead
2.10 %
Late Apop./Dead
5.45 %
12.10 %
Early Apop.
Live
Mannitol
Dead
1.60 %
Late Apop./Dead
5.80 %
5.75 %
Early Apop.
Live
HG
Dead
1.40 %
Late Apop./Dead
5.80 %
12.80 %
Early Apop.
Live
HG + miR-146a mimic
Dead
2.30 %
Late Apop./Dead
5.85 %
6.70 %
Early Apop.
Live
HG + mimic Neg CTRL
Dead
1.95 %
Late Apop./Dead
6.05 %
14.05 %
Early Apop.
Live
HG + miR-146a inhibitor
Dead
1.90 %
Late Apop./Dead
5.40 %
10.80 %
Early Apop.
Live
HG + inhibitor Neg CTRL
Dead
1.45 %
Late Apop./Dead
5.20 %
17.25 %
Early Apop.
Live

a

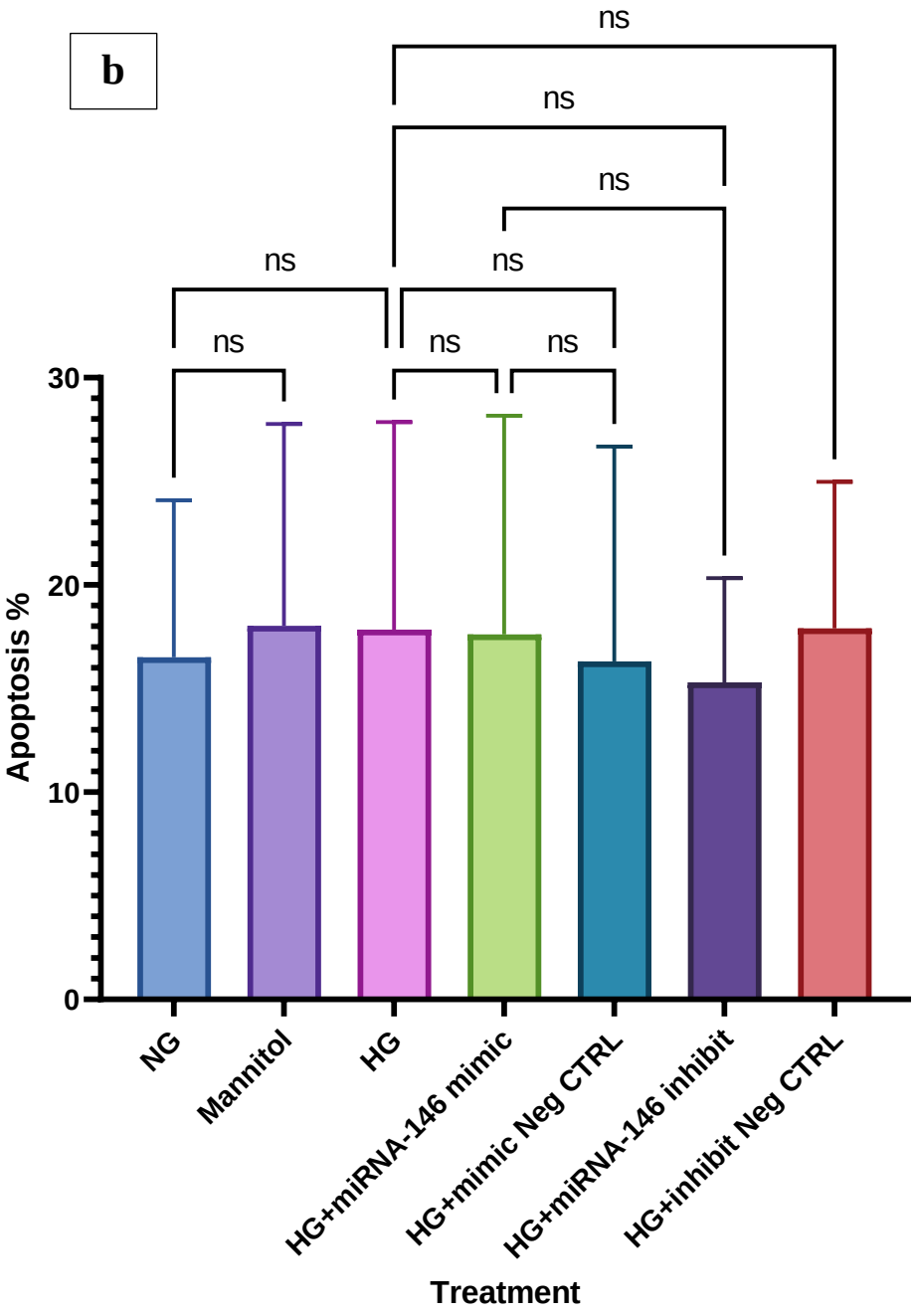
b
ns
ns
ns
ns
ns
ns
ns
ns
30
20
10
0
Apoptosis %
NG
Mannitol
HG
HG+miRNA-146 mimic
HG+mimic Neg CTRL
HG+miRNA-146 inhibit
HG+inhibit Neg CTRL
Treatment

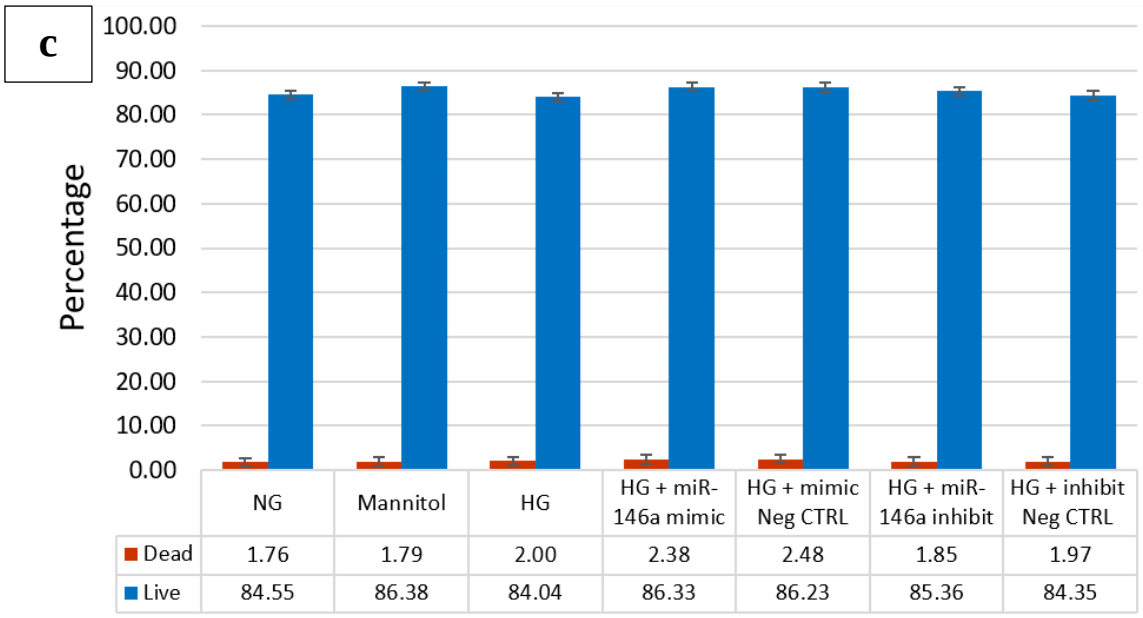

	NG	Mannitol	HG	HG + miR-146a mimic	HG + mimic Neg CTRL	HG + miR-146a inhibit	HG + inhibit Neg CTRL
Dead	1.76	1.79	2.00	2.38	2.48	1.85	1.97
Live	84.55	86.38	84.04	86.33	86.23	85.36	84.35

Figure 7: Live, dead, and Apoptosis data (a) Flow cytometry images obtained by Muse cell analyzer shows the percentage of live, dead, early, and late apoptotic cells in the different samples used in the study (b) Quantitative representation of total apoptosis (early and late) percentages of the samples used in the study (c) Quantitative representation of live and dead cells percentages of the samples used in the study. NG: Normal glucose; HG: High Glucose. All data in the graph present a mean and standard deviation of n=9 for each sample. miR-146a-5p mimic and inhibitory concentration= 10nM. ns: not significant. Two tailed p value is significant ≤ 0.05.

ROS production

ROS production in HRECs exposed to the different treatment and transfection conditions was assessed using CellROX™ Orange Reagent and analyzed on Tali analyzer. Our results showed that ROS production was significantly increased in HRECs exposed to chronic hyperglycemia compared to the normoglycemic control, as shown in Figure 8.

Then, the production of ROS was assessed in the samples with miR-146a-5p overexpressed using 10nM mimic, along with using scramble sequence as a negative control. As expected, the scramble sequence did not affect the ROS production; however, surprisingly, overexpressing miR-146a-5p with 10nM mimic significantly

increased the ROS production compared to hyperglycemia control Figure 8. Following that, the impact of miR-146a-5p knockout on ROS production was assessed. In line with the published literature, knocking out miR-146a-5p significantly increased ROS production compared to hyperglycemia control, Figure 8. Moreover, a comparison of ROS production rate between overexpressing miR-146a-5p with 10nM and knocking it out was performed. The data showed that knocking out miR-146a-5p significantly increased ROS production compared to overexpressing using 10nM mimic, Figure 9. Further, because of the unexpected effect of overexpressing miR-146a-5p with 10nM dose, its effect in normoglycemic condition was assessed. Interestingly, findings showed that 10nM miR-146a-5p significantly elevated ROS production compared to hyperglycemia as a control, Figure 9.

.

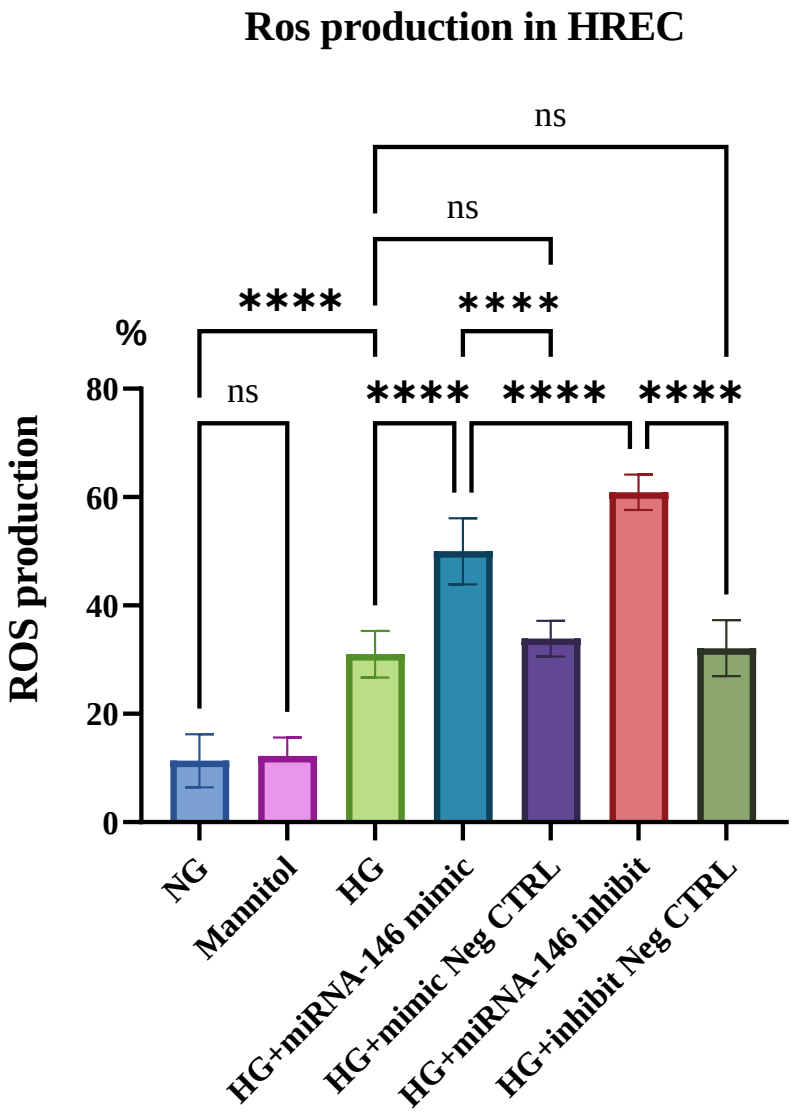

Figure 8: Comparison of ROS production between NG control and all the samples. Quantitative representation of ROS production in all samples used in the study compared to NG as control. NG: Normal glucose; HG: High Glucose. All data in the graph are presented as bars with a mean and standard deviation of n=9 for each sample. miR-146a-5p mimic and inhibitory concentration used is 10nM. ns: not significant; **** indicates P ≤ 0.0001. Two tailed p value is significant ≤0.05.

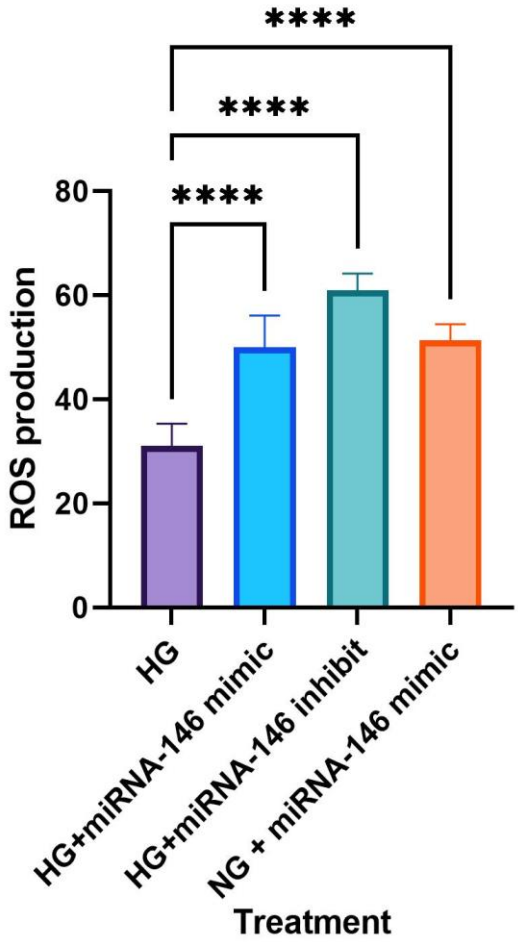

Figure 9: Comparison of ROS production between HG sample and the samples transfected with miR-146a-5p mimic and inhibit. Quantitative representation of ROS production in miR-146a-5p mimic and inhibit samples in comparison to HG treated sample. HG: High Glucose. All data in the graph are presented as a mean and standard deviation of n=9 for each sample. miR-146a-5p mimic and inhibitory concentration used is 10nM. **** indicates $P \leq 0.0001$. Two tailed p value is significant ≤ 0.05.

miR-146a-5p expression

This experiment was performed to identify the impact of hyperglycemia and transfection with 10 nM miR-146a-5p mimic and inhibitor on miR-146a-5p expression.

Expression during optimization

As shown in Figure 10, the CT values and expression of miR-146a-5p were significantly increased with miR-146a-5p mimic transfection by 18-folds, while miR-

146a-5p inhibit significantly decreased the miR-146a-5p expression by 500-folds compared to the negative control (scrambled sequence).

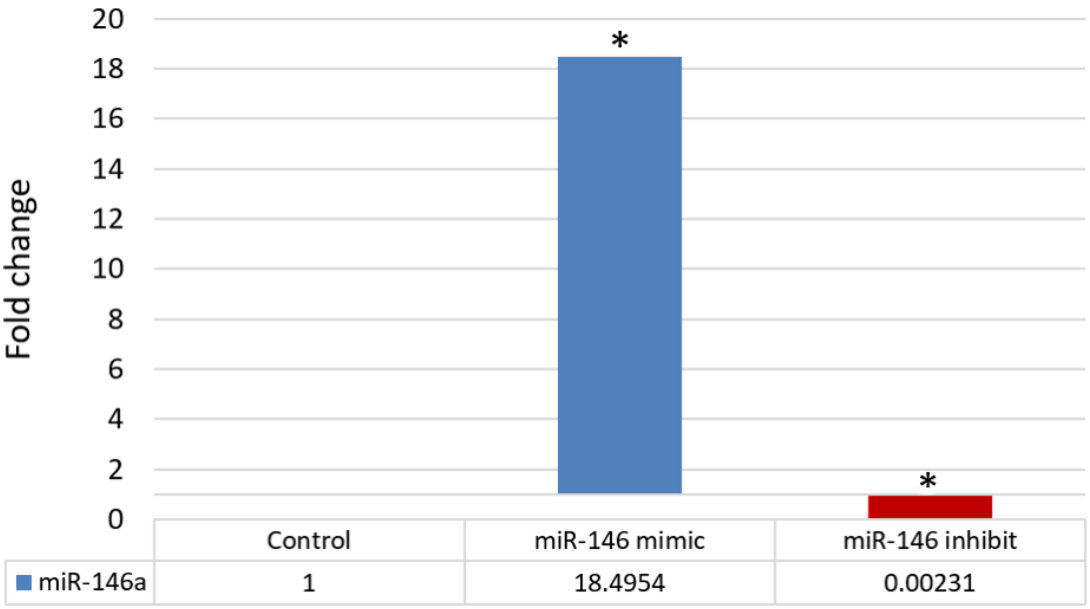

Figure 10: Assessing transfection efficacy. Quantitative representation of CT values. All data in the graph present a mean of n=4 for each sample. miR-320a was used as endogenous control. miR-146a-5p mimic and inhibitory concentration used is 10nM. * indicates value significantly different than the control group. Two tailed p value is significant ≤0.05.

Expression during transfection with 10nM

First, the effect of normoglycemia and hyperglycemia treatments were compared. Chronic hyperglycemia exposure caused a significant change in miR-146a-5p expression, decreasing it by 7 folds compared to the normoglycemia control, Figure 11 a. Then the expression of miR-146a-5p using 10nM miR-146a-5p mimic, along with using the scramble sequence as a negative transfection control was assessed. Data showed that transfection with 10nM miR-146a-5p mimic significantly increased the expression by 302 folds, while the scrambled sequence did not affect Figure 11 b. Further, miR-146a-5p expression post-miR-146a-5p inhibitor transfection, along with

using the scramble sequence as negative transfection control, was assessed. Findings showed that transfection with miR-146a-5p inhibitory significantly decreased the expression of miR-146a-5p by 7 folds while the scrambled sequence did not have any effect, Figure 11 c. Together, these results demonstrate that transfection with both miR-146a-5p mimic and inhibitory was effectively achieved.

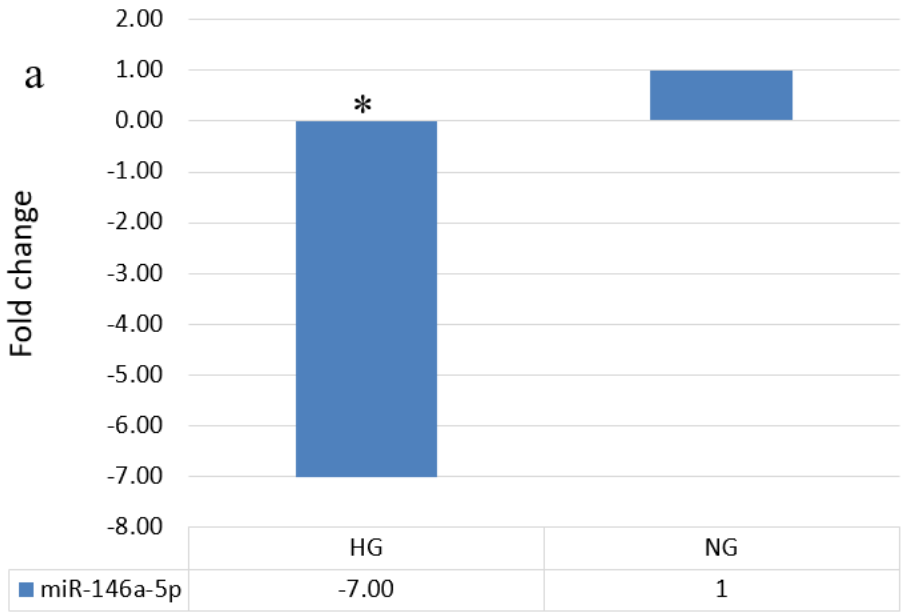

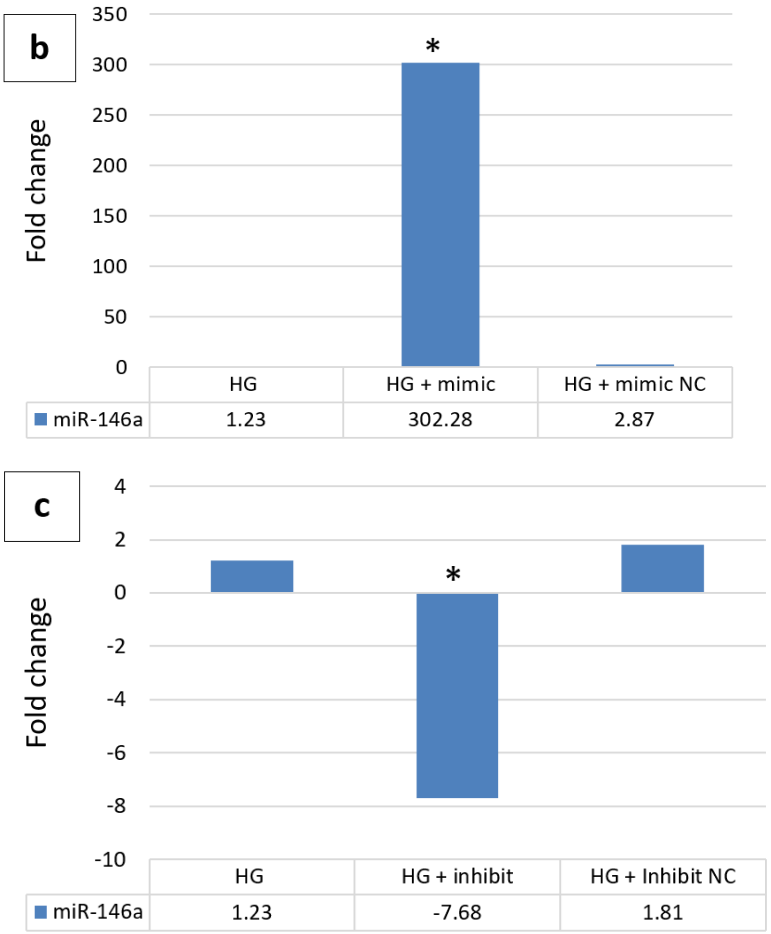

Figure 11: Quantitative representation of fold change in miR-146a-5p expression (a) Comparison of miR-146a-5p expression between NG and HG. (b) Comparison of miR-146a-5p expression between HG, HG+ 10 nM miR-14a-5p mimic and scramble sequence (c) HG+ 10 nM miR-14a-5p inhibit and scramble sequence. NG: Normal Glucose; HG: High Glucose; NC: Negative Control (scramble sequences). All data in the graph are presented as the mean of n=4 for each sample. miR-320a was used as endogenous control. miR-146a-5p mimic and inhibitory concentration used is 10nM. * indicates $P \leq 0.05$. Two tailed p value is significant ≤ 0.05.

Genes expression

The expression of four genes was tested TNF - α, ICAM 1, PPAR–α, and TRAF6, the main target gene of miR-146a-5P. TRAF6 expression was not changed significantly in any of the samples compared to NG or to the other samples; hence, the

below lines highlight the effect on TNF - α, PPAR–α, and ICAM 1.

First, assessing the effect of transfecting with 10 nM miR-146a-5p mimic under normoglycemic condition. This experiment aimed to identify the effect of 10 nM miR-146a-5p on gene expression in normoglycemic conditions. Our results showed an unexpected significant increase in TNF - α expression with 59998-fold, ICAM 1 with 48-folds, and PPAR- α around 3-folds compared to the NG sample Figure 12. These data indicated that overexpression of miR-146a-5p with a low dose could have a pro-inflammatory and pre-apoptotic effect, which affects the biological function of the cells adversely to the well-established functions of the studied genes.

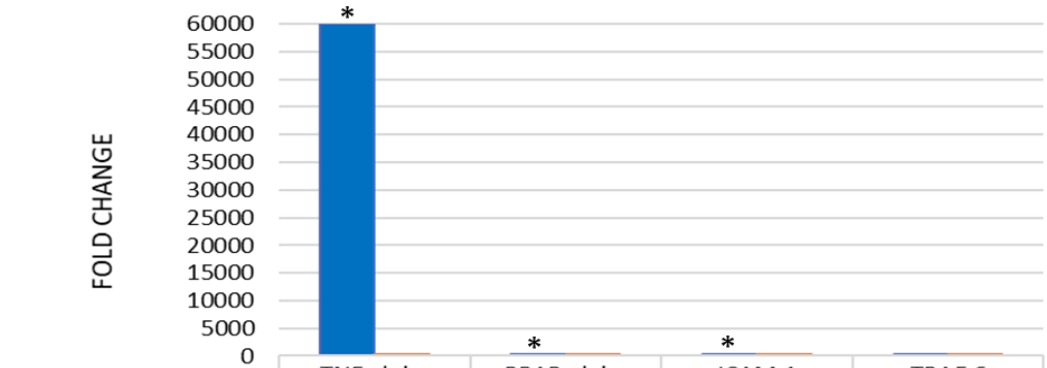

	TNF alpha	PPAR alpha	ICAM 1	TRAF 6
NG + miR-146a mimic	59998.54	2.55	48.24	1.037
NG	1	1	1	1

Figure 12: Expression genes in NG and NG+miR-146a-5p mimic. Comparison of TNF – α, PPAR – α, ICAM1, and TRAF 6 expression between NG and NG+miR-146a-5p mimic NG: Normal Glucose. All data in the graph are presented as the mean of n=4 for each sample. Beta-actin (ACTB) is used as endogenous control. miR-146a-5p mimic concentration= 10nM. TNF - α protein concentration used is 1ng/ml * indicates $P \leq 0.05$. Two tailed p value is significant ≤0.05.

In addition, we assessed the effect of treating samples exposed to normoglycemia condition with TNF - α protein at 1ng/ml for 4 hours. This experiment aimed to identify the effect of TNF-α which is a well-known pro-inflammatory and pro-apoptotic cytokine on HRECs on gene expression in normoglycemic conditions to

mimic inflammatory conditions observed in hyperglycemic conditions. We found that treatment with TNF – α protein significantly increased TNF-α expression by 6129-folds and ICAM1 by a 68-fold expression, whereas the expression of PPAR-α was not significantly affected as shown in Figure 13a, b. The results indicated that treatment with TNF-α could be pro-inflammatory and pre-apoptotic in terms of increasing expression of ICAM1. Interestingly, the expression of TNF–α was even greater with transfection with miR-146a-5p in the presence of TNF - α in the normoglycemic condition, by 54090-folds in comparison to the NG sample, Figure 14.

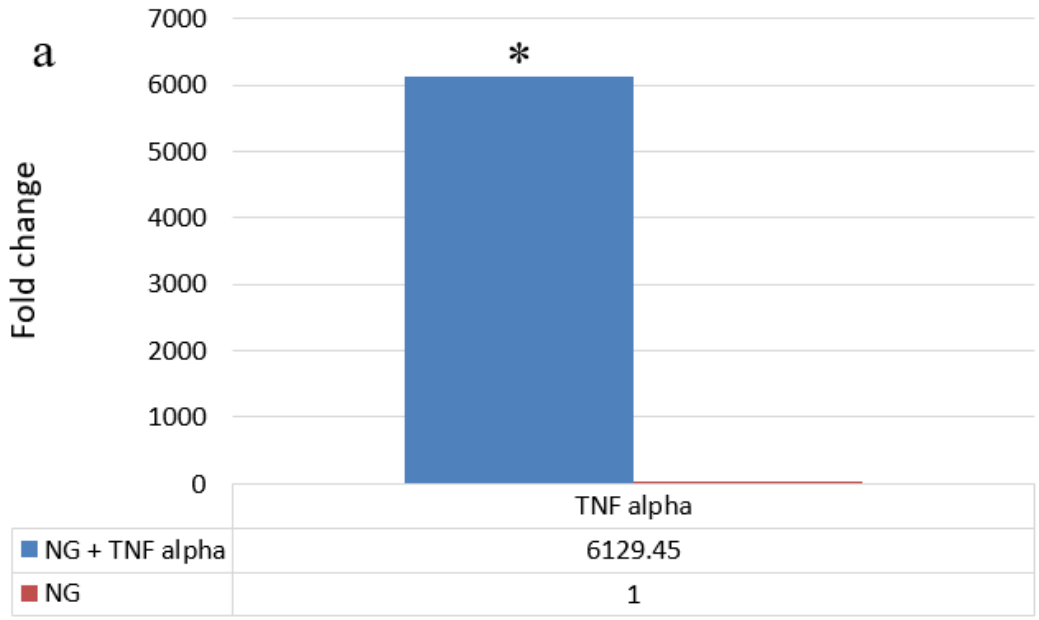

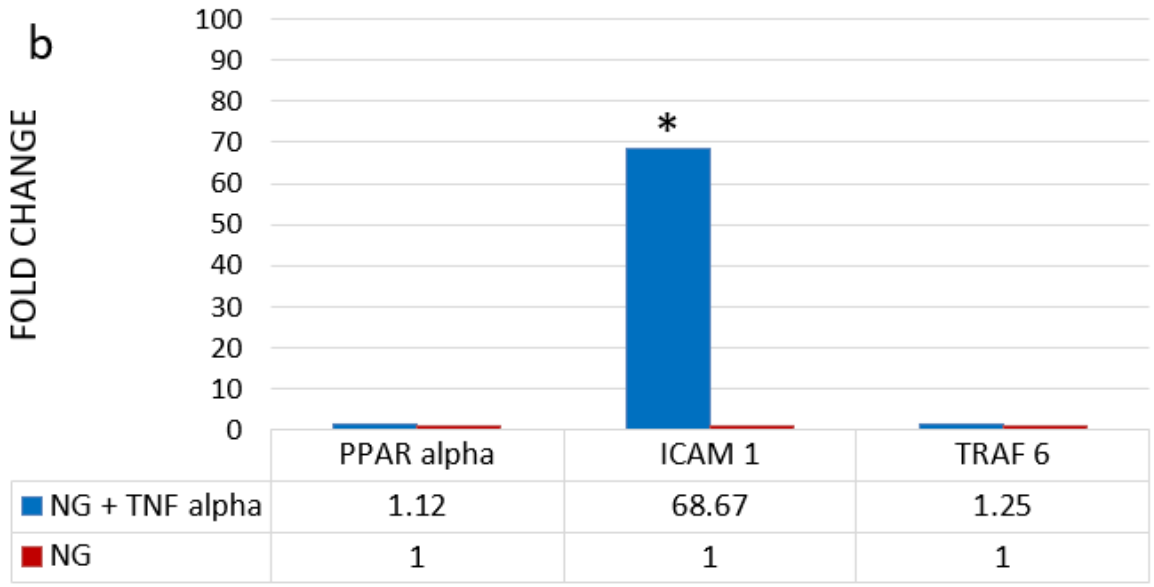

Figure 13: Expression of PPAR-α, ICAM-1, and TRAF6 genes in NG and NG+TNF – α (a) Comparison of TNF–α expression between NG and NG+ TNF – α (b) Comparison of PPAR – α, ICAM1 and TRAF 6 between NG, and NG+TNF- α. NG: Normal Glucose. All data in the graph represent the mean of n= 4 for each sample. Beta-actin (ACTB) is used as endogenous control. TNF-α protein concentration used is 1ng/ml. * indicates a significant difference between NG+TNF versus NG, P ≤ 0.05. Two tailed p value is significant ≤0.05.

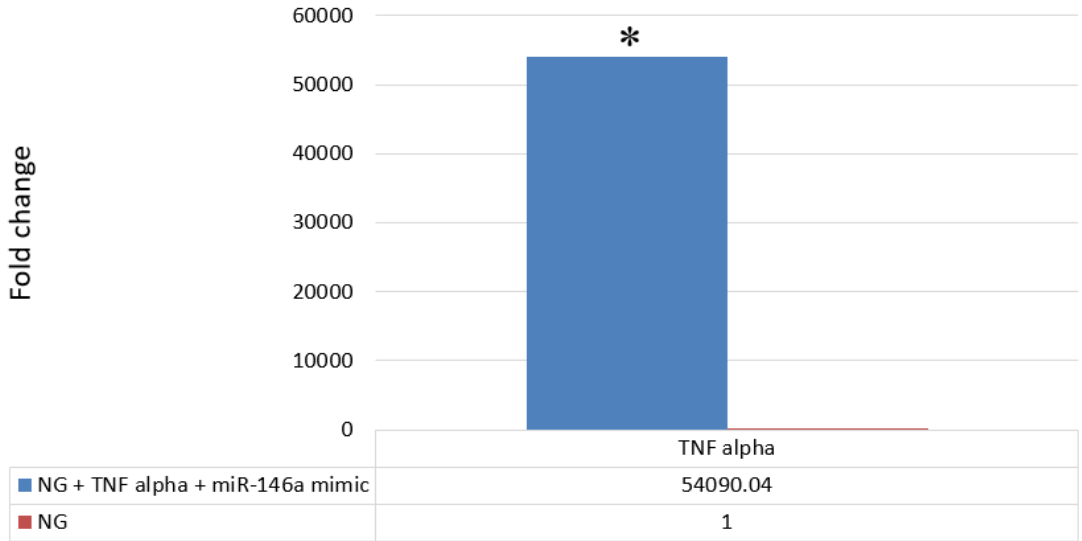

Figure 14: Expression of TNF - α in NG and NG+TNF - α+ miR-146a-5p mimic. NG: Normal Glucose. All data in the graph represent the mean of n= 4 for each sample. Beta-actin (ACTB) is used as endogenous control. miR-146a-5p mimic concentration

used is 10nM. TNF - α protein concentration used is 1ng/ml * indicates a significant difference between NG and NG+TNF - α+ miR-146a-5p mimic, P ≤ 0.05. Two tailed p value is significant ≤0.05.

Hence, we compared the gene expression in the normoglycemic sample treated with TNF - α at 1ng/mL for 4 hours with and without miR-146a-5p mimic to assess the impact of miR-146a-5p mimic on inflammation. Surprisingly, the result showed that 10 nM of miR-146a-5p mimic increased TNF-α expression significantly by almost 9-folds compared to only TNF–α treatment. The expression of PPAR-α and ICAM 1 were not affected, Figure 15. Further, interestingly, when the expression of the three genes was compared between normoglycemic samples with only 10 nM miR-146a-5p mimic or TNF - α at 1ng/mL for 4 hours, the miR-146a-5p mimic showed a significant increase in TNF - α expression almost 10-folds and PPAR–α by 2-folds in comparison to TNF - α treatment, Figure 16.

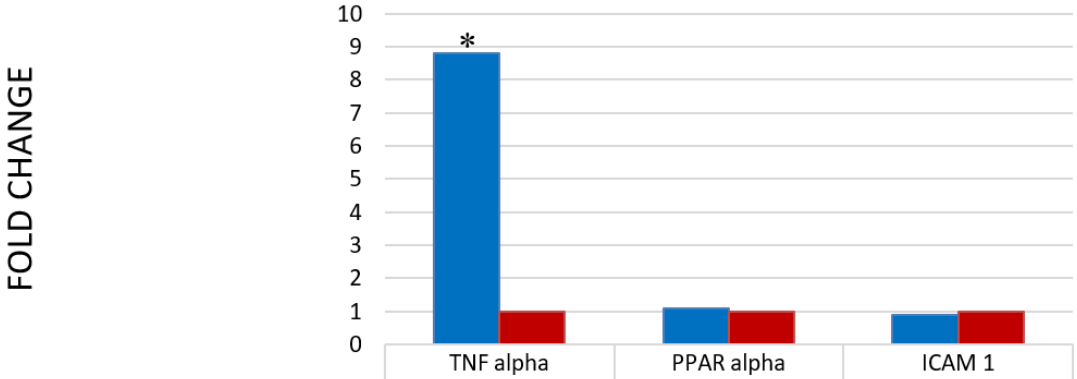

Figure 15: Expression of TNF - α, PPAR–α, ICAM1 in NG+TNF - α and NG+TNF - α+ miR-146a-5p mimic. NG: Normal Glucose. All data in the graph represent the mean of n= 4 for each sample. Beta-actin (ACTB) is used as endogenous control. miR-146a-5p mimic concentration used is 10nM. TNF - α protein concentration used is 1ng/ml *

indicates a significant difference between NG and NG+TNF - α+ miR-146a-5p mimic, P ≤ 0.05. Two tailed p value is significant ≤0.05.

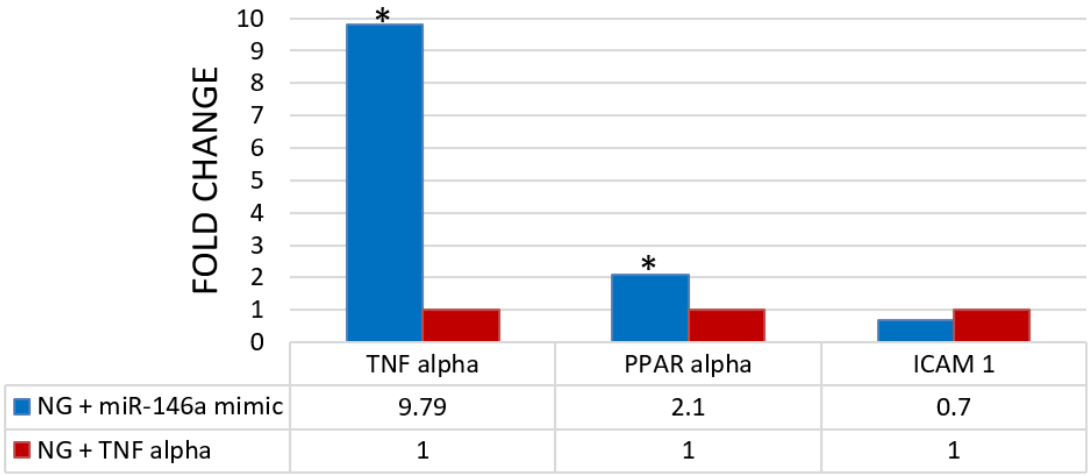

Figure 16: Expression of TNF - α, PPAR–α, ICAM1 in NG+TNF - α Vs. NG + miR-146a-5p mimic. NG: Normal Glucose. All data in the graph represent the mean of n= 4 for each sample. Beta-actin (ACTB) is used as endogenous control. miR-146a-5p mimic concentration= 10nM. TNF - α protein concentration= 1ng/ml. * indicates a significant difference between NG+ TNF alpha and NG+ miR-146a-5p mimic, P ≤ 0.05. Two tailed p value is significant ≤0.05.

On the other hand, a comparison of gene expression in the normoglycemic condition with transfection of miR-146a-5p mimic with and without TNF - α treatment at 1ng/mL for 4 hours did not show any significant difference, Figure 17.

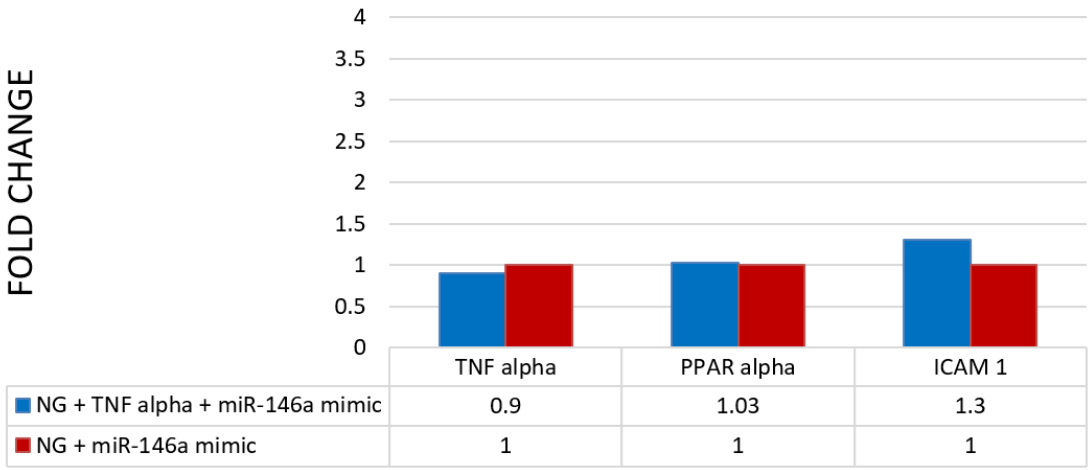

Figure 17: Expression of TNF - α, PPAR–α, ICAM1 in NG+TNF - α+miR-146a-5P and NG + miR-146a-5P mimic. NG: Normal Glucose. All data in the graph represent the mean of n= 4 for each sample. Beta-actin (ACTB) is used as endogenous control. miR-146a-5p mimic concentration used is 10nM. TNF - α protein concentration used is 1ng/ml. Two tailed p value is significant ≤0.05.

After that, we assessed the gene expression between normoglycemic and hyperglycemic conditions. We found that exposure to hyperglycemia significantly increased the expression of TNF – α, ICAM1, and TRAF-6 by 20-folds, 25-folds, and 12.6-folds, respectively, Figure 18.

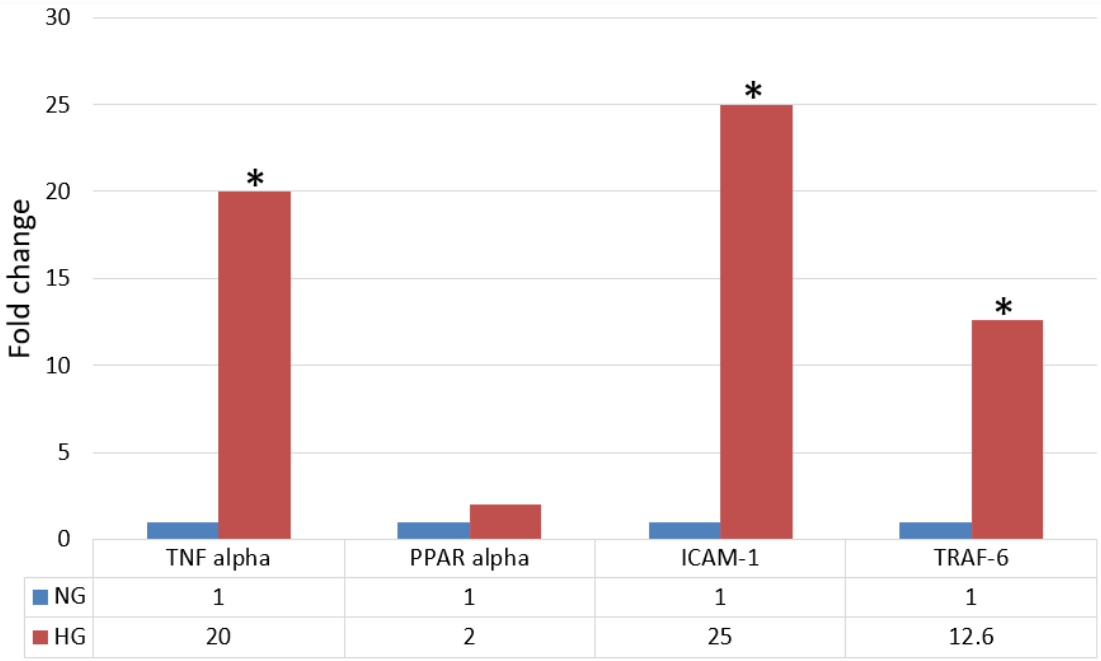

Figure 18 Expression of TNF – α, PPAR–α, ICAM1, TRAF-6 in NG and HG. NG: Normal Glucose; HG: High Glucose. All data in the graph represent the mean of n= 4 for each sample. Beta-actin (ACTB) is used as endogenous control. * indicates the significant differences of gene expression of TNF – α, PPAR–α, TRAF-6 in HG vs. NG. Two tailed p value is significant ≤0.05.

Surprisingly, when the hyperglycemic sample was transfected with miR-146a-5p mimic, TNF - α expression, PPAR–α, and ICAM1 increased significantly by 38404-folds, 1.48 -folds 43.5-folds, respectively, in comparison to the normoglycemic sample Figure 19a, b. Similarly, the expression of TNF - α, PPAR–α, and ICAM1 was also increased significantly when the hyperglycemic sample was transfected with miR-146a-5p inhibit by 30842-folds, 1.5-folds, and 33-folds, respectively, in comparison to the normoglycemic sample, Figure 20a, b.

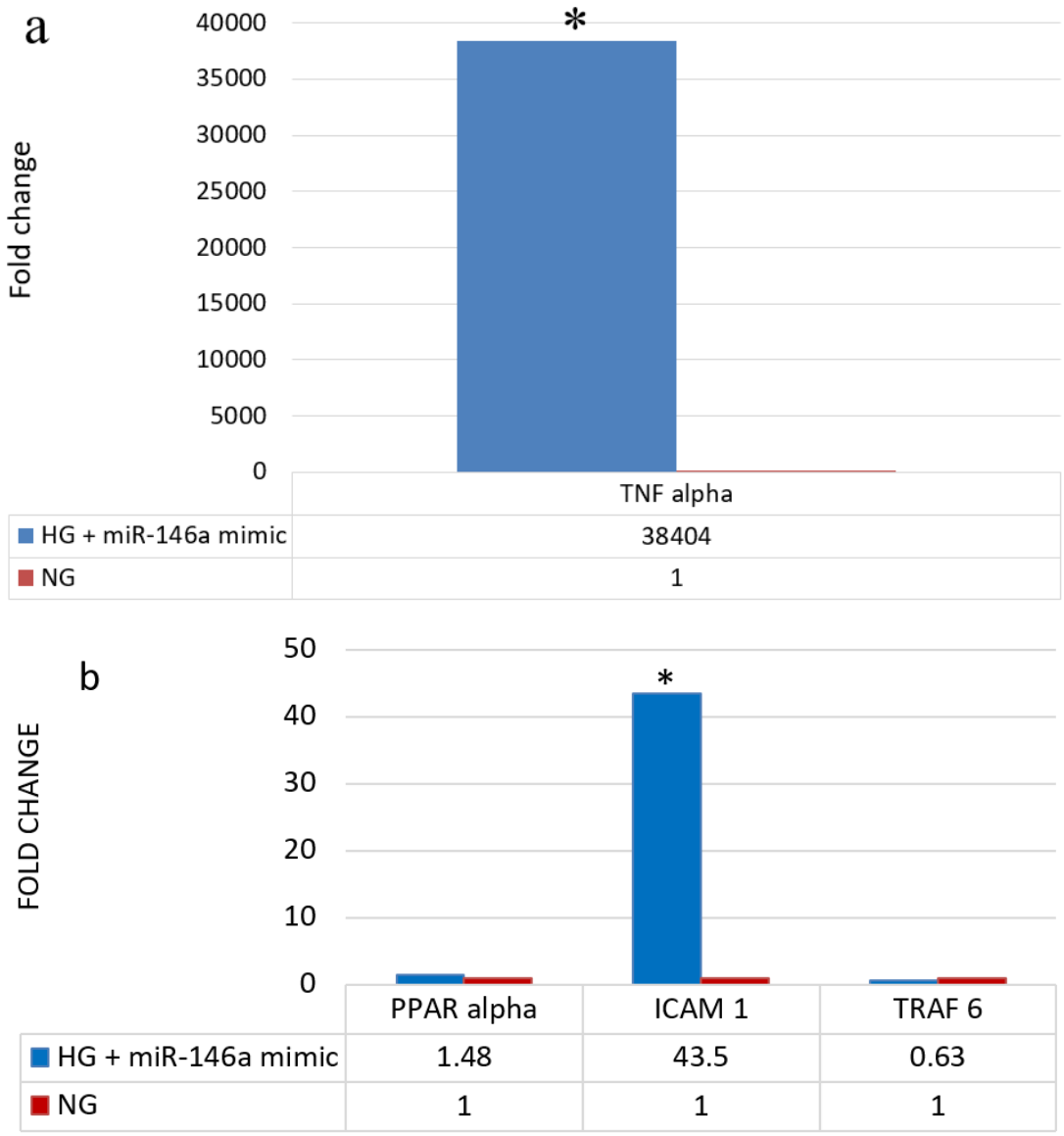

Figure 19 Expression of genes in NG and HG+miR-146a-5p mimic (a) Comparison of TNF – α expression between NG and HG+miR-146a-5p mimic (b) Comparison PPAR–α, ICAM1 and TRAF 6 expression between NG and HG+miR-146a-5p mimic. NG: Normal Glucose; HG: High Glucose. All data in the graph represent the mean of n= 4 for each sample. Beta-actin (ACTB) is used as endogenous control. miR-146a-5p mimic concentration used is 10nM. * indicates a significant difference of ICAM1 expression in HG+miR-146a-5p mimic vs. NG, $P \leq 0.05$. Two tailed p value is significant ≤0.05.

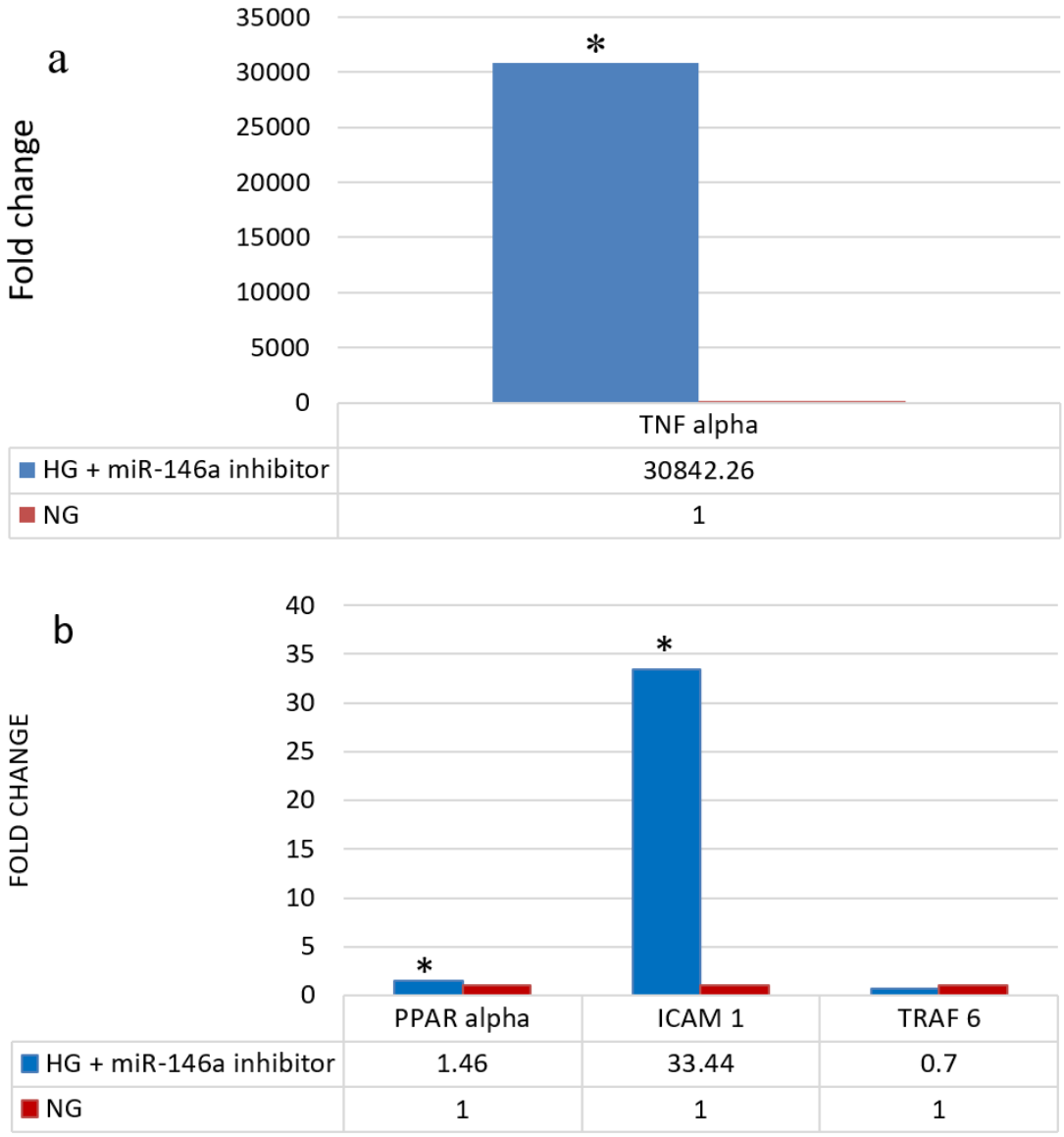

Figure 20 Expression of TNF – α, PPAR–α, ICAM1 in NG and HG+miR-146a-5p inhibit. NG: Normal Glucose; HG: High Glucose. All data in the graph represent the mean of n= 4 for each sample. Beta-actin (ACTB) is used as endogenous control. miR-146a-5p inhibitory concentration used is10nM. * indicates a significant difference of ICAM1 expression in HG+miR-146a-5p inhibitor vs. NG, $P \leq 0.05$. Two tailed p value is significant ≤0.05.

Subsequently, TNF - α, PPAR–α, and ICAM1 expression were significantly elevated by 15214-folds, 2-folds, and 52-folds, respectively, by transfecting the hyperglycemic samples using miR-146a-5p mimic when compared to hyperglycemia treatment only, Figure 21. In contrast, silencing of miR-146a-5p using inhibitor

transfection elevated only TNF-α expression by 15214-folds and ICAM1 by 52-folds, Figure 22.

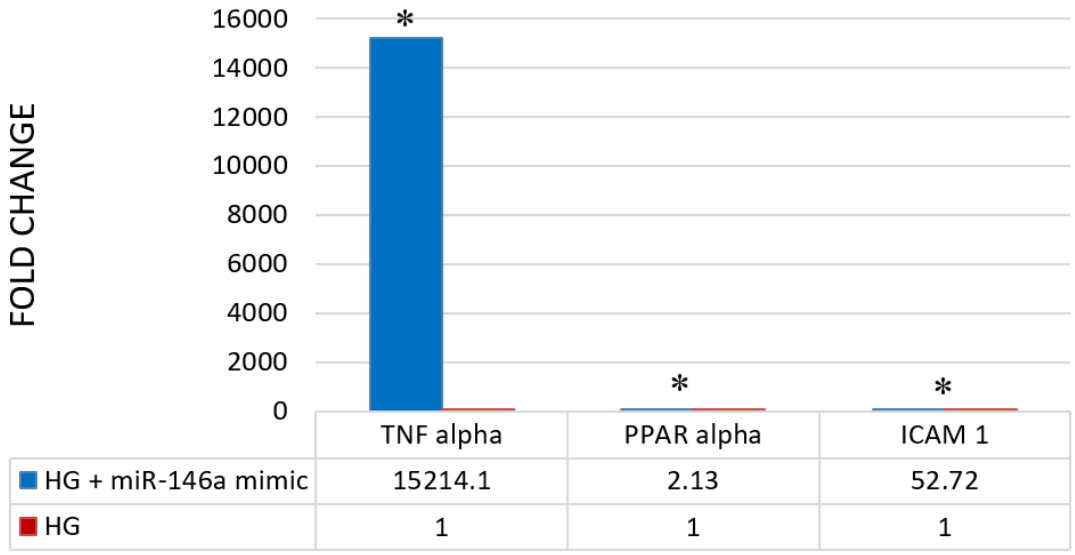

Figure 21 Expression of TNF - α, PPAR–α, ICAM1 in HG and HG+miR-146a-5p inhibit. HG: High Glucose. All data in the graph represent the mean of n= 4 for each sample. Beta-actin (ACTB) is used as endogenous control. miR-146a-5p mimic concentration used is 10nM. * indicates a significant difference of TNF - α expression in HG+miR-146a-5p mimic vs. HG, $P \leq 0.05$. Two tailed p value is significant ≤0.05.

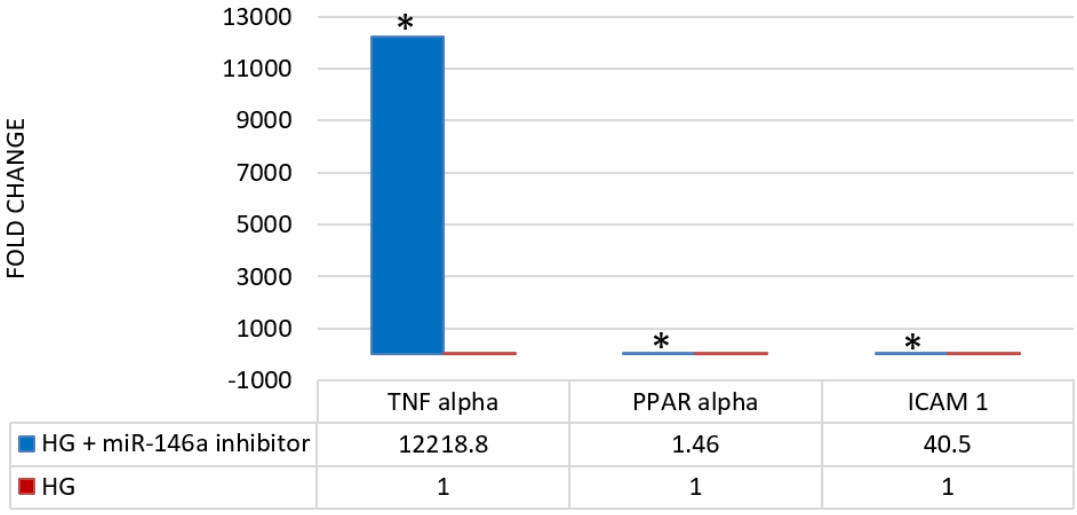

Figure 22 Expression of TNF - α, PPAR–α, ICAM1 in HG and HG+miR-146a-5p inhibit. HG: High Glucose. All data in the graph represent the mean of n= 4 for each sample. Beta-actin (ACTB) is used as endogenous control. miR-146a-5p inhibitor

concentration used is10nM. * indicates a significant difference of TNF - α expression in HG+miR-146a-5p inhibitor vs. HG, P ≤ 0.05. Two tailed p value is significant ≤0.05.

Finally, a comparison between the transfection of miR-146a-5P mimic and inhibitor in hyperglycemia condition was performed. Unexpectedly, no significant effect on the expression of TNF – α, PPAR–α, and ICAM1 was demonstrated with transfection with miR-146a-5p mimic and inhibit, Figure 23.

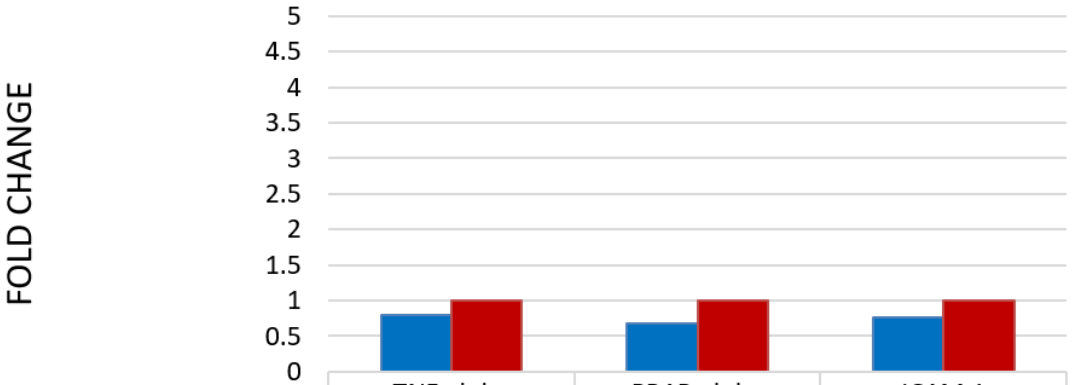

	TNF alpha	PPAR alpha	ICAM 1
HG + miR-146a inhibitor	0.8	0.68	0.76
HG + miR-146a mimic	1	1	1

Figure 23 Expression of TNF – α, PPAR–α, ICAM1 in HG+miR-14a mimic and HG+miR-146a-5p inhibit. HG: High Glucose. All data in the graph present the mean of n= 4 for each sample. Beta-actin (ACTB) is used as endogenous control. miR-146a-5p mimic and inhibitory concentration used is 10nM. Two tailed p value is significant ≤0.05.

B – Effect to a high dose (50 nM) of miR-146a-5p mimic

Expression of miR-146a-5p

First, we examined the change in miR-146a-5p when transfecting with 50 nM in hyperglycemic conditions. We compared the expression in HG only to the sample transfected with 50 nM miR-146a-5p using scramble sequence as a control transfecting with 50 nM miR-146a-5p significantly increased the expression of miR-146a-5p gene

by 710- fold in comparison with HG sample. Sample transfected with the scramble sequence did not show any significant change in miR-146a-5p expression, Figure 24.

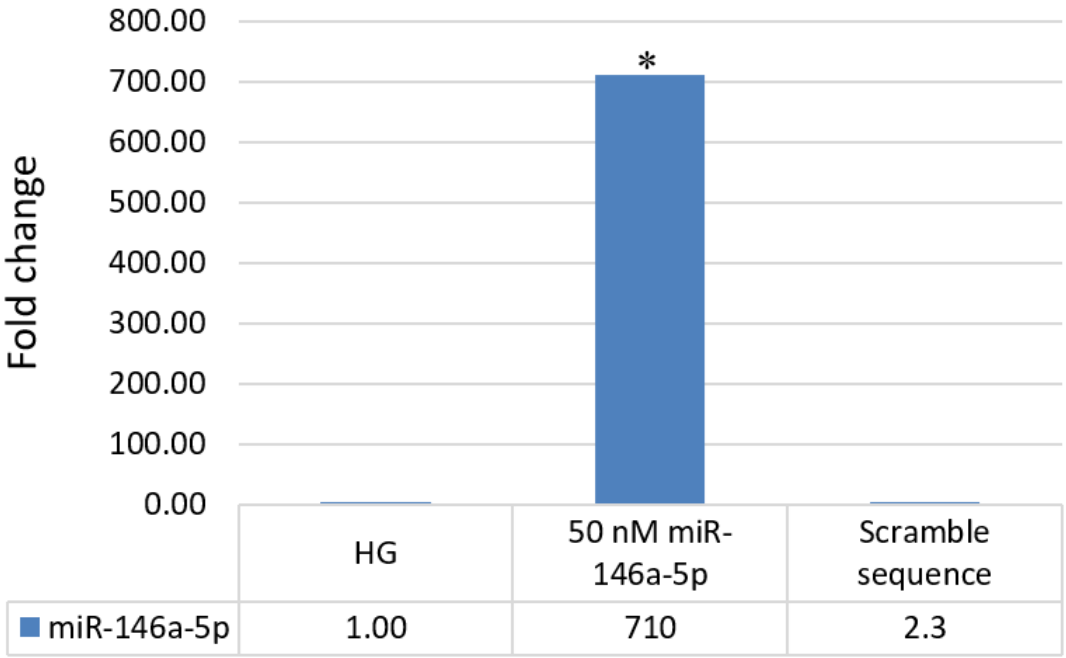

Figure 24 Quantitative representation of fold change in miR-146a-5p expression between HG, HG+ 50 nM miR-14a-5p mimic, and scramble sequence. HG: High Glucose; NC: Negative Control (scramble sequences). All data in the graph represent the mean of n= 3 for each sample. miR-320a was used as endogenous control. miR-146a-5p mimic concentration used is 50nM. * indicate a significant difference of miR-146a-5p expression in HG HRECs treated with 50nM miR-14a-5p mimic vs. HG HRECs without treatment, $P \leq 0.05$. Two tailed p value is significant ≤ 0.05.

Genes expression

Here we assessed the effect of transfecting 50 nM of miR-146a-5p mimic on the expression of four genes TNF - α, ICAM 1, PPAR–α, and TRAF6 in HRECs exposed to normoglycemia. We found that TNF – α was significantly upregulated by 3-folds, and TRAF-6 was decreased by 2-folds by 50 nM of miR-146a-5p mimic, while ICAM 1 and PPAR – α expression was not affected, Figure 25**.**

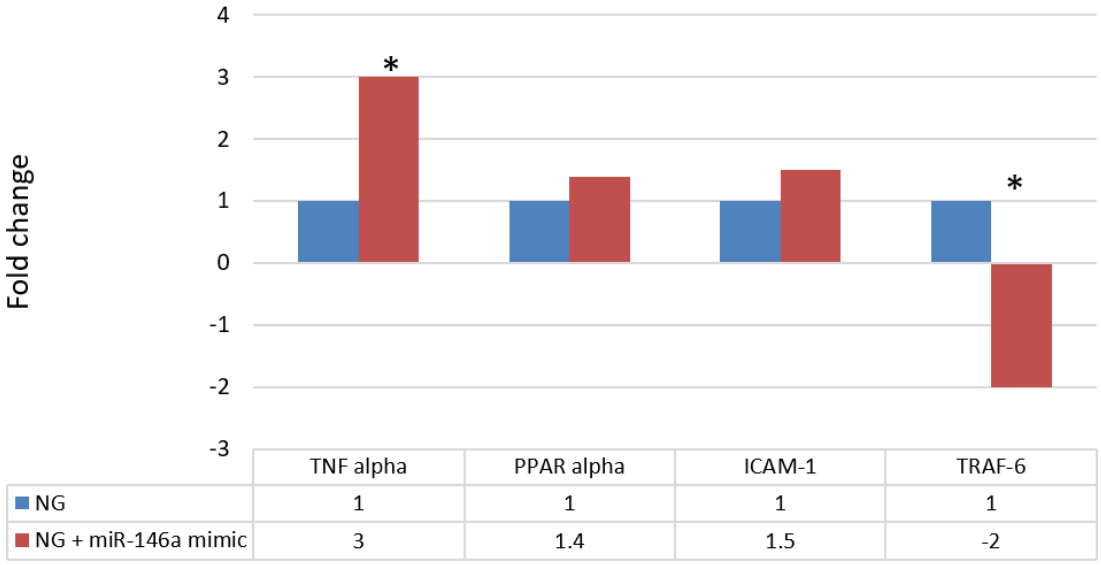

	TNF alpha	PPAR alpha	ICAM-1	TRAF-6
NG	1	1	1	1
NG + miR-146a mimic	3	1.4	1.5	-2

Figure 25 Expression of TNF - α, PPAR–α, ICAM1, TRAF6 in NG+miR-14a mimic. NG: Normal Glucose. All data in the graph represent the mean of n= 4 for each sample. Beta-actin (ACTB) is used as endogenous control. miR-146a-5p mimic concentration used is 50nM. * indicate a significant difference of genes expression in NG HRECs treated with 50nM miR-14a-5p mimic vs. NG HRECs without treatment, two tailed p value is significant ≤0.05.

Then, we studied the effect of 50 nM of miR-146a-5p mimic on the expression of four genes TNF - α, ICAM-1, and TRAF6 in HRECs exposed to chronic hyperglycemia. Interestingly, the results showed a significant reduction by 8-folds in TNF-α, ICAM 1, and TRAF6 expression, while expression was not significantly affected (Figure 26).

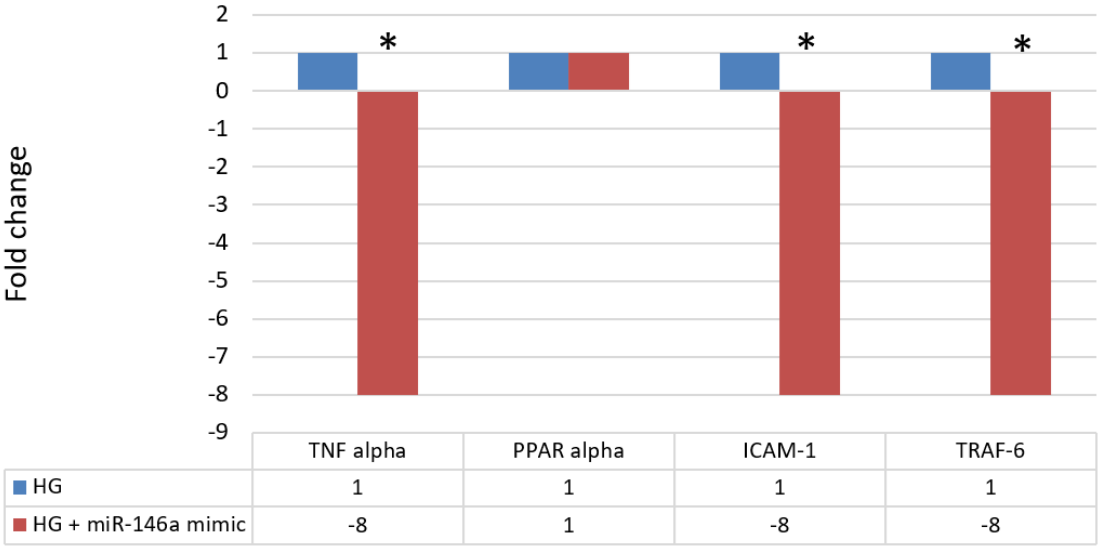

Figure 26 Expression of TNF - α, PPAR–α, ICAM1, TRAF6 in HG+miR-14a mimic. HG: High Glucose. All data in the graph represent the mean of n= 4 for each sample. Beta-actin (ACTB) is used as endogenous control. miR-146a-5p mimic concentration is used 50nM. * indicate a significant difference of genes expression in HG HRECs treated with 50nM miR-14a-5p mimic vs. HG HRECs without treatment, two tailed p value is significant ≤0.05.

Effect on oxidative stress regulation genes

In this experiment, we tested the expression level of several important genes included in regulating the oxidation stress process: Superoxide dismutase 1 (SOD1), Superoxide dismutase 2 (SOD2), Thioredoxin reductase 1 (TXNRD1), Chloramphenicol Acetyltransferase (CAT), Glutathione Peroxidase 1 (GPX1) and Peroxisome proliferation-activated receptor gamma (PPARγ) as a member of the family of ligand-regulated nuclear hormone receptors in hyperglycemia samples transfected with 10 nM miR-146a-5p and with 50 nM miR-146a-5p.

First, we assessed the expression level of the following genes; SOD1, SOD2, TXNRD1, CAT, GPX1, and PPARγ in HG cells treated with 10 nM miR-146a-5p, and with 50 nM miR-146a-5p and compared to the hyperglycemia samples without treatment as a control group, as shown in Figure 27. The results showed significant

upregulation in the expression of important anti-oxidative stress genes with transfecting 50 nM miR-146a-5p; CAT by 141.8 folds, TXNRD1 by 62 folds, SOD1 by 31 folds, and GPX1 by 5.6 folds, while the expression of SOD2 and PPARγ was not affected. Transfecting with 10 nM miR-146a-5p increased the expression of two genes only, SOD1 and TXNRD1, by approximately 5 folds and 4 folds, respectively.

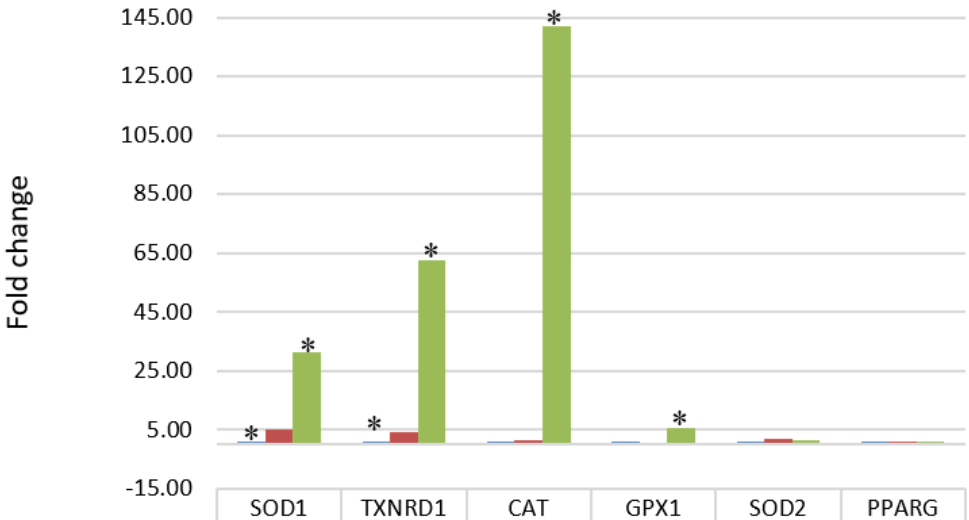

	SOD1	TXNRD1	CAT	GPX1	SOD2	PPARG
HG	1.00	1.00	1.00	1.00	1.00	1.00
10nM miR-146a	5.33	4.44	1.71	0.74	1.95	0.84
50nM miR-146a	31.20	62.73	141.79	5.64	1.31	1.11

Figure 27 Comparison of expression of genes included regulating oxidative stress between 10 nM and 50 nM miR-146a-5p with HG. Expression of SOD1, SOD2, TXNRD1, CAT, GPX1, and PPARγ in HG+ 10 nM miR-14a mimic and in HG+ 50 nM miR-14a mimic in comparison to HG sample. HG: High Glucose. All data in the graph represent the mean of n= 3 for each sample. Beta-actin (ACTB) is used as endogenous control. miR-146a-5p mimic concentration used are 10nM and 50nM. * indicate a significant difference of genes expression in HG HRECs treated with 10nM and 50nM miR-14a-5p mimic vs. HG HRECs without treatment, two tailed p value is significant ≤0.05.

Then, we assessed the expression level of SOD1, SOD2, TXNRD1, CAT, GPX1, and PPARγ genes between 10 nM miR-146a-5p and 50 nM miR-146a-5p in

hyperglycemia condition, Figure 28. The results showed significant upregulation in anti-oxidative stress genes' expression with transfecting 50 nM miR-146a-5p: CAT by 83 folds, TXNRD1 by 14 folds, SOD1 by 5.8 folds, and GPX1 by 7.5 folds in comparison to 10 nM miR-146a-5p. The finding revealed that 50 nM miR-146a-5p has a stronger anti-oxidative effect.

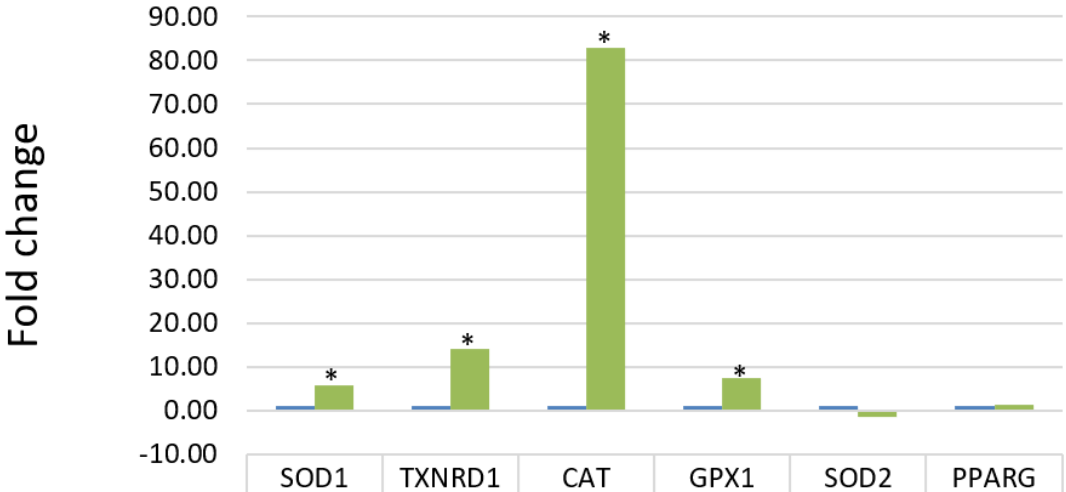

	SOD1	TXNRD1	CAT	GPX1	SOD2	PPARG
10nM miR-146a	1.00	1.00	1.00	1.00	1.00	1.00
50nM miR-146a	5.85	14.13	83.01	7.57	-1.48	1.32

Figure 28 Comparison of the expression of genes included in regulating oxidative stress between 10 nM and 50 nM miR-146a-5p. Expression of SOD1, SOD2, TXNRD1, CAT, GPX1, and PPARγ in HG+ 10 nM miR-14a mimic and in HG+ 50 nM miR-14a mimic. HG: High Glucose. All data in the graph represent the mean of n= 3 replicates for each sample. Beta-actin (ACTB) is used as endogenous control. miR-146a-5p mimic concentration= 10nM and 50nM. * indicate a significant difference of genes expression in HG HRECs treated with 50nM miR-14a-5p mimic vs. HG HRECs treated with 50nM miR-14a-5p mimic, two tailed p value is significant ≤0.05.

Effect on inflammatory and angiogenesis arrays

To identify genes or biological pathways, we determined the gene expression profiles of cells exposed to hyperglycemia (used as a control group) and cells exposed to HG + 50nM mimic miR-146a-5p (used as a treatment group). The cut-off value used

for significant expression in the present study was set as expressed fold changes of 2 and p-value of < 0.05. The expressed fold changes represent data of the treatment group (HG+ mimic miRNA) versus the control group (HG), as shown in Table 5. Table 5 shows a list of differential expressed genes in response to the application of 50nM mimic miR-146a-5p to hyperglycemic HRECs (treatment group) compared to HRECs exposed to hyperglycemia alone (control).

Table 5 List of angiogenesis and inflammatory panel genes identified by RT-PCR array profile, with their cellular location, molecular type, and expressed fold changes in hyperglycemic condition response to mimic miR-146a-5p transfection with a final concentration of 50nM.

Symbol	**Fold Change**	**Gene Name**	**Location**	**Type (s)**
IL21	10.32	interleukin 21	Extracellular Space	cytokine
CCR2	9.75	C-C motif chemokine receptor 2	Plasma Membrane	G-protein coupled receptor
THBS2	7.40	thrombospondin 2	Extracellular Space	other
CCL22	4.86	C-C motif chemokine ligand 22	Extracellular Space	cytokine
IL3	4.59	interleukin 3	Extracellular Space	cytokine
CCL23	4.09	C-C motif chemokine ligand 23	Extracellular Space	cytokine
CCR6	3.93	C-C motif chemokine receptor 6	Plasma Membrane	G-protein coupled receptor
CCL24	3.64	C-C motif chemokine ligand 24	Extracellular Space	cytokine
CSF3	3.34	colony stimulating factor 3	Extracellular Space	cytokine
TGFB2	3.26	transforming growth factor beta 2	Extracellular Space	growth factor

Symbol	Fold Change	Gene Name	Location	Type (s)
NADPH	3.11		Other	chemical - endogenous mammalian
CCR8	3.07	C-C motif chemokine receptor 8	Plasma Membrane	G-protein coupled receptor
TNFSF13	3.02	TNF superfamily member 13	Extracellular Space	cytokine
TNFSF11	2.91	TNF superfamily member 11	Extracellular Space	cytokine
IL1R1	2.86	interleukin 1 receptor type 1	Plasma Membrane	transmembrane receptor
ANGPTL4	2.50	angiopoietin like 4	Extracellular Space	other
PF4	2.32	platelet factor 4	Extracellular Space	cytokine
CCR1	2.31	C-C motif chemokine receptor 1	Plasma Membrane	G-protein coupled receptor
IL1RN	2.29	interleukin 1 receptor antagonist	Extracellular Space	cytokine
TNFRSF11B	2.19	TNF receptor superfamily member 11b	Plasma Membrane	transmembrane receptor
CDH5	2.17	cadherin 5	Plasma Membrane	other
SERPINE1	2.10	serpin family E member 1	Extracellular Space	other
CXCL12	2.09	C-X-C motif chemokine ligand 12	Extracellular Space	cytokine
PROK2	1.9	prokineticin 2	Extracellular Space	other
ANG	1.86	angiogenin	Extracellular Space	enzyme
CX3CL1	1.84	C-X3-C motif chemokine ligand 1	Extracellular Space	cytokine
TNFSF10	1.79	TNF superfamily member 10	Extracellular Space	cytokine

Symbol	Fold Change	Gene Name	Location	Type (s)
ENG	1.77	endoglin	Plasma Membrane	transmembrane receptor
FASLG	1.74	Fas ligand	Extracellular Space	cytokine
CCR3	1.62	C-C motif chemokine receptor 3	Plasma Membrane	G-protein coupled receptor
AKT1	1.62	AKT serine/threonine kinase 1	Cytoplasm	kinase
CCL13	1.61	C-C motif chemokine ligand 13	Extracellular Space	cytokine
IL10RB	1.61	interleukin 10 receptor subunit beta	Plasma Membrane	transmembrane receptor
IL10RA	1.57	interleukin 10 receptor subunit alpha	Plasma Membrane	transmembrane receptor
EPHB4	1.55	EPH receptor B4	Plasma Membrane	kinase
IGF1	1.55	insulin like growth factor 1	Extracellular Space	growth factor
CCL7	1.53	C-C motif chemokine ligand 7	Extracellular Space	cytokine
ID1	1.51	inhibitor of DNA binding 1, HLH protein	Nucleus	transcription regulator
NOS3	1.5	nitric oxide synthase 3	Cytoplasm	enzyme
ANPEP	1.47	alanyl aminopeptidase, membrane	Plasma Membrane	peptidase
NAMPT	1.36	nicotinamide phosphoribosyl transferase	Extracellular Space	cytokine
TNFSF13B	1.36	TNF superfamily member 13b	Extracellular Space	cytokine
FLT1	1.34	fms related receptor tyrosine kinase 1	Plasma Membrane	kinase
COL18A1	1.33	collagen type XVIII alpha 1 chain	Extracellular Space	other
LEP	1.31	leptin	Extracellular Space	growth factor

Symbol	Fold Change	Gene Name	Location	Type (s)
EDN1	1.3	endothelin 1	Extracellular Space	cytokine
IL17C	1.29	interleukin 17C	Extracellular Space	cytokine
PLAU	1.28	plasminogen activator, urokinase	Extracellular Space	peptidase
JAG1	1.24	jagged canonical Notch ligand 1	Extracellular Space	growth factor
IL16	1.22	interleukin 16	Extracellular Space	cytokine
IL15	1.16	interleukin 15	Extracellular Space	cytokine
CXCL9	1.15	C-X-C motif chemokine ligand 9	Extracellular Space	cytokine
PLG	1.15	plasminogen	Extracellular Space	peptidase
ITGAV	1.14	integrin subunit alpha V	Plasma Membrane	transmembrane receptor
CCR4	1.12	C-C motif chemokine receptor 4	Plasma Membrane	G-protein coupled receptor
IL33	1.12	interleukin 33	Extracellular Space	cytokine
THBS1	1.11	thrombospondin 1	Extracellular Space	other
FN1	1.1	fibronectin 1	Extracellular Space	enzyme
IL5	1.09	interleukin 5	Extracellular Space	cytokine
BMP2	1.03	bone morphogenetic protein 2	Extracellular Space	growth factor
IFNG	1.02	interferon gamma	Extracellular Space	cytokine
MMP2	1.01	matrix metallopeptidase 2	Extracellular Space	peptidase
TGFB1	1.01	transforming growth factor beta 1	Extracellular Space	growth factor

Symbol	Fold Change	Gene Name	Location	Type (s)
VEGFB	-1.01	vascular endothelial growth factor B	Extracellular Space	growth factor
TIMP2	-1.02	TIMP metallopeptidase inhibitor 2	Extracellular Space	other
KDR	-1.03	kinase insert domain receptor	Plasma Membrane	kinase
TEK	-1.03	TEK receptor tyrosine kinase	Plasma Membrane	kinase
CCL8	-1.07	C-C motif chemokine ligand 8	Extracellular Space	cytokine
IL9R	-1.07	interleukin 9 receptor	Plasma Membrane	transmembrane receptor
EFNB2	-1.08	ephrin B2	Plasma Membrane	kinase
CCL26	-1.09	C-C motif chemokine ligand 26	Extracellular Space	cytokine
NRP2	-1.09	neuropilin 2	Plasma Membrane	kinase
LTB	-1.10	lymphotoxin beta	Extracellular Space	cytokine
CXCR1	-1.11	C-X-C motif chemokine receptor 1	Plasma Membrane	G-protein coupled receptor
CNMD	-1.11	tenomodulin	Extracellular Space	other
CCN2	-1.13	cellular communication network factor 2	Extracellular Space	growth factor
MMP14	-1.13	matrix metallopeptidase 14	Extracellular Space	peptidase
SPHK1	-1.14	sphingosine kinase 1	Cytoplasm	kinase
CCR5	-1.15	C-C motif chemokine receptor 5 (gene/pseudogene)	Plasma Membrane	G-protein coupled receptor
PDGFA	-1.16	platelet derived growth factor subunit A	Extracellular Space	growth factor
CCL11	-1.17	C-C motif chemokine ligand 11	Extracellular Space	cytokine

Symbol	Fold Change	Gene Name	Location	Type (s)
EGF	-1.23	epidermal growth factor	Extracellular Space	growth factor
HIF1A	-1.23	hypoxia inducible factor 1 subunit alpha	Nucleus	transcription regulator
CXCL8	-1.26	C-X-C motif chemokine ligand 8	Extracellular Space	cytokine
FGF2	-1.28	fibroblast growth factor 2	Extracellular Space	growth factor
NRP1	-1.30	neuropilin 1	Plasma Membrane	transmembrane receptor
TGFA	-1.31	transforming growth factor alpha	Extracellular Space	growth factor
TIE1	-1.34	tyrosine kinase with immunoglobulin like and EGF like domains 1	Plasma Membrane	kinase
PTGS1	-1.41	prostaglandin-endoperoxide synthase 1	Cytoplasm	enzyme
MMP9	-1.42	matrix metallopeptidase 9	Extracellular Space	peptidase
S1PR1	-1.43	sphingosine-1-phosphate receptor 1	Plasma Membrane	G-protein coupled receptor
CCL20	-1.48	C-C motif chemokine ligand 20	Extracellular Space	cytokine
IL27	-1.52	interleukin 27	Extracellular Space	cytokine
PECAM1	-1.53	platelet and endothelial cell adhesion molecule 1	Plasma Membrane	other
TYMP	-1.56	thymidine phosphorylase	Extracellular Space	growth factor
OSM	-1.57	oncostatin M	Extracellular Space	cytokine
ITGB3	-1.59	integrin subunit beta 3	Plasma Membrane	transmembrane receptor
TGFBR1	-1.60	transforming growth factor beta receptor 1	Plasma Membrane	kinase
ANGPT2	-1.62	angiopoietin 2	Extracellular Space	growth factor

Symbol	Fold Change	Gene Name	Location	Type (s)
ERBB2	-1.62	erb-b2 receptor tyrosine kinase 2	Plasma Membrane	kinase
MDK	-1.69	midkine	Extracellular Space	growth factor
HPSE	-1.71	heparanase	Plasma Membrane	enzyme
EFNA1	-1.72	ephrin A1	Plasma Membrane	other
TIMP1	-1.72	TIMP metallopeptidase inhibitor 1	Extracellular Space	cytokine
IFNA1/IFNA13	-1.74	interferon alpha 1	Extracellular Space	cytokine
IL17A	-1.76	interleukin 17A	Extracellular Space	cytokine
MIF	-1.76	macrophage migration inhibitory factor	Extracellular Space	cytokine
IL1B	-1.76	interleukin 1 beta	Extracellular Space	cytokine
CCL15	-1.78	C-C motif chemokine ligand 15	Extracellular Space	cytokine
CXCL11	-1.79	C-X-C motif chemokine ligand 11	Extracellular Space	cytokine
ANGPT1	-1.85	angiopoietin 1	Extracellular Space	growth factor
FGFR3	-1.86	fibroblast growth factor receptor 3	Plasma Membrane	kinase
AIMP1	-1.93	aminoacyl tRNA synthetase complex interacting multifunctional protein 1	Extracellular Space	cytokine
CCL5	-1.97	C-C motif chemokine ligand 5	Extracellular Space	cytokine
IFNA2	-2.04	interferon alpha 2	Extracellular Space	cytokine
IL13	-2.05	interleukin 13	Extracellular Space	cytokine

Symbol	Fold Change	Gene Name	Location	Type (s)
CCL16	-2.27	C-C motif chemokine ligand 16	Extracellular Space	cytokine
PGF	-2.41	placental growth factor	Extracellular Space	growth factor
IL6	-2.42	interleukin 6	Extracellular Space	cytokine
VEGFC	-2.51	vascular endothelial growth factor C	Extracellular Space	growth factor
CXCR2	-2.57	C-X-C motif chemokine receptor 2	Plasma Membrane	G-protein coupled receptor
VEGFA	-2.83	vascular endothelial growth factor A	Extracellular Space	growth factor
HGF	-2.93	hepatocyte growth factor	Extracellular Space	growth factor
FGF1	-3.00	fibroblast growth factor 1	Extracellular Space	growth factor
NOTCH4	-3.00	notch receptor 4	Plasma Membrane	transcription regulator
CD40LG	-3.26	CD40 ligand	Extracellular Space	cytokine
TIMP3	-3.28	TIMP metallopeptidase inhibitor 3	Extracellular Space	other
CXCL6	-4.22	C-X-C motif chemokine ligand 6	Extracellular Space	cytokine
CCL3	-4.29	C-C motif chemokine ligand 3	Extracellular Space	cytokine
IL9	-4.35	interleukin 9	Extracellular Space	cytokine
COL4A3	-4.36	collagen type IV alpha 3 chain	Extracellular Space	other
SERPINF1	-4.84	serpin family F member 1	Extracellular Space	other
IL7	-5.00	interleukin 7	Extracellular Space	cytokine
TNFSF4	-6.12	TNF superfamily member 4	Extracellular Space	cytokine

Symbol	Fold Change	Gene Name	Location	Type (s)
IL5RA	-6.19	interleukin 5 receptor subunit alpha	Plasma Membrane	transmembrane receptor
F3	-6.35	coagulation factor III, tissue factor	Plasma Membrane	transmembrane receptor
CXCL5	-6.70	C-X-C motif chemokine ligand 5	Extracellular Space	cytokine
IL1A	-6.94	interleukin 1 alpha	Extracellular Space	cytokine
CCL17	-7.02	C-C motif chemokine ligand 17	Extracellular Space	cytokine
CXCL3	-7.72	C-X-C motif chemokine ligand 3	Extracellular Space	cytokine
TNF	-7.95	tumor necrosis factor	Extracellular Space	cytokine
TNF	-7.95	tumor necrosis factor	Extracellular Space	cytokine
TRAF6	-8.00	TNF receptor associated factor 6	Cytoplasm	enzyme
ICAM1	-8.00	intercellular adhesion molecule 1	Plasma Membrane	transmembrane receptor
CXCL10	-8.36	C-X-C motif chemokine ligand 10	Extracellular Space	cytokine
LTA	-8.49	lymphotoxin alpha	Extracellular Space	cytokine
VEGFD	-9.00	vascular endothelial growth factor D	Extracellular Space	growth factor
ADGRB1	-9.59	adhesion G protein-coupled receptor B1	Plasma Membrane	G-protein coupled receptor
CCL2	-11.04	C-C motif chemokine ligand 2	Extracellular Space	cytokine
IL17F	-14.86	interleukin 17F	Extracellular Space	cytokine
CX3CR1	-16.31	C-X3-C motif chemokine receptor 1	Plasma Membrane	G-protein coupled receptor
CSF1	-17.7	colony stimulating factor 1	Extracellular Space	cytokine

Symbol	Fold Change	Gene Name	Location	Type (s)
SPP1	-17.71	secreted phosphoprotein 1	Extracellular Space	cytokine
CXCL13	-18.24	C-X-C motif chemokine ligand 13	Extracellular Space	cytokine
CXCL1	-19.23	C-X-C motif chemokine ligand 1	Extracellular Space	cytokine
CXCL2	-19.29	C-X-C motif chemokine ligand 2	Extracellular Space	cytokine
CCL4	-21.38	C-C motif chemokine ligand 4	Extracellular Space	cytokine
CSF2	-24.26	colony stimulating factor 2	Extracellular Space	cytokine

The dataset displays 94 downregulated and 96 upregulated genes of both inflammatory and angiogenesis panels (Figure 29, 30). Only, twenty-two genes displayed fold change above 2, and 33 gens displayed fold change below 2. The Data represent the differentially expressed dysregulated genes (DRGs), which were further evaluated to obtain details of biological processes, cellular functions, networks, and

signaling pathways related to HRECs exposed to hyperglycemia and treated with 50nM mimic miR-146a-5p.

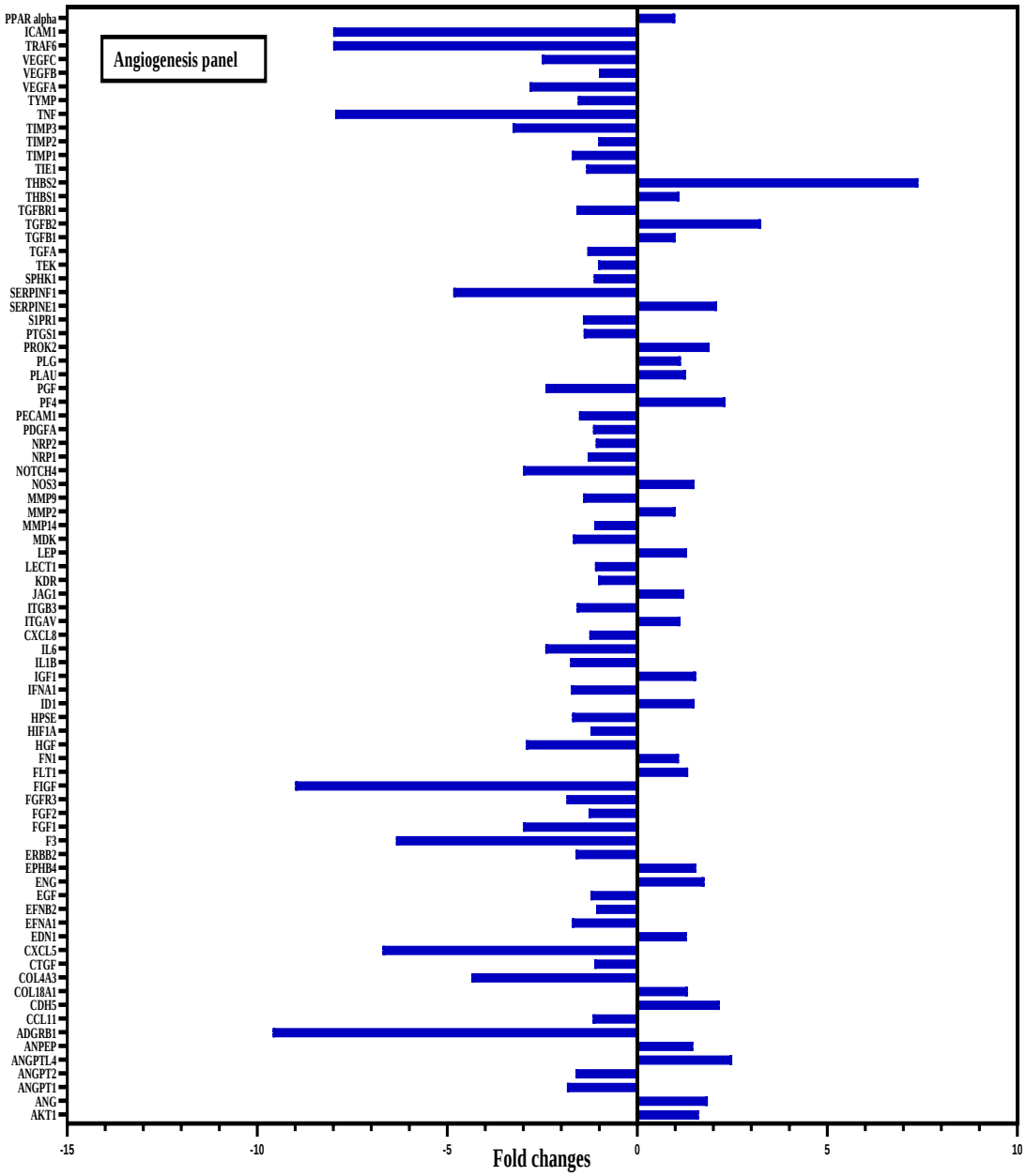

Figure 29 The list of differentially expressed genes of the angiogenesis panel in HRECs exposed to hyperglycemia and transfected with 50nM mimic miR-146a-5p compared to HRECs treated with only hyperglycemia. Data represent the fold changes in gene expression of the angiogenesis panel. n=1.

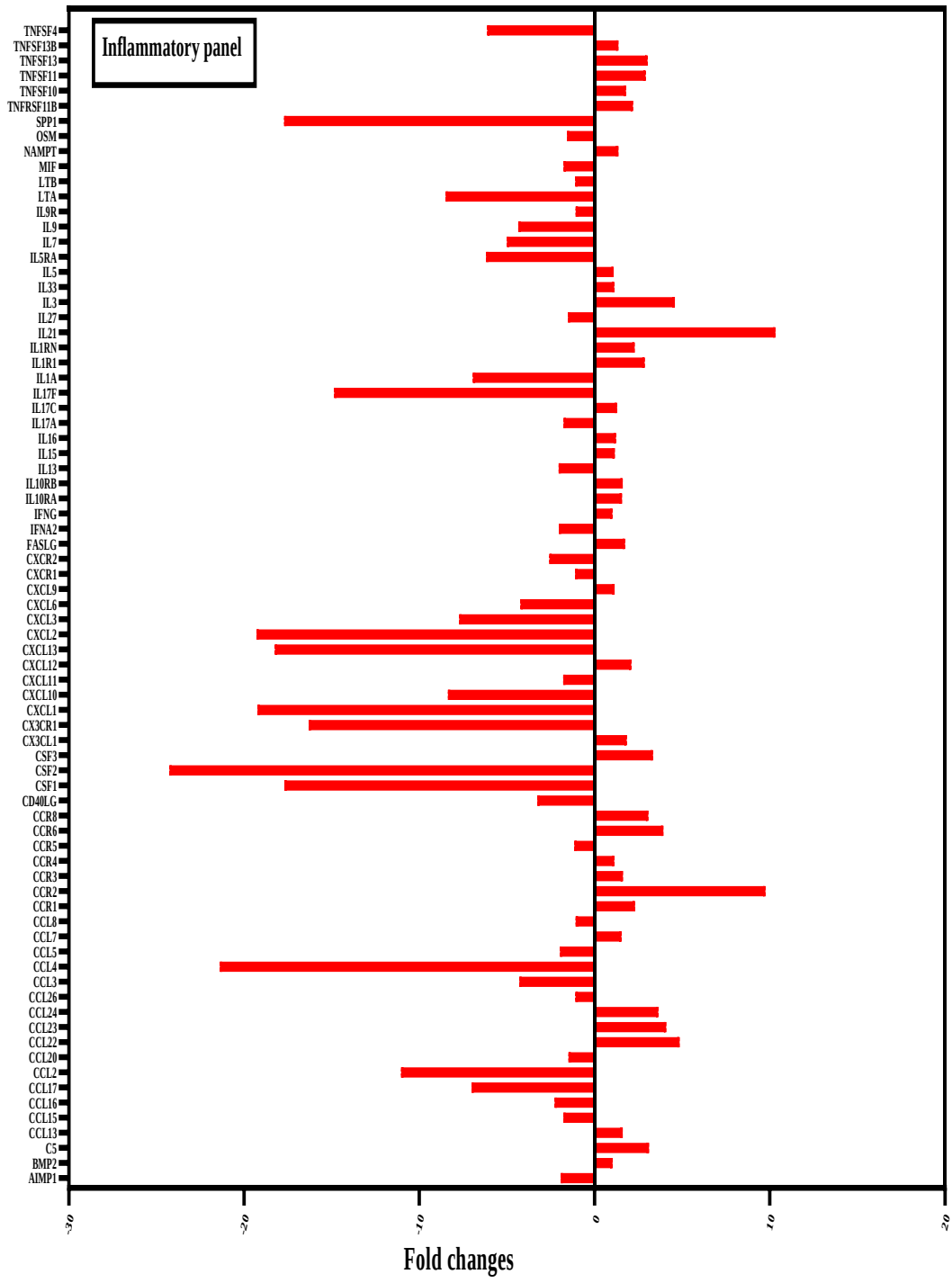

Figure 30 The list of differentially expressed genes of the inflammatory panel in HRECs exposed to hyperglycemia and transfected with 50nM mimic miR-146a-5pcompared to HRECs treated with only hyperglycemia. Data represent the fold changes in gene expression of the inflammatory panel. n=1.

Bioinformatics analysis

To further determine the biological significance and functional classification of the genes, bioinformatic tools were used. Metscape enrichment pathways analysis (metascape.org) demonstrated the most important enriched terms across the input gene lists for pathways and biological process, clustered and colored by p-values as shown in Table 6 and Figure 31. These pathways and biological processes are in order, and the top five with percentages were cytokine-cytokine receptor interaction (56.69%), angiogenesis (48.41%), chemotaxis (49.04%), positive regulation of locomotion (42.04%), Cytokine Signaling in Immune system (42.68%).

Table 6 Top 20 clusters with their representative enriched terms (one per cluster). Gene annotations extracted from the list of all angiogenesis and inflammatory panel genes in response to 50nM mimic miR-146a-5p in hyperglycemic conditions of HRECs, relative to HRECs treated with HG alone.

GO	Category	Description	Count	%	Log10 (P)	Log10 (q)
ko04060	KEGG Pathway	Cytokine-cytokine receptor interaction	89	56.69	-100.00	-96.12
GO:0001525	GO Biological Processes	angiogenesis	76	48.41	-84.43	-80.77
GO:0006935	GO Biological Processes	chemotaxis	77	49.04	-82.96	-79.38
GO:0040017	GO Biological Processes	positive regulation of locomotion	66	42.04	-67.07	-63.99
R-HSA-1280215	Reactome Gene Sets	Cytokine Signaling in Immune system	67	42.68	-64.11	-61.11
GO	**Category**	**Description**	**Count**	**%**	**Log10 (P)**	**Log10 (q)**

GO:0043410	GO Biological Processes	positive regulation of MAPK cascade	55	35.03	-53.24	-50.31
ko05323	KEGG Pathway	Rheumatoid arthritis	29	18.47	-43.13	-40.42
GO:0030155	GO Biological Processes	regulation of cell adhesion	49	31.21	-38.26	-35.63
hsa04151	KEGG Pathway	PI3K-Akt signaling pathway	39	24.84	-37.30	-34.68
GO:0050918	GO Biological Processes	positive chemotaxis	24	15.29	-36.98	-34.37
ko04657	KEGG Pathway	IL-17 signaling pathway	25	15.92	-34.86	-32.30
GO:0018108	GO Biological Processes	peptidyl-tyrosine phosphorylation	36	22.93	-33.28	-30.77
WP530	Wiki Pathways	Cytokines and Inflammatory Response	17	10.83	-32.22	-29.75
GO:0043491	GO Biological Processes	protein kinase B signaling	30	19.11	-29.40	-27.02
ko04933	KEGG Pathway	AGE-RAGE signaling pathway in diabetic complications	22	14.01	-28.64	-26.27
GO:0010631	GO Biological Processes	epithelial cell migration	32	20.38	-28.50	-26.14
GO:0009611	GO Biological Processes	response to wounding	37	23.57	-24.85	-22.56
GO:0048771	GO Biological Processes	tissue remodeling	23	14.65	-24.11	-21.86
GO:0030198	GO Biological Processes	extracellular matrix organization	29	18.47	-23.35	-21.11
GO:0002521	GO Biological Processes	leukocyte differentiation	32	20.38	-23.27	-21.04

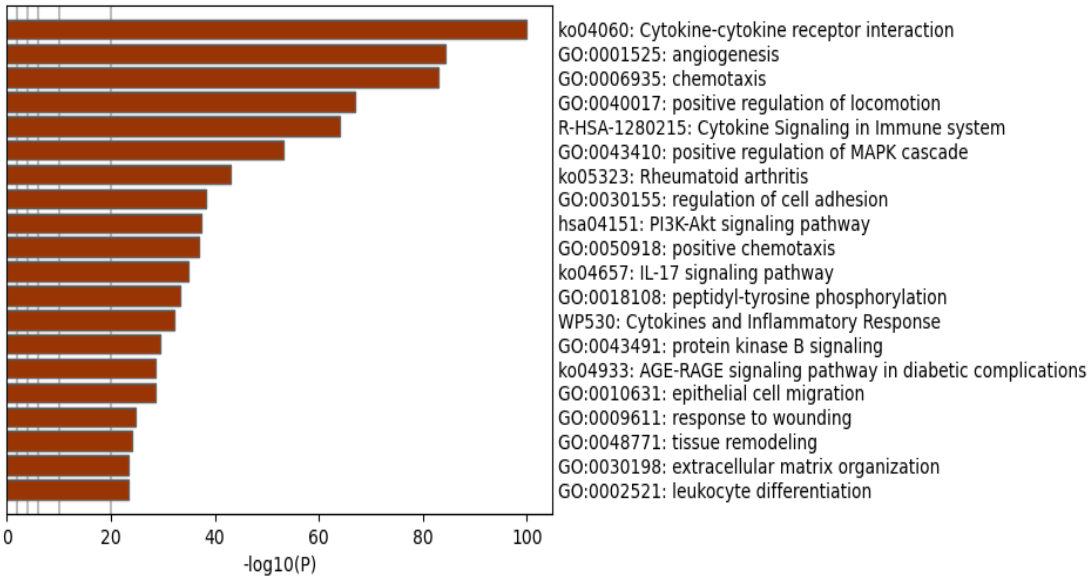

Figure 31 Bar graph of enriched terms across input gene lists, colored by p-values.

To better understand the detailed mechanisms involved, identify the primary cellular targets that modify endothelial dysfunction of microvascular retinal cells exposed to hyperglycemia, and to determine the changes caused by miR-146a-5p transfection, the dataset was integrated into Ingenuity Pathway Analysis (IPA) software using core analysis. Identifying each gene's role in the data set is important; however, the interaction of several genes plays a fundamental role in the outcome of various biological, cellular process, and molecular functions and regulations by transcription factors, hence important to be identified.

The most enriched canonical pathways detected in the hyperglycemic microvascular endothelial cells in response to transfection by miR-146a-5p based on log p value are shown in Table 7 and Figure 32. Notably, the dominant five pathways detected in the log p values are Il-17 signaling pathway; Agranulocyte Adhesion; and Diapedesis; HMGB1 Signaling; Glucocorticoid Receptor Signaling; and MSP-RON Signaling Pathway. As shown in Figure 32 and Table 7, several of these signaling pathways affect TRAF6 gene expression. In addition, data obtained from GO analysis

indicate that downregulation of the target genes of miR-146a-5p after transfection of hyperglycemic HRECs involved many signaling pathways, as indicated in Table 7 such as Il-17 signaling pathway, Glucocorticoid Receptor Signaling, IL-8 Signaling, p38 MAPK Signaling, IL-10 Signaling, Acute Phase Response Signaling, Toll-like Receptor Signaling, PPAR Signaling, Th17 Activation Pathway, and IL-6 Signaling. These results demonstrate the pleiotropic effects of miR-146a-5p on gene expression via different pathways, as displayed in Table 7.

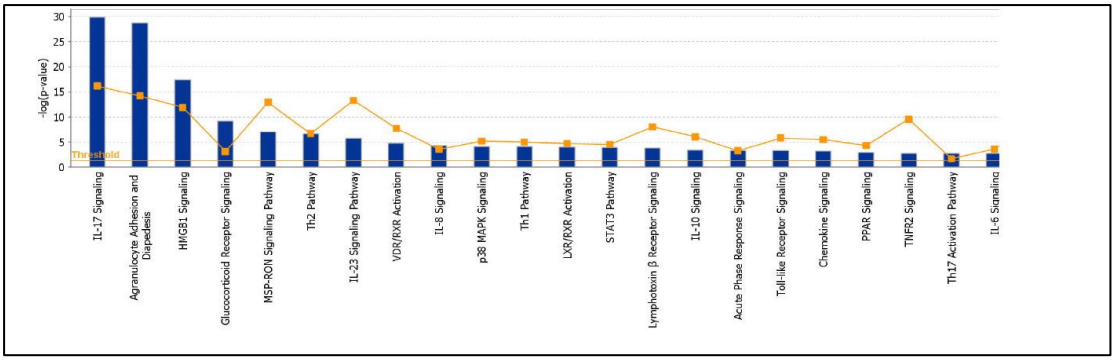

Figure 32 Displays a conical illustration of the top 22 significant enriched pathway analysis in the HRECs dataset, which is differentially expressed genes transfected with 50nM of miR-146a-5p mimic. Data are presented as a bar on X-axis. Y-axes indicate the log (p-value) of the dataset of the studied genes compared to the IPA knowledge base.

Table 7. Top 22 Canonical Pathways of genes of the HRECs transfected with mimic miR-146a-5p with their p- values. (Based on Core Analysis in Ingenuity Pathway Analysis (IPA). Bold word shown in molecules refers to three target genes evaluated after transfection of HRECs with 50nM of miR-146a-5p mimic. Data showed many signaling pathways contribute to its expression level, as shown in table 7.

IPA Canonical Pathways	**Log (p-value)**	**Ratio**	**Molecules**

IL-17 Signaling	30	0.106	CCL17, CCL2, CCL22, CD40LG, CSF2, CSF3, CXCL1, CXCL3, CXCL5, IL17F, IL1A, IL21, IL3, LTA, TGFB2, **TNF**, SF13, TNFSF4, **TRAF6**, VEGFD
Agranulocyte Adhesion and Diapedesis	28.8	0.093	CCL17, CCL2, CCL22, CCL23, CCL24, CCL3, CCL4, CCR2, CCR6, CCR8, CXCL1, CXCL10, CXCL13, CXCL2, CXCL3, CXCL5, CXCL6, **ICAM1**, IL1A, **TNF**
HMGB1 Signaling	17.4	0.0778	CCL2, CD40LG, CSF2, **ICAM1**, IL17F, IL1A, IL21, IL3, LTA, TGFB2, **TNF**, SF13, TNFSF4
Glucocorticoid Receptor Signaling	9.17	0.0203	CCL2, CCL3, CSF2, CXCL3, **ICAM1**, IL1A, IL3, IL5RA, IL9, TGFB2, **TNF, TRAF6**
MSP-RON Signaling Pathway	7.05	0.0847	CCL2, CCR2, CSF1, IL3, **TNF**
Th2 Pathway	6.66	0.0438	CCR8, **ICAM1**, IL3, IL9, NOTCH4, **TNF**, SF4
IL-23 Signaling Pathway	5.77	0.087	CSF2, IL17F, IL21, **TNF**
VDR/RXR Activation	4.83	0.0506	CSF2, CXCL10, SPP1, TGFB2
IL-8 Signaling	4.29	0.0233	CXCL1, **ICAM1**, IL9, **TRAF6**, VEGFD
p38 MAPK Signaling	4.14	0.0339	IL1A, TGFB2, **TNF**, **TRAF6**
Th1 Pathway	4.07	0.0325	CD40LG, **ICAM1**, LTA, NOTCH4
LXR/RXR Activation	3.98	0.0308	CCL2, IL1A, SERPINF1, **TNF**
STAT3 Pathway	3.9	0.0294	IL1A, IL5RA, IL9, TGFB2
Lymphotoxin β Receptor Signaling	3.77	0.0526	CXCL1, LTA, **TRAF6**
IL-10 Signaling	3.4	0.0395	IL1A, **TNF**, **TRAF6**

IPA Canonical Pathways	**Log (p-value)**	**Ratio**	**Molecules**
Acute Phase Response Signaling	3.37	0.0214	IL1A, SERPINF1, **TNF**, **TRAF6**

Toll-like Receptor Signaling	3.35	0.038	IL1A, **TNF, TRAF6**
Chemokine Signaling	3.27	0.0357	CCL2, CCL24, CCL4
PPAR Signaling	2.97	0.028	IL1A, **TNF, TRAF6**
TNFR2 Signaling	2.78	0.0625	LTA, **TNF**
Th17 Activation Pathway	2.76	0.0108	CCR6, CSF2, IL17F, IL21, **TRAF6**
IL-6 Signaling	2.74	0.0234	IL1A, **TNF, TRAF6**

Epigenetic factors involved in response to mimic miR-146a-5p

miR-146a-5p and transcription factors (TF)

The binding of miRNAs to 3′ UTR and coding regions of mRNA has silencing effects on gene expression. The miRNA interaction with the promoter region has been reported to induce transcription. Table 8 shows the most important TF.

Table 8. The transcription factors as upstream regulators in response to transfection of hyperglycemic HRECs by miR-146a-5p. Data represent the list of transcription factors, z- score of activation or inhibition, overlap p-value, and the target molecules affected by these TF as upstream regulators in response to t the transfection of hyperglycemic HRECs to mimic transfection of miR-146a-5p (50nM).

Upstream Regulator	**Predicted Activation State**	**Activation z-score**	**p-value of overlap**
ZNF281	Activated	2.646	9.88^{E-19}
ZFP36	Activated	2.242	1.1^{E-15}
HAND1	Activated	2.121	4.23^{E-11}

GFI1	Activated	2.112	1.8^{E-16}
TWIST2	Activated	2.195	4.62^{E-06}
FEM1A	Activated	2.415	1.91^{E-12}
KLF2	Activated	2.187	1.28^{E-56}
BCL6	Activated	2.443	3.34^{E-19}
GPS2	Activated	2.571	1.97^{E-07}
HNF4A	Activated	2.72	3.95^{E-5}
BCL3	Activated	3.713	1.33^{E-21}
NCOA2	Activated	2.044	4.24^{E-08}
MEOX2	Activated	2.938	3.29^{E-34}
SIRT1	Activated	2.023	1.57^{E-15}
ARID1A	Activated	2.449	8.66^{E-07}
CBL	Activated	2.003	4.07^{E-12}
CITED2	Activated	2.795	2.68^{E-13}
NFAT5	Inhibited	-2.118	2.87E-19
NOTCH4	Inhibited	-2.236	7.88^{E-07}
IRF8	Inhibited	-2.32	7.11^{E-13}
ISL1	Inhibited	-2.236	0.000479 4.79^{E-6}
TGIF1	Inhibited	-2.398	4.57^{E-15}

Upstream Regulator	**Predicted Activation State**	**Activation z-score**	**p-value of overlap**
STAT4	Inhibited	-2.396	1.25^{E-07}
JUN	Inhibited	-3.312	2.26^{E-38}
CEBPB	Inhibited	-2.018	4.55^{E-23}

POU5F1	Inhibited	-2.178	4.02^{E-20}
TFEB	Inhibited	-2.219	2.22^{E-05}
PML	Inhibited	-2.183	0.00686 6.86^{E-5}
IFI16	Inhibited	-2.452	3.03^{E-18}
EGR1	Inhibited	-2.194	1.21^{E-40}
SMAD3	Inhibited	-2.239	2.45^{E-35}
HOXB7	Inhibited	-2.043	5.1^{E-14}
TCF4	Inhibited	-2.333	5.78^{E-07}
NFKB1	Inhibited	-2.527	8.82^{E-46}
RELA	Inhibited	-3.01	2.24^{E-46}
BCL10	Inhibited	-2.01	3.31^{E-14}
IRF5	Inhibited	-2.036	5.76^{E-16}
CREBBP	Inhibited	-2.918	1.52^{E-15}
HMGB1	Inhibited	-3.62	3.79^{E-25}

As shown in Table 8, The most important TF involved based on the Z-score of activation is MEOX2 (z- score of 2.94), while HMGB1 is the most TF inhibited with (z–value of -3.62). Figure 33 shows the most TFs and canonical pathways involved in miR-146a-5p regulation. The data clearly indicate that many pathways, TF, and intermediate regulators interact to affect the downregulation of TNF expression through different mechanisms and pathways.

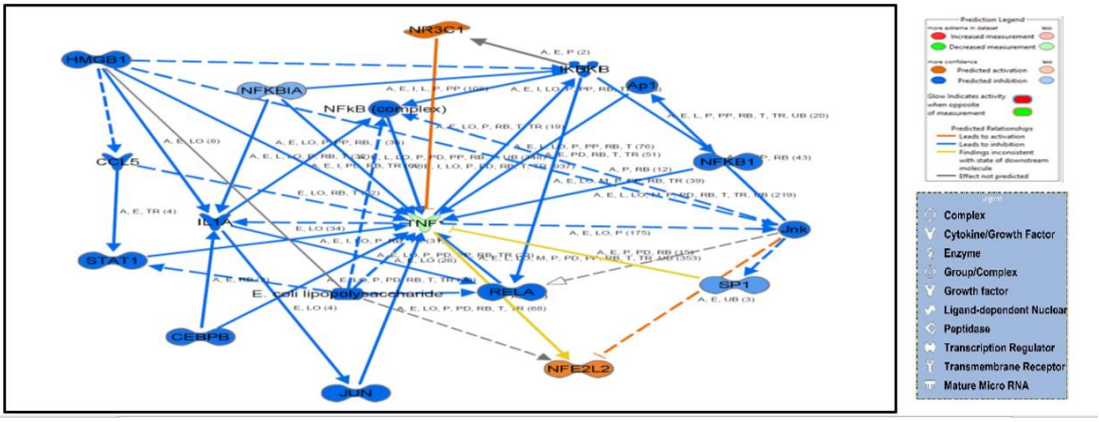

Figure 33 Regulation of TNF gene expression in response to transfection of hyperglycemic HRECs with miR-146a-5p by HMGB1 TF. Data represent nodes in blue indicating the inhibited activity of HMGB1 (blue) as a transcription factor and how it cross-talk with other TF and transcription regulators and molecules to affect TNF gene expression (green) via different mechanistic pathways and indirect effects in response to transfection by mimic miR-146a-5p. Abbreviation; blue arrow= inhibition, brown arrow= activation. Solid arrow = active, dot arrow-= weak effect. Blue color of nodes = inhibition and orange = activation. Green color of TNF means decreased expression. E= expression, LO= localization, A= activation, protein- DNA interaction (PD), (P), and transcription (T), causative (C).

Furthermore, in Table 9, the relations exerted by TF HMGB1on molecules in the network are shown.

Table 9 Displays the relationship exerted by the transcription factor HMGB1 on molecules of the network in Figure 33.

From Molecule(s)	Relationship Type	To Molecule(s)
HMGB1	activation	CCL5
HMGB1	activation	IKBKB
HMGB1	activation	IL1A
From Molecule(s)	**Relationship Type**	**To Molecule(s)**
HMGB1	activation	Jnk
HMGB1	activation	TNF

HMGB1	chemical-protein interactions	E. coli lipopolysaccharide
HMGB1	expression	IL1A
HMGB1	expression	TNF
HMGB1	localization	CCL5
HMGB1	localization	IL1A
HMGB1	localization	TNF
HMGB1	phosphorylation	Jnk
HMGB1	protein-protein interactions	TNF
HMGB1	transcription	TNF

Further, the pathways and TFs affecting the gene expression of TNF and Il-6 were investigated, as both genes are downregulated in response to transfection by mimic miR-146a-5p (50nM) in hyperglycemic HRECs. Previous data published by our lab indicated the critical role of these two molecules in the diabetic complications of human subjects (Cheema et al., 2020). Analysis of Figure 34 demonstrates that several TFs regulating TNF and IL6, such as Jun, STAT4, NFKB1, and RELA, are inhibited in response to miR-146a-5p (50nM) overexpression and by the activated TF MEOX2.

Furthermore, involvement of several CP pathways such as apoptosis, PPARα /RXRα, IL-10, IL-6, NFKB, TNFR2, and NO and ROS production was identified.

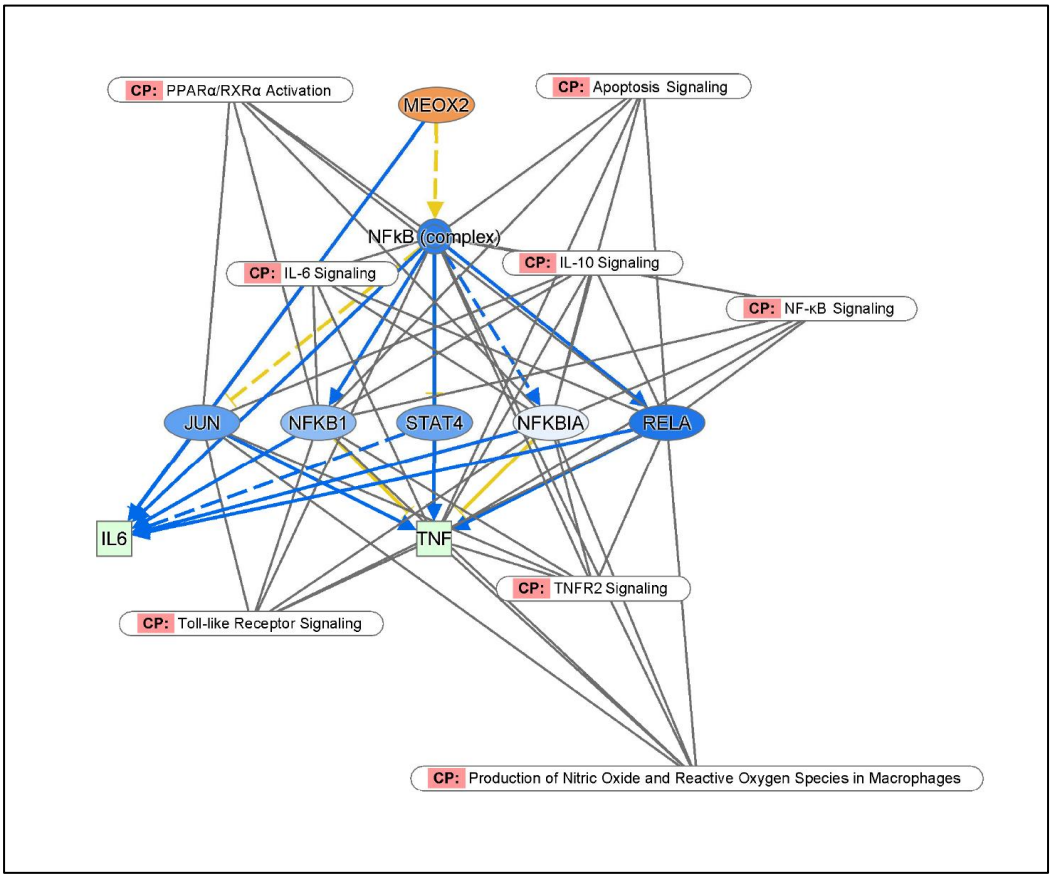

Figure 34 Regulation of TNF gene expression in response to transfection of hyperglycemic HRECs with miR-146a-5p (50nM) showing the most TFs and canonical pathways involved in its regulation. Data represent Nodes in blue indicating inhibited activity of JUN, NFKB1, STAT4, RELA (blue), while the increased activity of MEOX2 (orange) as a transcription factor and how it cross-talk with different canonical pathways to affect TNF and IL6 gene expression (green) via different mechanistic pathways whether direct and indirect effects in response to transfection by mimic miR-146a-5p (50nM). Abbreviation; blue arrow= inhibition, brown arrow= activation. Solid arrow = active, dot arrow-= weak effect. Blue color of nodes = inhibition and orange = activation. Green color of TNF means decreased expression. E= expression, LO= localization, A= activation, protein- DNA interaction (PD), (P), and transcription (T), causative (C). CP= canonical pathway.

Further, we investigated the mechanistic network by which miR-146a-5p exert its effects on the downstream target genes, as shown in Figure 35 and Table 10. As displayed, the RNA-RNA interactions: microRNA targeting could involve activation of activator protein-1, c-Jun (Ap1) as complex Group of TF, which in turn downregulates the expression of ICAM1 and VEGFA via different routes such as expression, transcription, and protein-DNA interactions. IL10, as is a cytokine that affects TNF expression via different mechanisms such as regulation of binding, expression, and localization. NFKB1 affects the expression and activation of ICAM1. In summary, overexpression of miR-146a-5p (50nM) in HRECs exposed to high glucose affects the expression of several genes of interest in this study, such as TARF6, TNF-α IL6, ICAM1, VEGFA, and MMP. These genes are involved in endothelial function, such as response to inflammation and angiogenesis.

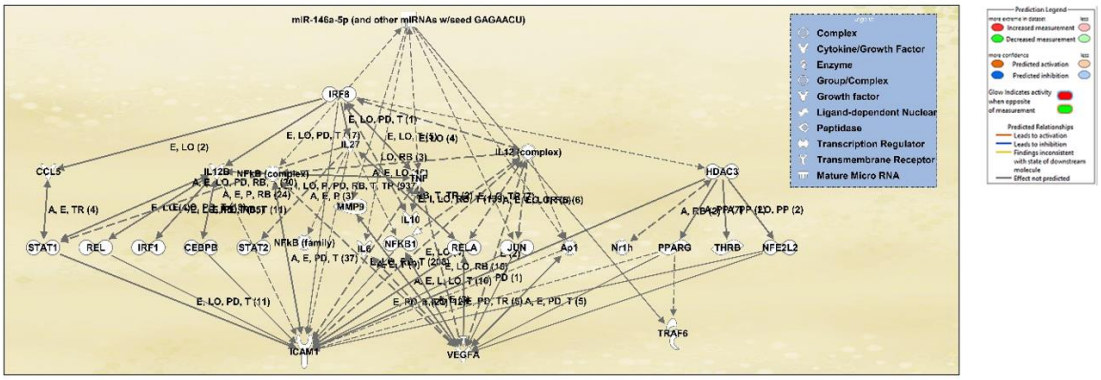

Figure 35 Mechanistic network showing the effect of overexpressed miRNA 146a-5p (50nM) in HRECs on the expression of TRAF6, VEGFA, TNF, MMP9, IL10, and ICAM1 genes in hyperglycemic conditions. Data represent the mechanistic pathways by which overexpression of miR-146a-5p regulates the downstream target genes TRAF6, VEGFA, TNF, MMP9, IL10, and ICAM1 genes in hyperglycemic conditions. Nodes in represent different regulators such as TF; JUN, NFKB1, STAT1, STAT 2, IRF1, RELA; ligand-dependent nuclear receptor such as PPARG; complex regulators such as NFkB (complex), and how it cross talk to affect the downstream gene

expression via different mechanistic pathways whether direct and indirect effects in response to transfection by mimic miRNA 146-a. Abbreviation; E= expression, LO= localization, A= activation, protein- DNA interaction (PD), (P), and transcription (T), causative (C). See legends for molecule type in blue and prediction legend too. See Table 10 for more details about relations.

Table 10 Displays the relationship exerted by the miR-146a-5p on molecules of the network in Figure 35

From Molecule(s)	Relationship Type	To Molecule(s)
miR-146a-5p	RNA-RNA interactions: microRNA targeting	TRAF6
miR-146a-5p	activation	Ap1
miR-146a-5p	activation	JUN
miR-146a-5p	activation	NFkB (complex)
miR-146a-5p	expression	IL6
miR-146a-5p	expression	TNF
miR-146a-5p	expression	TRAF6
miR-146a-5p	localization	IL6
miR-146a-5p	localization	MMP9
miR-146a-5p	phosphorylation	JUN

Further, in Figure 36, we explored the IL-8 signaling with crosstalk of miR-146a-5p (50nM) transfected in HRECs exposed to high glucose. As shown in Figure 35, the network illustrates the pathways and interactions between IL-8 signaling and endothelial functions of HRECs exposed to high glucose after transfection with miR-146a-5p. IL-8 causes activation of CXCR1/R2, which activates IRAK receptor, which

in turn activates TRAF6, while miR-146a-5p downregulates TRAF6 gene expression activates IRAK receptor, which activates TRAF6. In contrast, miRNA146a downregulates TRAF6 gene expression via its effects on protein-protein interactions and ubiquitination of STAT3 inhibition, which in turn causes inhibition of angiogenesis. Several pathways are illustrated, such as IL-8 may affect the phosphorylation of IκB, which affects the activity of P60NFkB, which in sequence affects transcription of Cox2 expression, which causes inhibition of the inflammation and downregulates the expression of VCAM1 and ICAM1, which causes inhibition of angiogenesis.

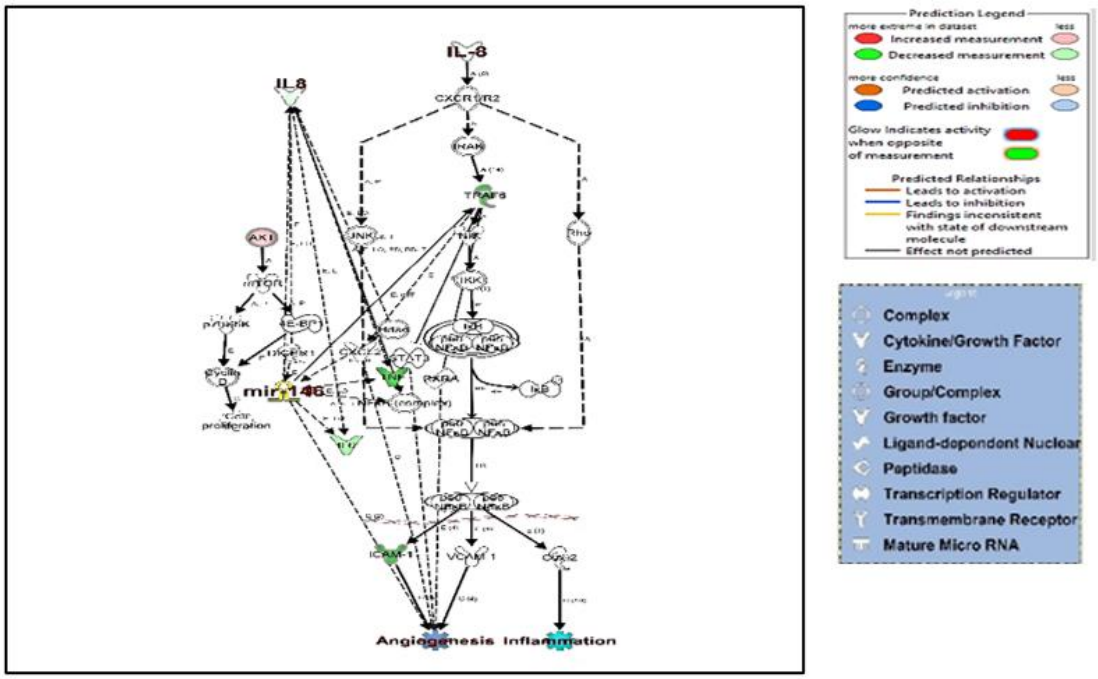

Figure 36 Network displays IL-8 signaling pathway and crosstalk with miR-146a-5p on inflammation and angiogenesis functions. Network illustrates the pathways and interactions between IL-8 signaling and endothelial functions of HRECs exposed to high glucose after transfection with miR-146a-5p (50nM). Il-8 causes activation of CXCR1/R2, which activates IRAK receptor, which activates TRAF6, while miRNA146a downregulates TRAF6 gene expression that affects protein-protein

interactions and ubiquitination of STAT3 inhibition, which in turn causes inhibition of angiogenesis. Several pathways are illustrated, such as IL-8 may affect the phosphorylation of IκB, which affects the activity of P60NFkB, which in sequence affects transcription of Cox2 expression, which causes inhibition of the inflammation and downregulates the expression of VCAM1and ICAM1, which causes inhibition of angiogenesis. See legends for details.

CHAPTER 6: DISCUSSION

Diabetic retinopathy is a microvascular complication of diabetes and a major cause of visual impairment and blindness among the working-age population. The stable condition of high blood glucose is the main factor of DR, which activates several mechanisms and pathways contributing to disease pathogenesis. Currently, there are several therapeutic options; however, the failure of a successful response to these available treatments is common among DR patients. A recent approach by researchers focuses on studying the effect of miRNAs and gene regulation in DR to develop effective molecular therapeutic strategies. One of the widely investigated miRNAs in DR is miR-146a-5p which has shown promising anti-inflammatory effects. In this study, we assessed the impact of transfecting low and high doses of miR-146a-5p mimic and inhibitor on HRECs exposed to hyperglycemia.

First, in the current study, we did not demonstrate any significant difference in cell viability between HRECs exposed to normoglycemia (5.5mM) or to high glucose (25mM), which contrasts the findings in other published studies (Bushra, Rizk, & Sharma, 2016; Fan, Qiao, & Tang, 2017; S. Jiang & Chen, 2017). However, this observation could be due to the difference in the glucose concentration that was used. In the current study, we used 25mM, while in the others was 30mM. S. Jiang & Chen, in their study, tested different concentrations of high glucose 22mM and 30mM and found that the way high glucose decreases the viability of HREC is dose dependent as 30mM glucose gradually decreased cell viability. Lower glucose concentration as 22mM, also reduced cell viability; however, the rate was not significant as compared to 30mM glucose (S. Jiang & Chen, 2017). In addition, HRECs viability was not affected with miRNA mimic and inhibitor transfection using the liquid medium Lipofectamine RNAiMAX. This finding is very important and shows that the

transfection reagents used in this study did not introduce any toxic effect on HRECs. Also, in our study, HRECs exposed to high glucose (25mM) for four days did not show increased apoptosis rate when compared to normoglycemia, which again was not in line with the findings of other published studies (Bushra et al., 2016; X. L. Chen et al., 2013; S. Jiang & Chen, 2017). This also could be due to the difference in high glucose concentration to which HRECs were exposed between our study and the other studies. Another factor could be the inherited properties of the primary cells used in the present study compared to other studies.

Hyperglycemia is reported by numerous studies to have pro-inflammatory, pro-oxidative, and pro-apoptotic effects. Hyperglycemia is also demonstrated to downregulate the expression of miR-146a-5p expression which is well known anti-inflammatory miRNA. Our findings showed a significant reduction in miR-146a-5p in HRECs exposed to high glucose. This finding is supported by other studies performed on HRECs and diabetic animal models (S. Chen, Feng, Thomas, & Chakrabarti, 2017; P. Zhuang et al., 2017).

Hence in the current study, the effect of overexpressing and silencing by transfecting miR-146a-5p in HRECs exposed to high glucose was assessed. Expression of miR-146a-5p is regulated through NF-κB pathway (Jixiang Zhang et al., 2016). As a negative feedback mechanism, miR-146a-5p downregulates NF-κB and its downstream targets TNF-α and ICAM-1 through targeting the signaling molecules IRAK1and TRAF6 (L. Zhang et al., 2020; P. Zhuang et al., 2017). In the current study, knockdown miR-146a-5p in HRECs exposed to hyperglycemia in vitro using a dose of 10nM antimir or inhibitor significantly elevated ROS production, upregulated TNF-α ICAM-1 expression, but TRAF 6 expression was not affected. These data enrich the published literature that low expression of miR-146a-5p obtained after silencing

increases the pro-inflammatory activities (Qiaoyun Gong et al., 2017; Q. Wang et al., 2014; Y. Xie et al., 2018; E.-A. Ye & Steinle, 2016). This finding demonstrates that low expression of miR-146a-5p could highlight the potential role in the pathogenesis of DR by enhancing inflammation and oxidative stress in the retina's vascular system of diabetic subjects. Further studies are needed to explore in detail these observations in vivo using animal models.

Overexpression of miR-146a-5p in the current study was achieved by transfection in vitro of HRECs using two doses of mimic: low dose (10nM) and a high dose (50nM). Overexpression of miR-146a-5p using a low dose of 10nM significantly elevated ROS production, upregulated the mRNA expression of TNF-α and ICAM-1 genes in HRECs exposed to hyperglycemia, and consequently, increases the pro-inflammatory activities. These findings contrast the clue that overexpression of miR-146a-5p diminishes inflammation and related activities in HRECs exposed to hyperglycemia. Cowan et al., in their study, transfected HRECs with 10nM miR-146a-5p mimic using liquid medium Lipofectamine RNAiMAX similar to the procedure that followed in the current study; however, instead of exposing the HRECs to high glucose, they treated the cells with 1 or 5 U/mL thrombin which is a strong pro-inflammatory factor (Cowan et al., 2014). They found that overexpression of miR-146 with 10 nM mimic significantly decreased thrombin's effect on NF-κB expression and the downstream inflammatory activities (Cowan et al., 2014). There is a hypothetical explanation for this inconsistent finding reported by the current study with the findings reported by Cowan et al. The overexpression of miR-146a-5p gene using 10nM was insufficient to decrease the massive inflammatory responses and activities that are produced by the chronic high glucose condition; however, it was adequate to diminish the transient state of inflammation caused by introducing thrombin. This interesting

finding could reveal that a small dose of mimic is not enough to maintain homeostasis of the negative feedback loop of miR-146a-5p and NF-κB pathway in chronic hyperglycemic conditions.

On the other hand, overexpression of miR-146a-5p using 50nM significantly downregulated the expression of TNF-α, ICAM-1, and TRAF6, indicating the anti-inflammatory and anti-apoptotic role of miR-146a-5p as per the established functions of the abovementioned genes. This finding supported that the transfection with a high dose 0f 50 nM was optimum to decrease the expression of TRAF6, a well-known target gene of miR-146a-5p. The finding of the current study is in line with the data reported by numerous published studies supporting the role of miR-146a-5p as an anti-inflammatory in DR and other vascular complications such as cardiovascular disorder and nephropathy (Luly et al., 2019; J. Xie et al., 2017; E.-A. Ye & Steinle, 2016; P. Zhuang et al., 2017). Since we were unable to assess the oxidative stress by measuring ROS production level, we examined the expression of six important genes involved in the oxidation process, which are SOD1, SOD2, TXNRD1 CAT, GPX1, and PPARγ in HRECs exposed to hyperglycemia and transfected with 10 nM and 50nM for 48 hours. The HRECs transfected with 50nM mimic of miR-146a-5p demonstrated significant upregulation in the expression of four genes, CAT, TXNRD1, SOD1, and GPX1, in comparison with the low dose of transfection using 10nM mimic. These data reveal the antioxidant function of overexpressed miR-146a-5p with 50nM mimic and its anti-inflammatory and anti-apoptotic roles. It also supports the data mentioned above that overexpression of miR-146a-5p with a low dose of mimic using 10nM increases ROS production. It can enhance oxidative stress due to the impaired upregulation of the expression of genes involved in the anti-oxidative process except for SOD1, and TXNRD1 which are significantly upregulated.

Following that, profiling arrays were performed to assess the effect of overexpression of miR-146a-5p using 50nM on inflammatory and angiogenesis gene expression to understand the potential mechanisms for anti-inflammatory and anti-angiogenesis function. We compared the HRECs cells exposed to high glucose as a control group compared to HRECs cells transfected with a high dose of 50nM mimic under high glucose conditions. The inflammatory profile showed a significant reduction in several genes notably, secreted phosphoprotein 1 (SSP1), IL17C, CXCL2, CXCL13, CXCL1, and CX3CR1. SSP1 gene has been reported to be present in sclerotium tissues only (M. Li & Rollins, 2009). This could be an interesting gene to examine further since the environment in the diabetic retina is vulnerable to hemorrhage with the process of neovascularization. The rest of the inflammatory genes dysregulated are chemokines and GM-CSF, which are well established to function in inflammatory conditions.

The angiogenesis profile supported the RT-PCR results of the current study and showed that overexpression miR-14a-5p using 50nM function through downregulating the expression of all the VEGF isomers: VEGFA, VEGFB, VEGFC, VEGFD/ FIGF in addition to TNF, ICAM1, TRAF6, and Adhesion G Protein-Coupled Receptor B1(ADGRB1). The two significantly most downregulated genes were VEGFD/ FIGF, a gene that has an important role in endothelial cell growth and proliferation, and ADGRB1, an angiogenesis gene associated with several diseases such as Glioblastoma. Overexpression miR-14a-5p specifically upregulated Thrombospondin-2 (THBS2) gene expression, a protein that regulates various cell interactions and functions as an anti-angiogenesis factor.

We initially hypothetically assumed that miR-146a-5p might regulate inflammation through PPAR-α. Our data showed no significant increase in PPAR-α expression in samples transfected with the 50nM of miR-146a-5p mimic. From the

results of inflammatory and angiogenesis gene arrays, we concluded that miR-146a-5p mediate its anti-inflammatory and anti-angiogenesis functions through targeting TRAF6 and, consequently, the downstream factors such as protein-protein interactions and ubiquitination of STAT3 inhibition, which in turn causes inhibition of angiogenesis. Figure 37 summarizes the findings of the study regarding pathways and molecules affected by miR-146a-5p.

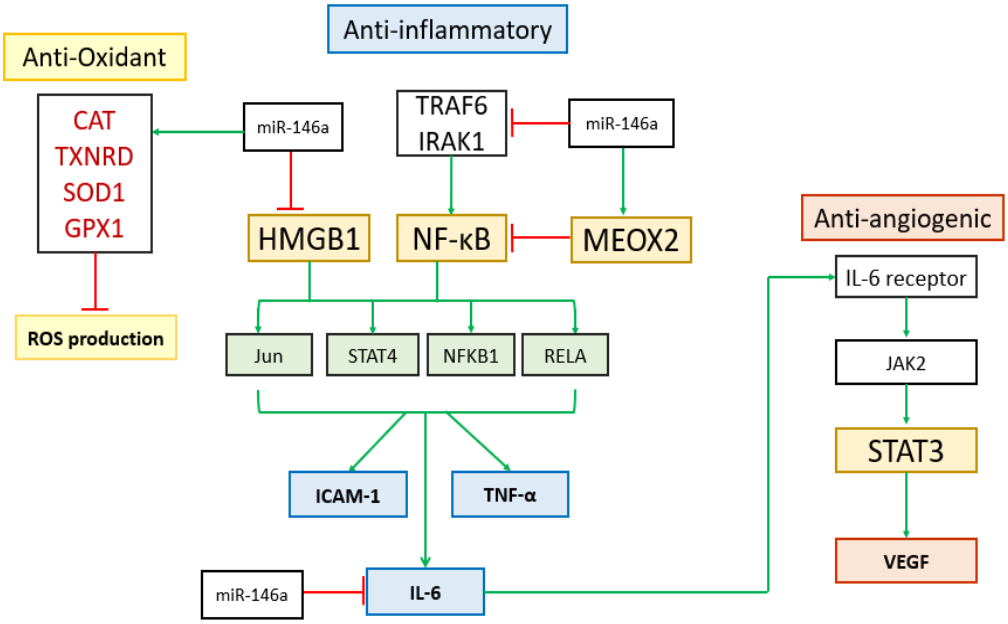

Figure 37 Summary of pathways and molecules targeted by miR-146a-5p in inflammation, angiogenesis, and oxidation process.

CHAPTER 7: CONCLUSION

In conclusion, our data strengthen and add to the current literature regarding the anti-inflammatory role of miR-146a-5p in DR and hypothetically in other vascular complications of diabetes. To summarize, the findings of the current study revealed that overexpressing of miR-146a-5p using 50nM decreases the expression level of pro-inflammatory, anti-apoptotic, anti-angiogenesis, and antioxidant genes, and hence inhibiting the inflammatory activities and the followed process which are involved in progressing and developing DR. The current study also shows the importance of determining the optimal effective dose of mimic to overexpress miR-146a-5p – in the current study 50nM showed to be optimum -, as using ineffective doses may result in adverse effects. Therefore, further comprehensive studies and dose-time curve experiments would help determine the effective therapeutic dose of miR-146a-5p that will provide the maximum advantage with minimum adverse effect.

LIMITATIONS AND FUTURE STUDIES

The present study has numerous limitations which need future investigations. Since we could not find data regarding the proper dose of miR-146a-5p mimic and inhibitor in the published studies, we initially started our experiments with 10 nM. The 10 nM miR-146a-5p mimic on cells exposed to chronic hyperglycemia at a concentration of 25 mM glucose showed a pro-inflammatory effect which contrasts what is published in the literature, hence we performed a small size pilot experiment to study the effect of a higher dose, and the 50 nM miR-146a-5p mimic demonstrated anti-inflammatory effect in cells exposed to chronic hyperglycemia. We recommend doing further studies to test the effect of more than a few doses of miR-146a-5p mimic (e.g. 5 nM, 10 nM, 30 nM, 50 nM, 100 nM) with different transfection periods (e.g. 24, 48, 72 hours) to establish dose/time curves. Also, the study aimed to assess the expression of the inflammatory proteins using western blot (WB); however, restrictions related to the SARS-COV-2 pandemic, which affected the reagents shipping, made it impossible to perform the test before the submission due date. Hence, we recommend evaluating the effect of miR-146a-5p on TNF – α and ICAM1 expression in future studies. Finally, due to the time constraint, we could not study the interaction between miR-146a-5p and the other miRNAs, which may have a potential role in regulating inflammation. Therefore, we recommend evaluating the HG + miR-146a-5p samples for the expression of miRNAs expression to identify and solve the puzzle of mechanisms and interaction of potential miRNAs regulating DR pathogenesis.

APPENDIX A: Research approval

جامعة قطر
QATAR UNIVERSITY

Qatar University
Institutional Bio-safety Committee

To: Dr. Nasser Rizk
Health Sciences Department
Qatar University

25 October 2020

Ref: Project Titled "The Functional Consequence of mi-146a on Human Retinal Endothelial Cells in Diabetic Conditions"
Research Grant #: QUST-2-CHS-2020- 15

Dear Dr. Nasser,

We would like to inform you that your application along with supporting documents provided for the above proposal have been reviewed by QU-IBC, and having met all the requirements, has been granted approval. The approval is for a period of one year and renewable for each year thereafter, should be sought and approved by QU-IBC period to continue.

Please note that QU-IBC approval is contingent upon your adherence to the following QU-IBC Guidelines:

- Ensuring compliance with QU Safety Plans and applicable national and international regulations.
- Ensuring experiments that require prior IBC approval are not conducted until IBC approval is obtained and making initial determination of containment levels required for experiments.
- Notifying the IBC of any changes to other hazardous material experiments previously approved by the IBC.
- Reporting any significant problems, violations of QU Safety Plans and applicable regulations/guidelines, or any significant research-related accidents and illnesses to the QU-IBC. Also, ensuring personnel receive appropriate orientation and specific training for the safe performance of the work.

Your research approval No. is: **QU-IBC-2020/077**. Please refer to this approval number in all your future correspondence pertaining to this research.

Best wishes,

Hadi M. Yassine, M.Sc., Ph.D
Chairperson, QU-IBC
Section Head of Research
Associate Professor of Infectious Diseases
Qatar University, Doha, Qatar.
Tel: +974 4403-6819
E-mail: hyassine@qu.edu.qa

APPENDIX B: RNA samples purity and integrity

Sample	RNA concentration	260/280 ratio	RNA Integrity Number (RIN)
NG	289.7	2.11	8.1
NG + miR-146a-5p mimic	110.1	1.85	7.9
Mannitol	296.8	1.93	.8
HG	225.3	1.81	8.2
HG + miR-146a-5p mimic	169.1	1.92	9.1
HG + miR-146a-5p mimic NC	246.7	2.01	8
HG + miR-146a-5p inhibit	294.3	1.84	8.2
HG + miR-146a-5p inhibit NC	211.6	1.82	8.6
NG + miR-146a-5p mimic + TNF-α	224.3	1.81	8.9
NG + TNF - α	381.9	1.84	9.2

APPENDIX C: Genes included in Inflammatory genes Array

Position	Symbol	Gene Name
A01	AIMP1	Aminoacyl tRNA synthetase complex-interacting multifunctional protein 1
A02	BMP2	Bone morphogenetic protein 2
A03	C5	Complement component 5
A04	CCL1	Chemokine (C-C motif) ligand 1
A05	CCL11	Chemokine (C-C motif) ligand 11
A06	CCL13	Chemokine (C-C motif) ligand 13
A07	CCL15	Chemokine (C-C motif) ligand 15
A08	CCL16	Chemokine (C-C motif) ligand 16
A09	CCL17	Chemokine (C-C motif) ligand 17
A10	CCL2	Chemokine (C-C motif) ligand 2
A11	CCL20	Chemokine (C-C motif) ligand 20
A12	CCL22	Chemokine (C-C motif) ligand 22
B01	CCL23	Chemokine (C-C motif) ligand 23
B02	CCL24	Chemokine (C-C motif) ligand 24
B03	CCL26	Chemokine (C-C motif) ligand 26
B04	CCL3	Chemokine (C-C motif) ligand 3
B05	CCL4	Chemokine (C-C motif) ligand 4
B06	CCL5	Chemokine (C-C motif) ligand 5
B07	CCL7	Chemokine (C-C motif) ligand 7
B08	CCL8	Chemokine (C-C motif) ligand 8
B09	CCR1	Chemokine (C-C motif) receptor 1

Position	Symbol	Gene Name
B10	CCR2	Chemokine (C-C motif) receptor 2
B11	CCR3	Chemokine (C-C motif) receptor 3
B12	CCR4	Chemokine (C-C motif) receptor 4
C01	CCR5	Chemokine (C-C motif) receptor 5
C02	CCR6	Chemokine (C-C motif) receptor 6
C03	CCR8	Chemokine (C-C motif) receptor 8
C04	CD40LG	CD40 ligand
C05	CSF1	Colony stimulating factor 1 (macrophage)
C06	CSF2	Colony stimulating factor 2 (granulocyte-macrophage)
C07	CSF3	Colony stimulating factor 3 (granulocyte)
C08	CX3CL1	Chemokine (C-X3-C motif) ligand 1
C09	CX3CR1	Chemokine (C-X3-C motif) receptor 1
C10	CXCL1	Chemokine (C-X-C motif) ligand 1 (melanoma growth stimulating activity, alpha)
C11	CXCL10	Chemokine (C-X-C motif) ligand 10
C12	CXCL11	Chemokine (C-X-C motif) ligand 11
D01	CXCL12	Chemokine (C-X-C motif) ligand 12
D02	CXCL13	Chemokine (C-X-C motif) ligand 13
D03	CXCL2	Chemokine (C-X-C motif) ligand 2
D04	CXCL3	Chemokine (C-X-C motif) ligand 3
D05	CXCL5	Chemokine (C-X-C motif) ligand 5
D06	CXCL6	Chemokine (C-X-C motif) ligand 6 (granulocyte chemotactic protein 2)
D07	CXCL9	Chemokine (C-X-C motif) ligand 9
D08	CXCR1	Chemokine (C-X-C motif) receptor 1

Position	Symbol	Gene Name
D09	CXCR2	Chemokine (C-X-C motif) receptor 2
D10	FASLG	Fas ligand (TNF superfamily, member 6)
D11	IFNA2	Interferon, alpha 2
D12	IFNG	Interferon, gamma
E01	IL10RA	Interleukin 10 receptor, alpha
E02	IL10RB	Interleukin 10 receptor, beta
E03	IL13	Interleukin 13
E04	IL15	Interleukin 15
E05	IL16	Interleukin 16
E06	IL17A	Interleukin 17A
E07	IL17C	Interleukin 17C
E08	IL17F	Interleukin 17F
E09	IL1A	Interleukin 1, alpha
E10	IL1B	Interleukin 1, beta
E11	IL1R1	Interleukin 1 receptor, type I
E12	IL1RN	Interleukin 1 receptor antagonist
F01	IL21	Interleukin 21
F02	IL27	Interleukin 27
F03	IL3	Interleukin 3 (colony-stimulating factor, multiple)
F04	IL33	Interleukin 33
F05	IL5	Interleukin 5 (colony-stimulating factor, eosinophil)
F06	IL5RA	Interleukin 5 receptor, alpha
F07	IL7	Interleukin 7

Position	Symbol	Gene Name
F08	CXCL8	Interleukin 8
F09	IL9	Interleukin 9
F10	IL9R	Interleukin 9 receptor
F11	LTA	Lymphotoxin alpha (TNF superfamily, member 1)
F12	LTB	Lymphotoxin beta (TNF superfamily, member 3)
G01	MIF	Macrophage migration inhibitory factor (glycosylation-inhibiting factor)
G02	NAMPT	Nicotinamide phosphoribosyl transferase
G03	OSM	Oncostatin M
G04	SPP1	Secreted phosphoprotein 1
G05	TNF	Tumor necrosis factor
G06	TNFRSF11B	Tumor necrosis factor receptor superfamily, member 11b
G07	TNFSF10	Tumor necrosis factor (ligand) superfamily, member 10
G08	TNFSF11	Tumor necrosis factor (ligand) superfamily, member 11
G09	TNFSF13	Tumor necrosis factor (ligand) superfamily, member 13
G10	TNFSF13B	Tumor necrosis factor (ligand) superfamily, member 13b
G11	TNFSF4	Tumor necrosis factor (ligand) superfamily, member 4
G12	VEGFA	Vascular endothelial growth factor-A

APPENDIX D: Genes included in Angiogenesis genes Array

Position	Symbol	Description
A01	AKT1	V-akt murine thymoma viral oncogene homolog 1
A02	ANG	Angiogenin, ribonuclease, RNase A family, 5
A03	ANGPT1	Angiopoietin 1
A04	ANGPT2	Angiopoietin 2
A05	ANGPTL4	Angiopoietin-like 4
A06	ANPEP	Alanyl (membrane) aminopeptidase
A07	ADGRB1	Brain-specific angiogenesis inhibitor 1
A08	CCL11	Chemokine (C-C motif) ligand 11
A09	CCL2	Chemokine (C-C motif) ligand 2
A10	CDH5	Cadherin 5, type 2 (vascular endothelium)
A11	COL18A1	Collagen, type XVIII, alpha 1
A12	COL4A3	Collagen, type IV, alpha 3 (Goodpasture antigen)
B01	CTGF	Connective tissue growth factor
B02	CXCL1	Chemokine (C-X-C motif) ligand 1 (melanoma growth stimulating activity, alpha)
B03	CXCL10	Chemokine (C-X-C motif) ligand 10
B04	CXCL5	Chemokine (C-X-C motif) ligand 5
B05	CXCL6	Chemokine (C-X-C motif) ligand 6 (granulocyte chemotactic protein 2)
B06	CXCL9	Chemokine (C-X-C motif) ligand 9
B07	EDN1	Endothelin 1
B08	EFNA1	Ephrin-A1
B09	EFNB2	Ephrin-B2
B10	EGF	Epidermal growth factor

Position	Symbol	Description
B11	ENG	Endoglin
B12	EPHB4	EPH receptor B4
C01	ERBB2	V-erb-b2 erythroblastic leukemia viral oncogene homolog 2, neuro/glioblastoma derived oncogene homolog (avian)
C02	F3	Coagulation factor III (thromboplastin, tissue factor)
C03	FGF1	Fibroblast growth factor 1 (acidic)
C04	FGF2	Fibroblast growth factor 2 (basic)
C05	FGFR3	Fibroblast growth factor receptor 3
C06	FIGF	C-fos induced growth factor (vascular endothelial growth factor D)
C07	FLT1	Fms-related tyrosine kinase 1 (vascular endothelial growth factor/vascular permeability factor receptor)
C08	FN1	Fibronectin 1
C09	HGF	Hepatocyte growth factor (hepapoietin A; scatter factor)
C10	HIF1A	Hypoxia inducible factor 1, alpha subunit (basic helix-loop-helix transcription factor)
C11	HPSE	Heparanase
C12	ID1	Inhibitor of DNA binding 1, dominant negative helix-loop-helix protein
D01	IFNA1	Interferon, alpha 1
D02	IFNG	Interferon, gamma
D03	IGF1	Insulin-like growth factor 1 (somatomedin C)
D04	IL1B	Interleukin 1, beta
D05	IL6	Interleukin 6 (interferon, beta 2)
D06	CXCL8	Interleukin 8
D07	ITGAV	Integrin, alpha V (vitronectin receptor, alpha polypeptide, antigen CD51)
D08	ITGB3	Integrin, beta 3 (platelet glycoprotein IIIa, antigen CD61)
D09	JAG1	Jagged 1

Position	Symbol	Description
D10	KDR	Kinase insert domain receptor (a type III receptor tyrosine kinase)
D11	LECT1	Leukocyte cell derived chemotaxin 1
D12	LEP	Leptin
E01	MDK	Midkine (neurite growth-promoting factor 2)
E02	MMP14	Matrix metallopeptidase 14 (membrane-inserted)
E03	MMP2	Matrix metallopeptidase 2 (gelatinase A, 72kDa gelatinase, 72kDa type IV collagenase)
E04	MMP9	Matrix metallopeptidase 9 (gelatinase B, 92kDa gelatinase, 92kDa type IV collagenase)
E05	NOS3	Nitric oxide synthase 3 (endothelial cell)
E06	NOTCH4	Notch 4
E07	NRP1	Neuropilin 1
E08	NRP2	Neuropilin 2
E09	PDGFA	Platelet-derived growth factor alpha polypeptide
E10	PECAM1	Platelet/endothelial cell adhesion molecule
E11	PF4	Platelet factor 4
E12	PGF	Placental growth factor
F01	PLAU	Plasminogen activator, urokinase
F02	PLG	Plasminogen
F03	PROK2	Prokineticin 2
F04	PTGS1	Prostaglandin-endoperoxide synthase 1 (prostaglandin G/H synthase and cyclooxygenase)
F05	S1PR1	Sphingosine-1-phosphate receptor 1
F06	SERPINE1	Serpin peptidase inhibitor, clade E (nexin, plasminogen activator inhibitor type 1), member 1
F07	SERPINF1	Serpin peptidase inhibitor, clade F (alpha-2 antiplasmin, pigment epithelium derived factor), member 1
F08	SPHK1	Sphingosine kinase 1

Position	Symbol	Description
F09	TEK	TEK tyrosine kinase, endothelial
F10	TGFA	Transforming growth factor, alpha
F11	TGFB1	Transforming growth factor, beta 1
F12	TGFB2	Transforming growth factor, beta 2
G01	TGFBR1	Transforming growth factor, beta receptor 1
G02	THBS1	Thrombospondin 1
G03	THBS2	Thrombospondin 2
G04	TIE1	Tyrosine kinase with immunoglobulin-like and EGF-like domains 1
G05	TIMP1	TIMP metallopeptidase inhibitor 1
G06	TIMP2	TIMP metallopeptidase inhibitor 2
G07	TIMP3	TIMP metallopeptidase inhibitor 3
G08	TNF	Tumor necrosis factor
G09	TYMP	Thymidine phosphorylase
G10	VEGFA	Vascular endothelial growth factor A
G11	VEGFB	Vascular endothelial growth factor B
G12	VEGFC	Vascular endothelial growth factor C

REFERENCES

Abougalambou, S. S. I., & Abougalambou, A. S. (2015). Risk factors associated with diabetic retinopathy among type 2 diabetes patients at teaching hospital in Malaysia. *Diabetes & Metabolic Syndrome: Clinical Research & Reviews, 9*(2), 98-103. doi:https://doi.org/10.1016/j.dsx.2014.04.019

Adamis, A. P., Shima, D. T., Yeo, K. T., Yeo, T. K., Brown, L. F., Berse, B., . . . Folkman, J. (1993). Synthesis and Secretion of Vascular Permeability Factor/Vascular Endothelial Growth Factor by Human Retinal Pigment Epithelial Cells. *Biochemical and Biophysical Research Communications, 193*(2), 631-638. doi:https://doi.org/10.1006/bbrc.1993.1671

Al-Kharashi, A. S. (2018). Role of oxidative stress, inflammation, hypoxia and angiogenesis in the development of diabetic retinopathy. *Saudi J Ophthalmol, 32*(4), 318-323. doi:10.1016/j.sjopt.2018.05.002

Al-Sadeq, D. W. (2018). The Expression of Retinal miRNA Evoked by Hyperglycemia and After Adiponectin Treatment in Human Retinal Endothelial Cells.

Amit-Cohen, B.-C., Rahat, M., & Rahat, M. (2013). Tumor cell-macrophage interactions increase angiogenesis through secretion of EMMPRIN. *Frontiers in Physiology, 4*, 178.

Aplin, A. C., Gelati, M., Fogel, E., Carnevale, E., & Nicosia, R. F. (2006). Angiopoietin-1 and vascular endothelial growth factor induce expression of inflammatory cytokines before angiogenesis. *Physiological Genomics, 27*(1), 20-28. doi:10.1152/physiolgenomics.00048.2006

Bansal, P., Gupta, R., & Kotecha, M. (2013, 2013 October-December). Frequency of diabetic retinopathy in patients with diabetes mellitus and its correlation with

duration of diabetes mellitus. *Medical Journal of Dr. D.Y. Patil University, 6(4),* 366.

Barot, M., Gokulgandhi, M. R., Patel, S., & Mitra, A. K. (2013). Microvascular complications and diabetic retinopathy: recent advances and future implications. *Future medicinal chemistry, 5*(3), 301-314. doi:10.4155/fmc.12.206

Birben, E., Sahiner, U. M., Sackesen, C., Erzurum, S., & Kalayci, O. (2012). Oxidative stress and antioxidant defense. *The World Allergy Organization journal, 5*(1), 9-19. doi:10.1097/WOX.0b013e3182439613

Bordet, R., Ouk, T., Petrault, O., Gelé, P., Gautier, S., Laprais, M., . . . Bastide, M. (2006). PPAR: a new pharmacological target for neuroprotection in stroke and neurodegenerative diseases. *Biochem Soc Trans, 34*(Pt 6), 1341-1346. doi:10.1042/bst0341341

Bushra, S., Rizk, N., & Sharma, I. (2016). ASSOCIATION BETWEEN INSULIN AND NITRIC OXIDE IN HUMAN RETINAL MICROVASCULAR ENDOTHELIAL CELLS IN VITRO. *Investigative Ophthalmology & Visual Science, 57*(12), 5426-5426.

Busik, J. V., Mohr, S., & Grant, M. B. (2008). Hyperglycemia-induced reactive oxygen species toxicity to endothelial cells is dependent on paracrine mediators. *Diabetes, 57*(7), 1952-1965. doi:10.2337/db07-1520

Calderon, G. D., Juarez, O. H., Hernandez, G. E., Punzo, S. M., & De la Cruz, Z. D. (2017). Oxidative stress and diabetic retinopathy: development and treatment. *Eye (Lond), 31*(8), 1122-1130. doi:10.1038/eye.2017.64

Caporali, A., & Emanueli, C. (2011). MicroRNA regulation in angiogenesis. *Vascular Pharmacology, 55*(4), 79-86. doi:https://doi.org/10.1016/j.vph.2011.06.006

Catalanotto, C., Cogoni, C., & Zardo, G. (2016). MicroRNA in Control of Gene Expression: An Overview of Nuclear Functions. *International journal of molecular sciences, 17*(10), 1712. doi:10.3390/ijms17101712

Cavarretta, E., & Frati, G. (2016). MicroRNAs in Coronary Heart Disease: Ready to Enter the Clinical Arena? *BioMed Research International, 2016,* 2150763. doi:10.1155/2016/2150763

Cheema, A. K., Kaur, P., Fadel, A., Younes, N., Zirie, M., & Rizk, N. M. (2020). Integrated Datasets of Proteomic and Metabolomic Biomarkers to Predict Its Impacts on Comorbidities of Type 2 Diabetes Mellitus. *Diabetes Metab Syndr Obes, 13,* 2409-2431. doi:10.2147/dmso.s244432

Chen, L., Deng, H., Cui, H., Fang, J., Zuo, Z., Deng, J., . . . Zhao, L. (2017). Inflammatory responses and inflammation-associated diseases in organs. *Oncotarget, 9*(6), 7204-7218. doi:10.18632/oncotarget.23208

Chen, N., Wang, J., Hu, Y., Cui, B., Li, W., Xu, G., . . . Liu, S. (2014). MicroRNA-410 reduces the expression of vascular endothelial growth factor and inhibits oxygen-induced retinal neovascularization. *PLoS One, 9*(4), e95665-e95665. doi:10.1371/journal.pone.0095665

Chen, S., Feng, B., Thomas, A. A., & Chakrabarti, S. (2017). miR-146a regulates glucose induced upregulation of inflammatory cytokines extracellular matrix proteins in the retina and kidney in diabetes. *PLOS ONE, 12*(3), e0173918. doi:10.1371/journal.pone.0173918

Chen, W., Esselman, W. J., Jump, D. B., & Busik, J. V. (2005). Anti-inflammatory effect of docosahexaenoic acid on cytokine-induced adhesion molecule expression in human retinal vascular endothelial cells. *Investigative*

Ophthalmology & Visual Science, 46(11), 4342-4347. doi:10.1167/iovs.05-0601

Chen, X. L., Zhang, X. D., Li, Y. Y., Chen, X. M., Tang, D. R., & Ran, R. J. (2013). Involvement of HMGB1 mediated signalling pathway in diabetic retinopathy: evidence from type 2 diabetic rats and ARPE-19 cells under diabetic condition. *Br J Ophthalmol, 97*(12), 1598-1603. doi:10.1136/bjophthalmol-2013-303736

Cohen, S. R., & Gardner, T. W. (2016). Diabetic Retinopathy and Diabetic Macular Edema. *Dev Ophthalmol, 55*, 137-146. doi:10.1159/000438970

Condorelli, G., Latronico, M., & Cavarretta, E. (2014). microRNAs in Cardiovascular Diseases Current Knowledge and the Road Ahead. *Journal of the American College of Cardiology, 63*. doi:10.1016/j.jacc.2014.01.050

Cornel, S., Adriana, I. D., Mihaela, T. C., Speranta, S., Algerino, D. S., Mehdi, B., & Jalaladin, H.-R. (2015). Anti-vascular endothelial growth factor indications in ocular disease. *Romanian journal of ophthalmology, 59*(4), 235-242.

Cowan, C., Muraleedharan, C. K., O'Donnell, J. J., 3rd, Singh, P. K., Lum, H., Kumar, A., & Xu, S. (2014). MicroRNA-146 inhibits thrombin-induced NF-κB activation and subsequent inflammatory responses in human retinal endothelial cells. *Invest Ophthalmol Vis Sci, 55*(8), 4944-4951. doi:10.1167/iovs.13-13631

Cristina, M., Adina, M., Simona Georgiana, P., Valerica, T., & Maria, M. (2013). Biochemistry of hyperglycemia induced vascular dysfunction. *Romanian Journal of Diabetes Nutrition and Metabolic Diseases, 20*(4), 419-425. doi:https://doi.org/10.2478/rjdnmd-2013-0042

Curtale, G., Citarella, F., Carissimi, C., Goldoni, M., Carucci, N., Fulci, V., . . . Macino, G. (2010). An emerging player in the adaptive immune response: microRNA-

146a is a modulator of IL-2 expression and activation-induced cell death in T lymphocytes. *Blood, 115*(2), 265-273. doi:10.1182/blood-2009-06-225987

Dantas da Costa E Silva, M. E., Polina, E. R., Crispim, D., Sbruzzi, R. C., Lavinsky, D., Mallmann, F., . . . Dos Santos, K. G. (2019). Plasma levels of miR-29b and miR-200b in type 2 diabetic retinopathy. *Journal of cellular and molecular medicine, 23*(2), 1280-1287. doi:10.1111/jcmm.14030

Das, A., Ganesh, K., Khanna, S., Sen, C. K., & Roy, S. (2014). Engulfment of apoptotic cells by macrophages: a role of microRNA-21 in the resolution of wound inflammation. *Journal of immunology (Baltimore, Md. : 1950), 192*(3), 1120-1129. doi:10.4049/jimmunol.1300613

de Pontual, L., Yao, E., Callier, P., Faivre, L., Drouin, V., Cariou, S., . . . Amiel, J. (2011). Germline deletion of the miR-17∼92 cluster causes skeletal and growth defects in humans. *Nature genetics, 43*(10), 1026-1030. doi:10.1038/ng.915

dell'Omo, R., Semeraro, F., Bamonte, G., Cifariello, F., Romano, M. R., & Costagliola, C. (2013). Vitreous mediators in retinal hypoxic diseases. *Mediators of Inflammation, 2013*, 935301-935301. doi:10.1155/2013/935301

Duh, E. J., Sun, J. K., & Stitt, A. W. (2017). Diabetic retinopathy: current understanding, mechanisms, and treatment strategies. *JCI insight, 2*(14), e93751. doi:10.1172/jci.insight.93751

Evans, J., Michelessi, M., & Virgili, G. (2014). Laser photocoagulation for proliferative diabetic retinopathy. *The Cochrane database of systematic reviews, 11*, CD011234. doi:10.1002/14651858.CD011234.pub2

Fabbri, M., Paone, A., Calore, F., Galli, R., Gaudio, E., Santhanam, R., . . . Croce, C. M. (2012). MicroRNAs bind to Toll-like receptors to induce prometastatic inflammatory response. *Proceedings of the National Academy of Sciences of the*

United States of America, 109(31), E2110-E2116. doi:10.1073/pnas.1209414109

Fan, C., Qiao, Y., & Tang, M. (2017). Notoginsenoside R1 attenuates high glucose-induced endothelial damage in rat retinal capillary endothelial cells by modulating the intracellular redox state. *Drug Des Devel Ther, 11*, 3343-3354. doi:10.2147/dddt.s149700

Fang, S., Ma, X., Guo, S., & Lu, J. (2017). MicroRNA-126 inhibits cell viability and invasion in a diabetic retinopathy model via targeting IRS-1. *Oncol Lett, 14*(4), 4311-4318. doi:10.3892/ol.2017.6695

Fasanaro, P., D'Alessandra, Y., Di Stefano, V., Melchionna, R., Romani, S., Pompilio, G., . . . Martelli, F. (2008). MicroRNA-210 modulates endothelial cell response to hypoxia and inhibits the receptor tyrosine kinase ligand Ephrin-A3. *The Journal of biological chemistry, 283*(23), 15878-15883. doi:10.1074/jbc.M800731200

Fiedler, J., Jazbutyte, V., Kirchmaier Bettina, C., Gupta Shashi, K., Lorenzen, J., Hartmann, D., . . . Thum, T. (2011). MicroRNA-24 Regulates Vascularity After Myocardial Infarction. *Circulation, 124*(6), 720-730. doi:10.1161/CIRCULATIONAHA.111.039008

Fish, J. E., Santoro, M. M., Morton, S. U., Yu, S., Yeh, R.-F., Wythe, J. D., . . . Srivastava, D. (2008). miR-126 regulates angiogenic signaling and vascular integrity. *Developmental cell, 15*(2), 272-284. doi:10.1016/j.devcel.2008.07.008

Friedman, R. C., Farh, K. K.-H., Burge, C. B., & Bartel, D. P. (2009). Most mammalian mRNAs are conserved targets of microRNAs. *Genome research, 19*(1), 92-105. doi:10.1101/gr.082701.108

Fu, Z., & Tindall, D. J. (2008). FOXOs, cancer and regulation of apoptosis. *Oncogene, 27*(16), 2312-2319. doi:10.1038/onc.2008.24

Gong, Q., & Su, G. (2017). Roles of miRNAs and long noncoding RNAs in the progression of diabetic retinopathy. *Biosci Rep, 37*(6). doi:10.1042/bsr20171157

Gong, Q., Xie, J. n., Liu, Y., Li, Y., & Su, G. (2017). Differentially Expressed MicroRNAs in the Development of Early Diabetic Retinopathy. *Journal of Diabetes Research, 2017*, 4727942. doi:10.1155/2017/4727942

Group, B. D. W., Atkinson Jr, A. J., Colburn, W. A., DeGruttola, V. G., DeMets, D. L., Downing, G. J., . . . Schooley, R. T. (2001). Biomarkers and surrogate endpoints: preferred definitions and conceptual framework. *Clinical Pharmacology & Therapeutics, 69*(3), 89-95.

Guo, R., Gu, J., Zhang, Z., Wang, Y., & Gu, C. (2015). MicroRNA-410 functions as a tumor suppressor by targeting angiotensin II type 1 receptor in pancreatic cancer. *IUBMB Life, 67*(1), 42-53. doi:10.1002/iub.1342

He, L., & Hannon, G. J. (2004). MicroRNAs: small RNAs with a big role in gene regulation. *Nature Reviews Genetics, 5*(7), 522-531. doi:10.1038/nrg1379

Heij, E., Tecim, S., Kessels, A., Liem, A., Japing, W., & Hendrikse, F. (2004). Clinical variables and their relation to visual outcome after vitrectomy in eyes with diabetic retinal traction detachment. *Graefe's archive for clinical and experimental ophthalmology = Albrecht von Graefes Archiv für klinische und experimentelle Ophthalmologie, 242*, 210-217. doi:10.1007/s00417-003-0815-5

IDF. (2019). IDF DIABETES ATLAS. Retrieved from https://diabetesatlas.org/en/

Israelian-Konaraki, Z., & Reaven, P. D. (2005). Peroxisome Proliferator-Activated Receptor-Alpha and Atherosclerosis: From Basic Mechanisms to Clinical Implications. *Cardiology, 103*(1), 1-9. doi:10.1159/000081845

Jiang, Q., Lyu, X.-M., Yuan, Y., & Wang, L. (2017). Plasma miR-21 expression: an indicator for the severity of Type 2 diabetes with diabetic retinopathy. *Bioscience reports, 37*(2), BSR20160589. doi:10.1042/BSR20160589

Jiang, Q., Zhao, F., Liu, X., Li, R., & Liu, J. (2015). Effect of miR-200b on retinal endothelial cell function under high glucose environment. *International journal of clinical and experimental pathology, 8*, 10482-10487.

Jiang, S., & Chen, X. (2017). HMGB1 siRNA can reduce damage to retinal cells induced by high glucose in vitro and in vivo. *Drug design, development and therapy, 11*, 783-795. doi:10.2147/DDDT.S129913

Khalfaoui, T., Lizard, G., & Ouertani-Meddeb, A. (2008). Adhesion molecules (ICAM-1 and VCAM-1) and diabetic retinopathy in type 2 diabetes. *Journal of Molecular Histology, 39*(2), 243-249. doi:10.1007/s10735-007-9159-5

Khurana, R., Simons, M., Martin John, F., & Zachary Ian, C. (2005). Role of Angiogenesis in Cardiovascular Disease. *Circulation, 112*(12), 1813-1824. doi:10.1161/CIRCULATIONAHA.105.535294

Kim, Y., & Park, C. W. (2019). Mechanisms of Adiponectin Action: Implication of Adiponectin Receptor Agonism in Diabetic Kidney Disease. *International journal of molecular sciences, 20*(7), 1782. doi:10.3390/ijms20071782

Knoepp, K., Teske, R., Korte, L., Dutzmann, J., Rieckmann, M., Daniel, J. M., . . . Sedding, D. G. (2020). MicroRNA-146a regulates angiogenesis and functional regeneration after myocardial infarction. *European Heart Journal, 41*(Supplement_2). doi:10.1093/ehjci/ehaa946.3637

Kollias, A. N., & Ulbig, M. W. (2010). Diabetic retinopathy: Early diagnosis and effective treatment. *Deutsches Arzteblatt international, 107*(5), 75-84. doi:10.3238/arztebl.2010.0075

Konstantinidis, L., Carron, T., de Ancos, E., Chinet, L., Hagon-Traub, I., Zuercher, E., & Peytremann-Bridevaux, I. (2017). Awareness and practices regarding eye diseases among patients with diabetes: a cross sectional analysis of the CoDiab-VD cohort. *BMC endocrine disorders, 17*(1), 56-56. doi:10.1186/s12902-017-0206-2

Kreth, S., Hübner, M., & Hinske, L. C. (2018). MicroRNAs as Clinical Biomarkers and Therapeutic Tools in Perioperative Medicine. *Anesthesia & Analgesia, 126*(2).

Krol, J., Loedige, I., & Filipowicz, W. (2010). The widespread regulation of microRNA biogenesis, function and decay. *Nature Reviews Genetics, 11*(9), 597-610. doi:10.1038/nrg2843

Kuehbacher, A., Urbich, C., Zeiher Andreas, M., & Dimmeler, S. (2007). Role of Dicer and Drosha for Endothelial MicroRNA Expression and Angiogenesis. *Circulation research, 101*(1), 59-68. doi:10.1161/CIRCRESAHA.107.153916

Kumarswamy, R., Volkmann, I., & Thum, T. (2011). Regulation and function of miRNA-21 in health and disease. *RNA biology, 8*(5), 706-713. doi:10.4161/rna.8.5.16154

Kwon, H., & Pessin, J. E. (2013). Adipokines mediate inflammation and insulin resistance. *Frontiers in endocrinology, 4*, 71-71. doi:10.3389/fendo.2013.00071

Leasher, J., Bourne, R., Flaxman, S., Jonas, J., Keeffe, J., Naidoo, K., . . . Taylor, H. (2016). Global Estimates on the Number of People Blind or Visually Impaired by Diabetic Retinopathy: A meta-analysis from 1990-2010. *Diabetes care, 39*, 1643-1649. doi:10.2337/dc15-2171

Li, E.-H., Huang, Q.-Z., Li, G.-C., Xiang, Z.-Y., & Zhang, X. (2017). Effects of miRNA-200b on the development of diabetic retinopathy by targeting VEGFA gene. *Bioscience reports, 37*(2), BSR20160572. doi:10.1042/BSR20160572

Li, M., & Rollins, J. A. (2009). The development-specific protein (Ssp1) from Sclerotinia sclerotiorum is encoded by a novel gene expressed exclusively in sclerotium tissues. *Mycologia, 101*(1), 34-43. doi:10.3852/08-114

Li, Y., & Shi, X. (2013). MicroRNAs in the regulation of TLR and RIG-I pathways. *Cellular & molecular immunology, 10*(1), 65-71. doi:10.1038/cmi.2012.55

Liu, C.-H., Huang, S., Britton, W. R., & Chen, J. (2020). MicroRNAs in Vascular Eye Diseases. *International journal of molecular sciences, 21*(2), 649. doi:10.3390/ijms21020649

Liu, Y., Song, Y., Tao, L., Qiu, W., Lv, H., Jiang, X., . . . Li, X. (2017). Prevalence of diabetic retinopathy among 13473 patients with diabetes mellitus in China: a cross-sectional epidemiological survey in six provinces. *BMJ open, 7*(1), e013199-e013199. doi:10.1136/bmjopen-2016-013199

Lu, Q., Zhang, J., Zhao, N., Wang, H., Tong, Q., & Wang, S. (2017). Association of IL-6 Gene (-174 and -572 G/C) Polymorphisms with Proliferative Diabetic Retinopathy of Type 2 Diabetes in a Chinese Population. *Ophthalmic Research, 58*(3), 162-167. doi:10.1159/000475670

Luly, F. R., Lévêque, M., Licursi, V., Cimino, G., Martin-Chouly, C., Théret, N., . . . Del Porto, P. (2019). MiR-146a is over-expressed and controls IL-6 production in cystic fibrosis macrophages. *Scientific Reports, 9*(1), 16259. doi:10.1038/s41598-019-52770-w

Ma, X., Becker Buscaglia, L. E., Barker, J. R., & Li, Y. (2011). MicroRNAs in NF-kappaB signaling. *Journal of molecular cell biology, 3*(3), 159-166. doi:10.1093/jmcb/mjr007

Madsen-Bouterse, S., Mohammad, G., & Kowluru, R. A. (2010). Glyceraldehyde-3-phosphate dehydrogenase in retinal microvasculature: implications for the development and progression of diabetic retinopathy. *Investigative Ophthalmology & Visual Science, 51*(3), 1765-1772. doi:10.1167/iovs.09-4171

Magliah, S. F., Bardisi, W., Al Attah, M., & Khorsheed, M. M. (2018). The prevalence and risk factors of diabetic retinopathy in selected primary care centers during the 3-year screening intervals. *Journal of family medicine and primary care, 7*(5), 975-981. doi:10.4103/jfmpc.jfmpc_85_18

Mahesh, G., & Biswas, R. (2019). MicroRNA-155: A Master Regulator of Inflammation. *Journal of interferon & cytokine research : the official journal of the International Society for Interferon and Cytokine Research, 39*(6), 321-330. doi:10.1089/jir.2018.0155

Maier, M. M. J. A. M. (2006). *Angiogenesis: An Overview*: New Frontiers in Angiogenesis. Springer, Dordrecht.

Mancuso, P. (2016). The role of adipokines in chronic inflammation. *ImmunoTargets and therapy, 5*, 47-56. doi:10.2147/ITT.S73223

Martinez, B., & Peplow, P. V. (2019). MicroRNAs as biomarkers of diabetic retinopathy and disease progression. *Neural regeneration research, 14*(11), 1858-1869. doi:10.4103/1673-5374.259602

Mastropasqua, R., Toto, L., Cipollone, F., Santovito, D., Carpineto, P., & Mastropasqua, L. (2014). Role of microRNAs in the modulation of diabetic

retinopathy. *Progress in retinal and eye research, 43*, 92-107. doi:10.1016/j.preteyeres.2014.07.003

Mazzeo, A., Beltramo, E., Lopatina, T., Gai, C., Trento, M., & Porta, M. (2018). Molecular and functional characterization of circulating extracellular vesicles from diabetic patients with and without retinopathy and healthy subjects. *Experimental Eye Research, 176*, 69-77. doi:https://doi.org/10.1016/j.exer.2018.07.003

McArthur, K., Feng, B., Wu, Y., Chen, S., & Chakrabarti, S. (2011). MicroRNA-200b regulates vascular endothelial growth factor-mediated alterations in diabetic retinopathy. *Diabetes, 60*(4), 1314-1323. doi:10.2337/db10-1557

Meissner, M., Stein, M., Urbich, C., Reisinger, K., Suske, G., Staels, B., . . . Gille, J. (2004). PPARalpha activators inhibit vascular endothelial growth factor receptor-2 expression by repressing Sp1-dependent DNA binding and transactivation. *Circulation research, 94*(3), 324-332. doi:10.1161/01.res.0000113781.08139.81

Metin, T., Dinç, E., Görür, A., Erdoğan, S., Ertekin, S., Sarı, A. A., . . . Çelik, Y. (2018). Evaluation of the plasma microRNA levels in stage 3 premature retinopathy with plus disease: preliminary study. *Eye (London, England), 32*(2), 415-420. doi:10.1038/eye.2017.193

Mohamed, Q., Gillies, M. C., & Wong, T. Y. (2007). Management of Diabetic RetinopathyA Systematic Review. *JAMA, 298*(8), 902-916. doi:10.1001/jama.298.8.902

Musat, O., Cernat, C., Labib, M., Gheorghe, A., Toma, O., Zamfir, M., & Boureanu, A. M. (2015). DIABETIC MACULAR EDEMA. *Romanian journal of ophthalmology, 59*(3), 133-136.

Negi, G., Kumar, A., Joshi, R., P K, R., & Sharma, S. (2011). Oxidative stress and diabetic neuropathy: Current status of antioxidants. *IIOAB Journal, 2*, 71-78.

Nejad, C., Stunden, H. J., & Gantier, M. P. (2018). A guide to miRNAs in inflammation and innate immune responses. *The FEBS Journal, 285*(20), 3695-3716. doi:10.1111/febs.14482

Nentwich, M. M., & Ulbig, M. W. (2015). Diabetic retinopathy - ocular complications of diabetes mellitus. *World journal of diabetes, 6*(3), 489-499. doi:10.4239/wjd.v6.i3.489

Noda, K., Nakao, S., Ishida, S., & Ishibashi, T. (2012). Leukocyte Adhesion Molecules in Diabetic Retinopathy. *Journal of ophthalmology, 2012*, 279037. doi:10.1155/2012/279037

O'Connell, R., Rao, D., Chaudhuri, A., & Baltimore, D. (2010). Physiological and pathological roles of microRNAs in the immune system. *Nature reviews. Immunology, 10*, 111-122. doi:10.1038/nri2708

Osada, H., & Takahashi, T. (2007). MicroRNAs in biological processes and carcinogenesis. *Carcinogenesis, 28*(1), 2-12. doi:10.1093/carcin/bgl185

Otrock, Z. K., Mahfouz, R. A. R., Makarem, J. A., & Shamseddine, A. I. (2007). Understanding the biology of angiogenesis: Review of the most important molecular mechanisms. *Blood Cells, Molecules, and Diseases, 39*(2), 212-220. doi:https://doi.org/10.1016/j.bcmd.2007.04.001

Otsuka, M., Zheng, M., Hayashi, M., Lee, J.-D., Yoshino, O., Lin, S., & Han, J. (2008). Impaired microRNA processing causes corpus luteum insufficiency and infertility in mice. *The Journal of clinical investigation, 118*(5), 1944-1954. doi:10.1172/JCI33680

Palazzo, A. F., & Lee, E. S. (2015). Non-coding RNA: what is functional and what is junk? *Frontiers in genetics, 6*, 2-2. doi:10.3389/fgene.2015.00002

Park, J. E., Keller, G. A., & Ferrara, N. (1993). The vascular endothelial growth factor (VEGF) isoforms: differential deposition into the subepithelial extracellular matrix and bioactivity of extracellular matrix-bound VEGF. *Molecular biology of the cell, 4*(12), 1317-1326. doi:10.1091/mbc.4.12.1317

Qin, L.-L., An, M.-X., Liu, Y.-L., Xu, H.-C., & Lu, Z.-Q. (2017). MicroRNA-126: a promising novel biomarker in peripheral blood for diabetic retinopathy. *International journal of ophthalmology, 10*(4), 530-534. doi:10.18240/ijo.2017.04.05

Qing, S., Yuan, S., Yun, C., Hui, H., Mao, P., Wen, F., . . . Liu, Q. (2014). Serum MiRNA Biomarkers serve as a Fingerprint for Proliferative Diabetic Retinopathy. *Cellular Physiology and Biochemistry, 34*(5), 1733-1740. doi:10.1159/000366374

Rezk, N. A., Sabbah, N. A., & Saad, M. S. S. (2016). Role of MicroRNA 126 in screening, diagnosis, and prognosis of diabetic patients in Egypt. *IUBMB Life, 68*(6), 452-458. doi:10.1002/iub.1502

Romano, G. L., Platania, C. B. M., Drago, F., Salomone, S., Ragusa, M., Barbagallo, C., . . . Bucolo, C. (2017). Retinal and Circulating miRNAs in Age-Related Macular Degeneration: An In vivo Animal and Human Study. *Frontiers in pharmacology, 8*, 168-168. doi:10.3389/fphar.2017.00168

Roy, S., Kern, T. S., Song, B., & Stuebe, C. (2017). Mechanistic Insights into Pathological Changes in the Diabetic Retina: Implications for Targeting Diabetic Retinopathy. *The American journal of pathology, 187*(1), 9-19. doi:10.1016/j.ajpath.2016.08.022

Rungger-Brändle, E., Dosso, A. A., & Leuenberger, P. (2000). Glial Reactivity, an Early Feature of Diabetic Retinopathy. *Investigative Ophthalmology & Visual Science, 41*, 1971-1980.

Rübsam, A., Parikh, S., & Fort, P. E. (2018). Role of Inflammation in Diabetic Retinopathy. *Int J Mol Sci, 19*(4). doi:10.3390/ijms19040942

Rübsam, A., Parikh, S., & Fort, P. E. (2018). Role of Inflammation in Diabetic Retinopathy. *International journal of molecular sciences, 19*(4), 942. doi:10.3390/ijms19040942

Sakurai, E., Taguchi, H., Anand, A., Ambati, B. K., Gragoudas, E. S., Miller, J. W., . . . Ambati, J. (2003). Targeted Disruption of the CD18 or ICAM-1 Gene Inhibits Choroidal Neovascularization. *Investigative Ophthalmology & Visual Science, 44*(6), 2743-2749. doi:10.1167/iovs.02-1246

Santos, J. M., Tewari, S., & Kowluru, R. A. (2012). A compensatory mechanism protects retinal mitochondria from initial insult in diabetic retinopathy. *Free radical biology & medicine, 53*(9), 1729-1737. doi:10.1016/j.freeradbiomed.2012.08.588

Sheedy, F. J. (2015). Turning 21: Induction of miR-21 as a Key Switch in the Inflammatory Response. *Frontiers in Immunology, 6*, 19.

Shibuya, M. (2011). Vascular Endothelial Growth Factor (VEGF) and Its Receptor (VEGFR) Signaling in Angiogenesis: A Crucial Target for Anti- and Pro-Angiogenic Therapies. *Genes & cancer, 2*(12), 1097-1105. doi:10.1177/1947601911423031

Silva, V. A. O., Polesskaya, A., Sousa, T. A., Corrêa, V. M. A., André, N. D., Reis, R. I., . . . De Lucca, F. L. (2011). Expression and cellular localization of microRNA-29b and RAX, an activator of the RNA-dependent protein kinase

(PKR), in the retina of streptozotocin-induced diabetic rats. *Molecular vision, 17*, 2228-2240.

Simó, R., & Hernández, C. (2009). Advances in the medical treatment of diabetic retinopathy. *Diabetes care, 32*(8), 1556-1562. doi:10.2337/dc09-0565

Singh, R., & Mo, Y.-Y. (2013). Role of microRNAs in breast cancer. *Cancer biology & therapy, 14*(3), 201-212. doi:10.4161/cbt.23296

Solomon, S. D., Chew, E., Duh, E. J., Sobrin, L., Sun, J. K., VanderBeek, B. L., . . . Gardner, T. W. (2017). Diabetic Retinopathy: A Position Statement by the American Diabetes Association. *Diabetes care, 40*(3), 412-418. doi:10.2337/dc16-2641

Song, J., Ouyang, Y., Che, J., Li, X., Zhao, Y., Yang, K., . . . Yuan, W. (2017). Potential Value of miR-221/222 as Diagnostic, Prognostic, and Therapeutic Biomarkers for Diseases. *Frontiers in Immunology, 8*, 56.

Sorrentino, F. S., Matteini, S., Bonifazzi, C., Sebastiani, A., & Parmeggiani, F. (2018). Diabetic retinopathy and endothelin system: microangiopathy versus endothelial dysfunction. *Eye (Lond), 32*(7), 1157-1163. doi:10.1038/s41433-018-0032-4

Srivastava, S., Zaidi, A., Afreen, S., Eba, A., shwar, M., & Raza, S. (2019). DIAGNOSTIC IMPORTANCE OF MIRNA IN DIABETIC RETINOPATHY. *Era's Journal of Medical Research, 6*, 131-138. doi:10.24041/ejmr2019.143

Stewart, M. W. (2016). Treatment of diabetic retinopathy: Recent advances and unresolved challenges. *World journal of diabetes, 7*(16), 333-341. doi:10.4239/wjd.v7.i16.333

Su, Z. F., Sun, Z. W., Zhang, Y., Wang, S., Yu, Q. G., & Wu, Z. B. (2017). Regulatory effects of miR-146a/b on the function of endothelial progenitor cells in acute

ischemic stroke in mice. *Kaohsiung J Med Sci, 33*(8), 369-378. doi:10.1016/j.kjms.2017.05.010

Sun, J. K., Lin, M. M., Lammer, J., Prager, S., Sarangi, R., Silva, P. S., & Aiello, L. P. (2014). Disorganization of the Retinal Inner Layers as a Predictor of Visual Acuity in Eyes With Center-Involved Diabetic Macular Edema. *JAMA Ophthalmology, 132*(11), 1309-1316. doi:10.1001/jamaophthalmol.2014.2350

Suárez, Y., & Sessa, W. C. (2009). MicroRNAs as novel regulators of angiogenesis. *Circulation research, 104*(4), 442-454. doi:10.1161/CIRCRESAHA.108.191270

Taganov, K., Boldin, M., & Baltimore, D. (2007). MicroRNAs and Immunity: Tiny Players in a Big Field. *Immunity, 26*, 133-137. doi:10.1016/j.immuni.2007.02.005

Taganov, K. D., Boldin, M. P., Chang, K.-J., & Baltimore, D. (2006). NF-kappaB-dependent induction of microRNA miR-146, an inhibitor targeted to signaling proteins of innate immune responses. *Proceedings of the National Academy of Sciences of the United States of America, 103*(33), 12481-12486. doi:10.1073/pnas.0605298103

Tan, G. S., Ikram, M. K., Sabanayagam, C., Neelam, K., Lamoureux, E. L., Tai, E. S., . . . Wong, T. Y. (2014). Serum levels of Leptin and Adiponectin are associated with diabetic retinopathy in an Asian population with diabetes mellitus. *Investigative Ophthalmology & Visual Science, 55*(13), 5344-5344.

Tang, J., & Kern, T. S. (2011). Inflammation in diabetic retinopathy. *Progress in retinal and eye research, 30*(5), 343-358. doi:10.1016/j.preteyeres.2011.05.002

Tarr, J. M., Kaul, K., Chopra, M., Kohner, E. M., & Chibber, R. (2013). Pathophysiology of diabetic retinopathy. *ISRN ophthalmology, 2013*, 343560-343560. doi:10.1155/2013/343560

Thomas, R. L., Halim, S., Gurudas, S., Sivaprasad, S., & Owens, D. R. (2019). IDF Diabetes Atlas: A review of studies utilising retinal photography on the global prevalence of diabetes related retinopathy between 2015 and 2018. *Diabetes research and clinical practice, 157*, 107840.

Usui, Y., Westenskow, P. D., Murinello, S., Dorrell, M. I., Scheppke, L., Bucher, F., . . . Friedlander, M. (2015). Angiogenesis and Eye Disease. *Annual Review of Vision Science, 1*(1), 155-184. doi:10.1146/annurev-vision-082114-035439

Vujosevic, S., Micera, A., Bini, S., Berton, M., Esposito, G., & Midena, E. (2015). Aqueous Humor Biomarkers of Müller Cell Activation in Diabetic Eyes. *Investigative Ophthalmology & Visual Science, 56*(6), 3913-3918. doi:10.1167/iovs.15-16554

Vujosevic, S., Micera, A., Bini, S., Berton, M., Esposito, G., & Midena, E. (2016). Proteome analysis of retinal glia cells-related inflammatory cytokines in the aqueous humour of diabetic patients. *Acta Ophthalmologica, 94*(1), 56-64. doi:10.1111/aos.12812

Wang, Q., Bozack, S. N., Yan, Y., Boulton, M. E., Grant, M. B., & Busik, J. V. (2014). Regulation of retinal inflammation by rhythmic expression of MiR-146a in diabetic retina. *Investigative Ophthalmology & Visual Science, 55*(6), 3986-3994. doi:10.1167/iovs.13-13076

Wang, Q., Navitskaya, S., Chakravarthy, H., Huang, C., Kady, N., Lydic, T. A., . . . Busik, J. V. (2016). Dual Anti-Inflammatory and Anti-Angiogenic Action of

miR-15a in Diabetic Retinopathy. *EBioMedicine, 11*, 138-150. doi:10.1016/j.ebiom.2016.08.013

Wang, S., Aurora, A. B., Johnson, B. A., Qi, X., McAnally, J., Hill, J. A., . . . Olson, E. N. (2008). The endothelial-specific microRNA miR-126 governs vascular integrity and angiogenesis. *Developmental cell, 15*(2), 261-271. doi:10.1016/j.devcel.2008.07.002

Wang, S., & Olson, E. N. (2009). AngiomiRs--key regulators of angiogenesis. *Current opinion in genetics & development, 19*(3), 205-211. doi:10.1016/j.gde.2009.04.002

Wang, W., & Lo, A. C. Y. (2018). Diabetic Retinopathy: Pathophysiology and Treatments. *Int J Mol Sci, 19*(6). doi:10.3390/ijms19061816

Wang, Y., Yuan, Y., & Jiang, H. (2014). Serum and vitreous levels of visfatin in patients with diabetic retinopathy. *Medical science monitor : international medical journal of experimental and clinical research, 20*, 2729-2732. doi:10.12659/MSM.891292

Weinreb, R. N., Aung, T., & Medeiros, F. A. (2014). The pathophysiology and treatment of glaucoma: a review. *JAMA, 311*(18), 1901-1911. doi:10.1001/jama.2014.3192

Whitehead, M., Wickremasinghe, S., Osborne, A., Van Wijngaarden, P., & Martin, K. R. (2018). Diabetic retinopathy: a complex pathophysiology requiring novel therapeutic strategies. *Expert Opin Biol Ther, 18*(12), 1257-1270. doi:10.1080/14712598.2018.1545836

Xie, J., Ikram, M. K., Cotch, M. F., Klein, B., Varma, R., Shaw, J. E., . . . Wong, T. Y. (2017). Association of Diabetic Macular Edema and Proliferative Diabetic Retinopathy With Cardiovascular Disease: A Systematic Review and Meta-

analysis. *JAMA Ophthalmol, 135*(6), 586-593. doi:10.1001/jamaophthalmol.2017.0988

Xie, Y., Chu, A., Feng, Y., Chen, L., Shao, Y., Luo, Q., . . . Chen, Y. (2018). MicroRNA-146a: A Comprehensive Indicator of Inflammation and Oxidative Stress Status Induced in the Brain of Chronic T2DM Rats. *Frontiers in Pharmacology, 9*, 478.

Yang, T. T., Song, S. J., Xue, H. B., Shi, D. F., Liu, C. M., & Liu, H. (2015). Regulatory T cells in the pathogenesis of type 2 diabetes mellitus retinopathy by miR-155. *European review for medical and pharmacological sciences, 19*, 2010-2015.

Yang, W., Yang, D., Na, S., Sandusky, G., Zhang, Q., & Zhao, G. (2005). Dicer Is Required for Embryonic Angiogenesis during Mouse Development. *The Journal of biological chemistry, 280*, 9330-9335. doi:10.1074/jbc.M413394200

Yau, J. W. Y., Rogers, S. L., Kawasaki, R., Lamoureux, E. L., Kowalski, J. W., Bek, T., . . . Meta-Analysis for Eye Disease Study, G. (2012). Global prevalence and major risk factors of diabetic retinopathy. *Diabetes care, 35*(3), 556-564. doi:10.2337/dc11-1909

Ye, E.-A., & Steinle, J. J. (2016). miR-146a Attenuates Inflammatory Pathways Mediated by TLR4/NF-κB and TNFα to Protect Primary Human Retinal Microvascular Endothelial Cells Grown in High Glucose. *Mediators of Inflammation, 2016*, 3958453. doi:10.1155/2016/3958453

Ye, E.-A., & Steinle, J. J. (2017a). miR-146a suppresses STAT3/VEGF pathways and reduces apoptosis through IL-6 signaling in primary human retinal microvascular endothelial cells in high glucose conditions. *Vision research, 139*, 15-22. doi:10.1016/j.visres.2017.03.009

Ye, E.-A., & Steinle, J. J. (2017b). Regulatory role of microRNA on inflammatory responses of diabetic retinopathy. *Neural regeneration research, 12*(4), 580-581. doi:10.4103/1673-5374.205095

Ye, J., Guo, R., Shi, Y., Qi, F., Guo, C., & Yang, L. (2016). miR-155 Regulated Inflammation Response by the SOCS1-STAT3-PDCD4 Axis in Atherogenesis. *Mediators of Inflammation, 2016*, 8060182-8060182. doi:10.1155/2016/8060182

Yee, D., Shah, K. M., Coles, M. C., Sharp, T. V., & Lagos, D. (2017). MicroRNA-155 induction via TNF-α and IFN-γ suppresses expression of programmed death ligand-1 (PD-L1) in human primary cells. *The Journal of biological chemistry, 292*(50), 20683-20693. doi:10.1074/jbc.M117.809053

Yilmaz, M., Sonmez, A., Acikel, C., Celik, T., Bingol, N., Pinar, M., . . . Ozata, M. (2004). Adiponectin may play a part in the pathogenesis of diabetic retinopathy. *European journal of endocrinology / European Federation of Endocrine Societies, 151*, 135-140. doi:10.1530/eje.0.1510135

Yoshida, S., Yoshida, A., & Ishibashi, T. (2004). Induction of IL-8, MCP-1, and bFGF by TNF-α in retinal glial cells: implications for retinal neovascularization during post-ischemic inflammation. *Graefe's Archive for Clinical and Experimental Ophthalmology, 242*(5), 409-413. doi:10.1007/s00417-004-0874-2

Yun, J. S., Lim, T. S., Cha, S. A., Ahn, Y. B., Song, K. H., Choi, J. A., . . . Ko, S. H. (2016). Clinical Course and Risk Factors of Diabetic Retinopathy in Patients with Type 2 Diabetes Mellitus in Korea. *Diabetes & metabolism journal, 40*(6), 482-493. doi:10.4093/dmj.2016.40.6.482

Zaki, W. M. D. W., Zulkifley, M. A., Hussain, A., Halim, W. H. W. A., Mustafa, N. B. A., & Ting, L. S. (2016). Diabetic retinopathy assessment: Towards an automated system. *Biomedical Signal Processing and Control, 24*, 72-82. doi:https://doi.org/10.1016/j.bspc.2015.09.011

Zampetaki, A., Willeit, P., Burr, S., Yin, X., Langley, S. R., Kiechl, S., . . . Mayr, M. (2016). Angiogenic microRNAs Linked to Incidence and Progression of Diabetic Retinopathy in Type 1 Diabetes. *Diabetes, 65*(1), 216. doi:10.2337/db15-0389

Zhang, J., Wang, X., Vikash, Ye, Q., Wu, D., Liu, Y., & Dong, W. (2016). ROS and ROS-mediated cellular signaling. *Oxidative Medicine and Cellular Longevity, 2016 (2016)*. doi:10.1155/2016/4350965

Zhang, J., Wu, L., Chen, J., Lin, S., Cai, D., Chen, C., & Chen, Z. (2018). Downregulation of MicroRNA 29a/b exacerbated diabetic retinopathy by impairing the function of Müller cells via Forkhead box protein O4. *Diab Vasc Dis Res, 15*(3), 214-222. doi:10.1177/1479164118756239

Zhang, L., Dong, L., Tang, Y., Li, M., & Zhang, M. (2020). MiR-146b protects against the inflammation injury in pediatric pneumonia through MyD88/NF-κB signaling pathway. *Infectious Diseases, 52*(1), 23-32. doi:10.1080/23744235.2019.1671987

Zhou, Q., Gallagher, R., Ufret-Vincenty, R., Li, X., Olson, E. N., & Wang, S. (2011). Regulation of angiogenesis and choroidal neovascularization by members of microRNA-23~27~24 clusters. *Proceedings of the National Academy of Sciences of the United States of America, 108*(20), 8287-8292. doi:10.1073/pnas.1105254108

Zhu, K., Pan, Q., Zhang, X., Kong, L.-Q., Fan, J., Dai, Z., . . . Zhou, J. (2013). MiR-146a enhances angiogenic activity of endothelial cells in hepatocellular carcinoma by promoting PDGFRA expression. *Carcinogenesis, 34*(9), 2071-2079. doi:10.1093/carcin/bgt160

Zhuang, P., Muraleedharan, C. K., & Xu, S. (2017). Intraocular Delivery of miR-146 Inhibits Diabetes-Induced Retinal Functional Defects in Diabetic Rat Model. *Investigative Ophthalmology & Visual Science, 58*(3), 1646-1655. doi:10.1167/iovs.16-21223

Zhuang, Z., Xiao, q., Hu, H., Tian, S.-y., Lu, Z.-j., Zhang, T.-z., & Bai, Y.-l. (2015). Down-regulation of microRNA-155 attenuates retinal neovascularization via the PI3K/Akt pathway. *Molecular vision, 21*, 1173-1184.

Zorena, K., Jachimowicz-Duda, O., Ślęzak, D., Robakowska, M., & Mrugacz, M. (2020). Adipokines and Obesity. Potential Link to Metabolic Disorders and Chronic Complications. *International journal of molecular sciences, 21*(10), 3570. doi:10.3390/ijms21103570

Zou, H.-L., Wang, Y., Gang, Q., Zhang, Y., & Sun, Y. (2017). Plasma level of miR-93 is associated with higher risk to develop type 2 diabetic retinopathy. *Graefe's Archive for Clinical and Experimental Ophthalmology, 255*(6), 1159-1166. doi:10.1007/s00417-017-3638-5

Zuazo-Gaztelu, I., & Casanovas, O. (2018). Unraveling the Role of Angiogenesis in Cancer Ecosystems. *Frontiers in Oncology, 8*, 248.

Zur, D., Iglicki, M., & Loewenstein, A. (2019). The Role of Steroids in the Management of Diabetic Macular Edema. *Ophthalmic Research, 62*(4), 231-236. doi:10.1159/000499540